A CONSTITUTIVE MODEL FOR OVERCONSOLIDATED CLAYS

PART 1: MODEL FORMULATION
PART 2: MODEL EVALUATION

By Andrew J. Whittle

MITSG 90-15

Sea Grant College Program
Massachusetts Institute of Technology
Cambridge, Massachusetts 02139

Grant No: NA84AA-D00046
NA86AA-D-SG089
Project No: RO-12/RO-17

ABSTRACT

This report presents a new constitutive model, MIT-E3, which was developed to describe the mechanical behaviour of overconsolidated clays and clays under cyclic loading. The report is divided into two parts; a) model formulation, and b) evaluation:

MIT-E3 is a generalized effective stress model for describing the rate independent behaviour of normally to moderately overconsolidated clay (with OCR's less than 8) which exhibit normalised behaviour. The model formulation comprises three components; a) an elasto-plastic model for normally consolidated clay including anisotropic and strain softening behaviour, b) equations to describe the small strain nonlinearity and hysteretic response in unloading and reloading, and c) bounding surface plasticity for irrecoverable, anisotropic and path dependent behaviour of overconsolidated clays. Model complexity is controlled through the use of input parameters which can be obtained from a small number of standard soil tests. A complete procedure is described to select the input parameters for a given clay.

Input parameters for the model are selected for a low plasticity clay of moderate sensitivity (Boston Blue Clay) using the procedure outlined above. Comparison of selected values for three different types of clay is used to illustate potential ranges of these input parameters. Model predictions of monotonic undrained shear tests are compared with laboratory data for different modes of shearing and for overconsolidation ratios up to 8. The predictive capabilities of the model for describing anisotropic stress-strain-strength of soft clays are further evaluated by comparison with unique data from the Directional Shear Cell and Multi-directional Direct Simple Shear devices. The overall assessment of model shows that the model captures accurately many of the observed features of clay behaviour. This provides the basis for further evaluations of predictions for cyclic load histories and for predicting the performance of friction piles.

ACKNOWLEDGEMENTS

This work was sponsored in part through the MIT Sea Grant College Program through grants NA84AA-D00046 and NA86AA-D-SG-089, and most recently through the Doherty Professorship in Ocean Utilization. Funding was also provided by a consortium of oil companies including Amoco Production Company, Chevron Oil Field Research, Exxon Production Research, Marathon Oil Company, Mobil Research and Development, and Shell Development Company.

The author is indebted to Professor Mohsen Baligh for his assistance and guidance throughout this work and would also like to thank: Professor Charles C. Ladd, for his meticulous review of the manuscript; Dr John T. Germaine for his help in interpreting soil behaviour; and the numerous former graduate students of the Massachusetts Institute of Technology whose experimental data has contributed so significantly to this work.

FORWARD

A three year research program entitled "Behaviour of Piles Supporting Tension Leg Platforms", was initiated in January 1985, at the Massachusetts Institute of technology. The research attempts to achieve a better understanding of the important factors controlling the behaviour of offshore tension piles in order to develop more reliable and rational methods for analysing and predicting the behaviour of foundations supporting tension leg platforms. The proposed study included three phases:

1. Development of a generalised constitutive model for simulating the behaviour of clays subject to cyclic loading.
2. Analysis of the soil deformations, stresses and pore pressures during the stages in the life of a pile (i.e. from installation to cyclic loading) using the generalised soil model in conjunction with the strain path methods developed previously by Baligh and Levadoux (MITSG Report Nos. 80-12, 80-13).
3. Evaluation and validation of predictions by means of in-situ measurements on a model pile.

The results of the project were originally submitted in a series of three annual research reports to the sponsoring oil companies. This report summarizes the final version of the constitutive model, MIT-E3, which was developed during Phase 1 of the project.

Part 1: Model Formulation

INTRODUCTION

Constitutive equations, which model accurately the behaviour of soils, are a necessary component of all rational numerical analyses used to model practical geotechnical problems and are essential if reliable predictions of performance are to be achieved. Significant difficulties in developing such models are associated with the complexity of soil behaviour, observed from standard laboratory tests, and the need to use this limited experimental information to formulate appropriate equations for general histories of stress and strain.

Soils are complex multi-phase materials whose stress-strain-strength is characterised by pressure dependency with coupling between volumetric and shear behaviour. For example, during drained shearing, dense sands and highly overconsolidated clays tend to dilate, while loose sands and normally consolidated clays tend to contract (when drainage is prevented, undrained shearing is accompanied by shear induced pore pressures). In general, soils do not have a well defined region of linear behaviour (even at small strain levels), and exhibit unstable strain softening behaviour in some modes of deformation. Anisotropic properties are asasociated with the structure, depositional environment and subsequent straining of most natural soils. Time dependent behaviour (such as variation in response at different strain rates, creep and relaxation) can be significant for some soils, but is often difficult to distingush in the field from consolidation effects where soil deformations are accompanied by displacement of pore water.

In view of these complexities it is not possible to think in terms of developing a completely generalized model for all soils. It is important to tailor the modelling of material behaviour to the particular problem of interest and the required accuracy of solution. The model described in this paper was developed to study the performance of offshore friction piles supporting tension leg platforms (Whittle & Baligh, 1990). For this problem, the materials of primary interest are recent marine sediments which are normally to lightly overconsolidated (OCR's up to 4.0). The critical aspect of foundation performance is the behaviour under cyclic loading due to wave action on the compliant superstructure. Problems of this type are particularly difficult to analyse using simple constitutive models as the load histories involve large numbers of load cycles with variable amplitude and

frequency under conditions with ill-defined drainage conditions. In this work, attention is limited to the behaviour of saturated clays obeying normalised behaviour (i.e. excluding highly structured clays; Leroueil & Vaughn, 1989) which are rate independent.

The development of the model can be summarized as follows:

1. Establish features of behaviour to be modelled based on reliable experimental data[2].
2. Formulate the model using theories of behaviour which satisfy the axioms of continuum mechanics. In the current paper, the model is formulated within the theory of incremental elasto-plasticity.
3. Establish a procedure to determine the input parameters for the constitutive model to characterize a given material. Ideally, the parameters should be measured directly in standard (or readily available) laboratory tests and have a clear physical meaning. As model complexity increases, this task often becomes very difficult and represents a major obstacle to the use of 'sophisticated soil models'.
4. Evaluate predictions at the element level to establish the accuracy and limitations of the model formulation. One possible approach is to compare model predictions with reliable experimental data (other than tests from which the model was constructed or from which the input parameters were defined). Typically a hierarchical sequence of evaluation is used to evaluate the predictive capabilities and limitations of the proposed model (Whittle, 1990a).

MODELLING OF OVERCONSOLIDATED CLAY BEHAVIOUR

Most natural clays involve some degree of overconsolidation due to processes of mechanical unloading such as erosion, excavations, changes in groundwater pressures etc. Other sources of 'overconsolidation' include phenomena such as desiccation, secondary compression, cementations etc. Traditionally, the degree of overconsolidation is expressed by a single scalar, the overconsolidation ratio[3], $OCR=\sigma'_p/\sigma'_v$, where σ'_p is the preconsolidation pressure (maximum past vertical

[2]This indicates that the model is primarily phenomenological in nature and reflects the difficulty in determining adequate parameters to describe the internal structure ('fabric') of a clay.

[3]A similar measure can be defined using mean effective stress, $R=\sigma'_m/\sigma'$

effective stress) measured from one-dimensional consolidation tests and σ'_v is the current vertical effective stress. This parameter is a basic element of normalized soil behaviour as described by Critical State soil mechanics (Schofield & Wroth, 1968) as well as the SHANSEP procedure (Ladd & Foott, 1974).

The most widely used, generalized models of clay behaviour are based on the theory of work hardening, elasto-plasticity (Drucker, Gibson & Henkel, 1956) as exemplified by the Modified Cam Clay (MCC) model (Roscoe & Burland, 1968). In these models, 'overconsolidated states' of the soil are defined as the locus of effective stress states within the current yield surface developed by the normally consolidated clay. The stress-strain behaviour of the overconsolidated clay is modelled as isotropic and elastic, its shear strength is controlled by the location of the yield surface and failure is described by a critical state failure criterion. Stress paths within the yield surface are fully reversible (i.e. involve no plastic strains). For example, hydrostatic unloading and reloading, are described by a swelling line of constant slope, κ, in an e-$\log_e\sigma'$ space. There is no coupling between volumetric and shear response until yield occurs (due to the assumptions of isotropy and linearity). The model then predicts that, for undrained shearing within the yield surface, no shear induced pore pressures occur. Hence, elastic shakedown is predicted for uniform, (stress controlled) undrained cyclic loading of overconsolidated clays.

A detailed study of clay behaviour, as measured in standard laboratory tests, identified key aspects of the behaviour of overconsolidated clays for which improved modelling is required:

1. Although researchers have observed that the small strain behaviour of certain overconsolidated clays is substantially linear (e.g. Graham & Houlsby, 1983), there is increasing evidence to suggest that most overconsolidated soils are highly non-linear even at axial strain levels as small as ε_a=0.005% (e.g. Jardine et al., 1984). In triaxial tests, conventional instrumentation is inaccurate for strain levels, ε_a<0.05%. Thus the importance of soil non-linearity is often not appreciated from standard triaxial tests. However, accurate modelling of small strain stiffness can be critically important in the accurate solution of boundary value problems (Jardine et al., 1986).
2. The location of the yield surface is critically important in the formulation of an

elasto-plastic model due to the sharp change in response described at yield. Such behaviour has been measured from drained stress path tests on a number of highly sensitive clays (e.g. Tavenas et al, 1979). However, a more common observation is that the yield becomes increasingly less distinct as a function of the total amount of unloading experienced by the soil element (e.g. Roscoe & Burland, 1968).

3. Uniform, undrained cyclic loading of overconsolidated clays causes an accumulation of shear induced pore pressures and can lead to failure even when the magnitude of the load cycles is a fraction of the monotonic undrained shear strength of the clay (e.g. Azzouz et al., 1988). Thus coupling of volumetric and shear behaviour is essential for accurate modelling of overconsolidated clays under cyclic loading even at small to medium stress (or strain) levels.

Limitations in the modelling of overconsolidated clays using simple elasto-plastic models have long been recognised. Numerous extensions of the elasto-plastic framework have been proposed:

1. Inclusion of plastic strains within the yield surface. In their original paper Roscoe & Burland (1968) proposed the introduction of a second yield surface within MCC to capture more realistically the shear behaviour of overconsolidated clays. Subsequently plastic strains have been introduced for overconsolidated clays through a variety of approaches including; a) two surface and multi-surface models with anisotropic hardening (Mróz et al., 1978, 1981; Prevost, 1977, 1978), b) bounding surface models (Dafalias & Herrmann, 1982; Anandarajah & Dafalias, 1986), and c) subloading surface models (Hashiguchi, 1977, 1980). All of these models preserve the essential structure of the elasto-plastic framework by defining flow rules, hardening rules and magnitude of the elasto-plastic modulus for all 'overconsolidated stress states'. Models that use multiple yield surfaces have the disadvantage of geometric complexity and accumulate large numbers of state variables. In contrast, the 'bounding surface' and 'subloading surface' models, link plastic strains explicitly to the behaviour on the normally consolidated surface (through mapping rules) and are extremely parsimonious in their use of material constants and state parameters.
2. A number of authors have modified the formulation for the elastic strain

components. For example, Hueckel (1976) describes an elasto-plastic coupling formulation in which the elastic moduli are related to the plastic deformation. Hueckel & Nova (1979) introduce a more elaborate piecewise elastic formulation, which describes the small strain non-linearity of overconsolidated clays and models the hysteretic unload-reload behaviour.

Evaluation of these models shows that while they capture some aspects of the observed behaviour of overconsolidated clays, no single model describes fully the observed aspects summarised above. In addition, only limited success has been achieved using the models to predict cyclic loading. This is partly due to the lack of reliable experimental data from which to construct models and partly due to the extra complexity of modelling load histories which involve load reversals (Whittle, 1990b).

MODEL FORMULATION

This section presents a new constitutive model, referred to as MIT-E3, for describing the behaviour of overconsolidated clays and predicting the behaviour of soft (normally to lightly overconsolidated) clays under cyclic loading. Experimental data indicate that the unloading and reloading characteristics of a clay in drained shearing (σ'=const) and hydrostatic compression exhibit similar features; a) much stiffer response than the primary loading curve, b) hysteretic stress-strain behaviour, c) small irrecoverable deformations on completion of the unload-reload cycle, and d) reloading transition to the primary loading curve (normally consolidated condition). These observations are modelled in MIT-E3 using a simple mechanical model. Figure 1 shows the conceptual framework used by the model for hydrostatic unloading and reloading. It is assumed throughout that the soil can be modelled as a rate independent material (i.e. creep effects are not considered). The measured behaviour of a clay is most closely described by A-B-C (figure 1b). For modelling purposes, MIT-E3 subdivides this behaviour into two components:

1. A closed, symmetric, hysteresis loop (figure 1a) which matches the observed behaviour during unloading. This response is referred to as 'Perfectly Hysteretic' and is described through a formulation similar to that proposed by Hueckel & Nova (1979).

2. For reloading, plastic (irrecoverable) strains are assumed to develop as the Virgin Consolidation Line (VCL) is approached, resulting in residual plastic strains, Δ^p, at A. The magnitude of plastic strains is determined by the proximity of the current stress state to the VCL. Thus the plasticity is conveniently described using a bounding surface (Dafalias & Popov, 1977) or subloading surface (Hashiguchi, 1977) model.

Within this subdivision, MIT-E3 implicitly contains a number of important assumptions concerning the behaviour of overconsolidated clays:

1. The behaviour of overconsolidated clays can not be fully described by the overconsolidation ratio (OCR) of the soil. Additional information of the loading history is also required to distinguish between 'unloading' and 'reloading' at a particular overconsolidated stress state. i.e. extra state variables must be included in the material description.
2. A load cycle in stress space always involves some plastic strains, so that there is no purely reversible (elastic) range of behaviour.
3. Inclusion of plastic strains, using bounding surface plasticity, provides the means of coupling volumetric and shear behaviour and is also the mechanism by which anisotropic properties are described for overconsolidated clays. Bounding surface plasticity also ensures a smooth transition to normally consolidated behaviour, so that 'yielding' is smoothed out (hence the classical role of the 'yield surface' is no longer of critical importance).

The third component of the MIT-E3 model is a plasticity formulation to describe the generalized behaviour of K_0-normally consolidated clays. In particular, the normally consolidated clay model captures; a) the anisotropic properties of K_0-consolidated clays and their evolution with subsequent loading, and b) strain softening behaviour which is observed experimentally for certain modes of deformation. The model used in MIT-E3 is a modified version on an earlier model developed by Kavvadas (1982, 1983), which is referred to as MIT-E1.

Incremental Effective Stress-Strain Relations

The formulation of MIT-E3 is based on the incrementally, linearized theory of rate independent, elasto-plasticity (e.g. Prévost, 1977). The main assumption in this framework is that the (infinitesimal) incremental strains (or strain rates) can

be subdivided into elastic and plastic components:

$$\dot{\underset{\sim}{\varepsilon}} = \dot{\underset{\sim}{\varepsilon}}^{e} + \dot{\underset{\sim}{\varepsilon}}^{p} \qquad (1)$$

The elastic strain increments are assumed to be isotropically related to the stress increments by:

$$\dot{\sigma}' = K\dot{\varepsilon}^{e} \qquad (2.a)$$

$$\dot{\underset{\sim}{s}} = 2G\dot{\underset{\sim}{e}}^{e} \qquad (2.b)$$

where K, G are the incremental (tangential) elastic bulk and shear modulus, respectively. The tensors of effective stress and strains are divided into octahedral (volumetric) and deviatoric components:

$$\underset{\sim}{\sigma}' = \frac{1}{3}\sigma' \underset{\sim}{I} + \underset{\sim}{s} \qquad (3.a)$$

$$\underset{\sim}{\varepsilon} = \frac{1}{3}\varepsilon \underset{\sim}{I} + \underset{\sim}{e} \qquad (3.b)$$

$\underset{\sim}{I}$ is the identity tensor.

A load direction, $\underset{\sim}{Q}$, is introduced to define the occurence of plastic strains:

$$K Q \dot{\varepsilon} + 2G\left(\underset{\sim}{Q}' : \dot{\underset{\sim}{e}}\right) \begin{cases} \geq 0 & \text{Loading} \\ < 0 & \text{Unloading} \end{cases} \qquad (4)$$

where, Q and $\underset{\sim}{Q}'$ are the volumetric and deviatoric components of $\underset{\sim}{Q}$. The symbol ":", indicates the double decomposition of the associated second order tensors.

In classical plasticity, the load direction is chosen as the gradient of the yield surface (i.e. $\underset{\sim}{Q} = \partial f / \partial \underset{\sim}{\sigma}'$).

The plastic strain increments are defined by a general flow rule:

$$\dot{\varepsilon}^{p} = \dot{\Lambda} P \qquad (5a)$$

$$\dot{\underset{\sim}{e}}^{p} = \dot{\Lambda} \underset{\sim}{P}' \qquad (5b)$$

where P and $\underset{\sim}{P}'$ are the volumetric and deviatoric components of a second order tensor, $\underset{\sim}{P}$, which defines the directions of the plastic strain increments. $\dot{\Lambda}$ is a scalar which controls the magnitude of the plastic strains:

$$\dot{\Lambda} = \frac{1}{H}\left(Q\dot{\sigma}' + \underset{\sim}{Q}' : \dot{\underset{\sim}{s}}\right) \qquad (6)$$

and H is the elasto-plastic modulus.

Finally, combining equations 1 to 6, the general incremental effective stress-strain relations can be written:

$$\dot{\sigma}' = K\left(\dot{\varepsilon} - \left\langle \dot{\Lambda} P \right\rangle\right) \qquad (7a)$$

$$\dot{\underset{\sim}{s}} = 2G\left(\dot{\underset{\sim}{e}} - \left\langle \dot{\Lambda} \underset{\sim}{P}' \right\rangle\right) \qquad (7b)$$

where: $\left\langle \dot{\Lambda} P \right\rangle = \begin{cases} \dot{\Lambda} P & \text{if } \dot{\Lambda} P \geq 0 \\ 0 & \text{if } \dot{\Lambda} P < 0 \end{cases}$

and $\dot{\Lambda}$ can be written in terms of the strain increments as:

$$\dot{\Lambda} = \frac{K Q \dot{\varepsilon} + 2G \left(\underset{\sim}{Q}' : \underset{\sim}{\dot{e}} \right)}{H + KQP + 2G \left(\underset{\sim}{Q}' : \underset{\sim}{P}' \right)} \qquad (8)$$

This general framework of elasto-plasticity is first used to develop a model for the normally consolidated clay through the introduction of a yield surface (MIT-E1). For overconsolidated clays, the perfectly hysteretic model is developed to describe the tangential elastic moduli (K, G; eqn. 2) during unloading and reloading; while plastic strain increments are related through mapping functions to the behaviour described for the normally consolidated clay. The model uses transformed measures for all tensorial quantities (Appendix A; following Mróz, 1967; Prevost, 1977) in order to solve practical problems with a reduced number of variables.

MIT-E1 for Normally Consolidated Clay

The MIT-E1 model assumes that the mechanical behaviour of soil elements normally consolidated along radial effective stress paths ($\underset{\sim}{s} / \sigma' = \text{const.}$), can be described by a yield surface which is initially oriented along the direction of consolidation. The yield function is written (Kavvadas,1982):

$$f = \left(\underset{\sim}{s} - \sigma' \underset{\sim}{b} \right) : \left(\underset{\sim}{s} - \sigma' \underset{\sim}{b} \right) - c^2 \sigma' \left(2\,\alpha' - \sigma' \right) = 0 \qquad (9)$$

where, α' controls the size of the yield surface, $\underset{\sim}{b}$ is a second order tensor describing the orientation of the yield surface in effective stress space (σ', $\underset{\sim}{s}$) and c is the ratio of the semi-axes of the ellipsoid (figure 2). For the case when $\underset{\sim}{b} = \underset{\sim}{0}$, the yield surface of MIT-E1 reduces to the same form as that used in the MCC model (Roscoe & Burland, 1968).

A 'virgin normally consolidated' soil element (i.e. one consolidated from a slurry along a radial effective stress path), is described by the stress state at the tip of the yield surface such that:

$$\sigma' = 2\alpha' \qquad (10a)$$

$$\underset{\sim}{s} = 2\alpha' \underset{\sim}{b} \qquad (10b)$$

The load direction, $\underset{\sim}{Q}$, for stress states located on the yield surface is given by the gradient of the yield surface:

$$Q = 2c^2 \left(\sigma' - \alpha' \right) - 2 \left(\underset{\sim}{s} - \sigma' \underset{\sim}{b} \right) : \underset{\sim}{b} \qquad (11a)$$

$$\underset{\sim}{Q}' = 2 \left(\underset{\sim}{s} - \sigma' \underset{\sim}{b} \right) \qquad (11b)$$

Failure conditions are represented by an anisotropic failure criterion:

$$h = \left(\underset{\sim}{s} - \sigma'\underset{\sim}{\xi}\right) : \left(\underset{\sim}{s} - \sigma'\underset{\sim}{\xi}\right) - k^2\sigma'^2 = 0 \qquad (12)$$

where h describes a cone in effective stress space, with apex at the origin and axes along the direction $\left(\underset{\sim}{I} + \underset{\sim}{\xi}\right)$ (fig. 2).

In general, the components of $\underset{\sim}{\xi}$ cannot be determined from standard laboratory tests. Instead, MIT-E1 assumes that the orientation tensor is fully defined by the friction angles measured in triaxial compression and extension tests (ϕ'_{TC} and ϕ'_{TE} respectively) at large strain conditions (typically $\varepsilon_a \approx 10\%$, in undrained shear tests). In triaxial space (σ', S_1) (Appendix A), the failure criterion is now written:

$$h = (S_1 - \sigma'\xi_1)^2 - k^2\sigma'^2 = 0 \qquad (13)$$

where the values of ξ_1 and k are:

$$\xi_1 = \frac{1}{2}(C_c - C_e) \quad ; \quad k = \frac{1}{2}(C_c + C_e)$$

$$C_c = \sqrt{\frac{2}{3}}\frac{6\sin\phi'_{TC}}{3 - \sin\phi'_{TC}} \quad ; \quad C_e = \sqrt{\frac{2}{3}}\frac{6\sin\phi'_{TE}}{3 + \sin\phi'_{TE}}$$

These assumptions lead to a final form of the failure criterion used in the MIT-E1 model:

$$h = \sum_{i=1}^{n} S_i^2 - 2\sigma' S_1\xi_1 + \sigma'^2\left(\xi_1^2 - k^2\right) \qquad (14)$$

(for a general stress space, n=5).

The model assumes two hardening rules to describe changes in the size and orientation of the yield surface, respectively:

$$\dot{\alpha}' = \alpha'\,\zeta\,\dot{\varepsilon}^p \qquad (15)$$

$$\dot{\underset{\sim}{b}} = \psi_0\,(r_x)\,\frac{1}{\alpha'}\left(\underset{\sim}{s} - \sigma'\underset{\sim}{b}\right)\dot{\varepsilon}^p \qquad (16)$$

where ζ is a dimensionless function of the state variables which is obtained by invoking the consistency requirement ($\dot{f} = 0$), ψ_0 is a material constant controlling the rate of rotation of the yield surface, and r_x is a scalar which describes the relative orientation of the yield surface to the critical state cone (figure 2):

$\overrightarrow{C\,R_x} = r_x.\overrightarrow{O'\,R_x}$

r_x=1 when $\underset{\sim}{b}$=0, ξ_1=0 (i.e. for an isotropic material)

r_x=0 when $\underset{\sim}{b}$=$\underset{\sim}{\xi}$, where $\underset{\sim}{\xi}$ defines the orientation of the critical state cone.

Equation 16 describes the rotational hardening of the yield surface and hence controls the rate of change of anisotropy of the clay. The general form of the

equation is such that the principal axes of anisotropy rotate towards the principal stress axes. Hence, the mechanism of evolving anisotropy is similar to the concept of evolving anisotropy described by Hashiguchi (1977) and to the swept-out-memory concept of Gudehus (1976). For the specific case when the principal axes of stress ($\underset{\sim}{\sigma}'$) and anisotropy ($\underset{\sim}{b}$) coincide, there are no rotations of the principal directions of anisotropy ($\dot{\underset{\sim}{b}} = \underset{\sim}{0}$). The variable r_x imposes limits on the principal directions of anisotropy. The form of r_x is selected such that a K_0-normally consolidated material (i.e. a sample with anisotropic structure due to its consolidation history), changes its anisotropic structure more slowly than a hydrostatically consolidated sample (which is isotropic due to the stress history) loaded under the same conditions.

A non-associated flow rule is used in the MIT-E1 model in order to generate: a) critical state failure conditions; and b) K_0 conditions for a 'virgin normally consolidated clay'. The critical state condition requires that, at large strain levels, as the stress path approaches the failure locus (eqn. 14), the sample continues to deform with no further change in volume. This is achieved by imposing the condition that P=0 (i.e. there is no further alteration of the yield surface at critical state, $\dot{\alpha} = 0$, $\dot{\underset{\sim}{b}} = \underset{\sim}{0}$). K_0 conditions are imposed by using the measured value of K_{0NC} as an input parameter and selecting the flow direction such that the virgin K_0 consolidation (from a slurry, along a radial effective stress path with K_0 conditions) generates conditions of no lateral straining in the sample. The flow rule used in MIT-E1 is given as follows:

$$P = 2\, c^2\, \alpha'\, r_c \qquad (17a)$$

$$\underset{\sim}{P}' = c^2 \times \left(\underset{\sim}{Q}' + \langle r_c \rangle \underset{\sim}{s} \right) \qquad (17b)$$

where x is a constant which defines the K_{0NC} condition:

$$x = \left(\frac{\lambda}{\lambda-\kappa}\right)\left\{ \frac{1+2K_{0NC}}{3(1-K_{0NC})} - \frac{K}{2G}\left(\frac{\kappa}{\lambda}\right)\right\} \qquad (18)$$

The parameter r_c is a scalar variable (analogous to r_x in equation 16) which describes the location of the current stress state relative to the failure surface as shown in figure 2:

$\overrightarrow{PR_c} = r_c.\overrightarrow{CR_c}$

The variable r_c has a maximum value when the stress state is located at the tip of the yield surface (r_c=1) and decreases such that at critical state conditions,

r_c=0.

The elasto-plastic modulus, H, is defined by detailed consideration of the behaviour of K_0-normally consolidated clays. The functional form of H is selected in order to describe: a) virgin consolidation lines (VCL) with slope λ in e-logσ' space for all radial consolidation paths in effective stress (σ', $\underset{\sim}{s}$) space; and b) strain hardening, peak strength, strain softening and critical state conditions for undrained shearing of K_0-normally consolidated clays:

$$H = 2c^2 \left(\frac{\kappa}{\lambda-\kappa}\right) K \left\{ \alpha' P - S_t 2c^2 \alpha' \times (r_c) \left(\underset{\sim}{Q}' : \underset{\sim}{b} \right) \right\} \qquad (19)$$

where S_t is a material constant.

Having selected the functional form of the elasto-plastic modulus the model formulation is completed by invoking the consistency requirement (Prager, 1956) that the stress state remain in contact with the yield surface for loading of a normally consolidated clay. For MIT-E1 with hardening parameters α' and $\underset{\sim}{b}$, this requirement is expressed by:

$$\dot{f} = \frac{\partial f}{\partial \underset{\sim}{\sigma}'} : \dot{\underset{\sim}{\sigma}} + \frac{\partial f}{\partial \alpha} \dot{\alpha} + \frac{\partial f}{\partial \underset{\sim}{b}} : \dot{\underset{\sim}{b}} = 0 \qquad (20)$$

From equations 6, 9, 15 and 16, this equation can be satisfied by solving for the constant ζ (eqn. 15) (Kavvadas, 1982):

$$\zeta = \frac{1}{\alpha'} \left\{ \frac{1}{2c^2 \alpha'} \frac{H}{P} - \psi_0 (r_x) \frac{\sigma'}{\alpha'} (2\alpha' - \sigma') \right\} \qquad (21)$$

Hysteretic Model

For a load cycle in stress space, the perfectly hysteretic model describes a closed symmetric hysteresis loop in the stress-strain response of the material. This behaviour is obtained using a formulation which is piecewise continuous (i.e. the moduli vary smoothly) between stress reversal points as suggested by Hueckel & Nova (1979). The model requires a) the definition of a 'stress reversal point' and b) the development of suitable expressions to describe the (secant or tangent) moduli relative to the stress reversal point.

It is assumed that the perfectly hysteretic response is based on the incremental, isotropic, relations between effective stress and elastic strain rates, equation 2. Furthermore, the Poisson's ratio for the soil skeleton, ν, is assumed to be constant, (i.e. K/2G=const). Thus, there is no coupling between volumetric and shear behaviour in the perfectly hysteretic equations (c.f. Graham & Houlsby, 1983).

Also, for proportional paths in stress space (constant ratio of deviatoric to mean effective stress rates), there are proportional paths in strain space and vice-versa. For example, K_0 swelling conditions ($\varepsilon_h=0$, $\varepsilon_v\neq 0$) describe a linear effective stress path (from eqn. 2). Observed deviations from the proportional stress (or strain) paths of overconsolidated clays are due solely to plastic strains. The perfectly hysteretic model is constructed by introducing a dimensionless distance (in stress space), ξ, which relates the current stress state to the stress reversal state (as shown in figure 3 for hydrostatic conditions):

$$\xi = \begin{cases} \sigma' / \sigma'_{rev} & \text{for } \sigma' > \sigma'_{rev} \\ \sigma'_{rev} / \sigma' & \text{for } \sigma'_{rev} > \sigma' \end{cases} \qquad (22)$$

where, σ'_{rev} is the mean effective stress at the stress reversal point.

The parameter ξ unifies the unloading and reloading behaviour and describes a symmetric, closed hysteresis loop by specifying the variation of the tangential (or secant) modulus as a function of ξ. A second stress amplitude is introduced to describe non-linearity in shear which accounts for changes in the stress ratio, $\underset{\sim}{\eta} = \underset{\sim}{s}/\sigma'$, using the following non-dimensional distance in stress space:

$$\xi_s = \left\{ \left(\underset{\sim}{\eta} - \underset{\sim}{\eta}_{rev}\right) : \left(\underset{\sim}{\eta} - \underset{\sim}{\eta}_{rev}\right) \right\}^{1/2} \qquad (23)$$

where, $\underset{\sim}{\eta}_{rev}$ = stress ratio at the most recent stress reversal state.

The model is extended for general stress states using the following assumptions:

1. The variation of moduli are described using the two measures of stress amplitude ξ and ξ_s corresponding to volumetric and shear behaviour. This takes advantage of the uncoupled nature of the incremental stress-strain relations (eqn. 1).
2. The moduli are related to the most recent stress reversal state. This implies that the small strain behaviour of an overconsolidated clay is controlled by the most recent stress history as suggested by Hight et al. (1983).

The volumetric behaviour of overconsolidated clays can be examined from the unloading behaviour in either hydrostatic or 1-dimensional swelling (triaxial, oedometer or constant rate of strain (CRS) tests, with lateral stress measurement). Both types of test produce very similar volumetric swelling behaviour (ε vs σ'). Figure 4 shows typical data from CRS tests (ε_a vs. ξ_v, where ξ_v is defined in terms of vertical effective stress) on two clays: a) a low plasticity, sensitive clay

(Boston Blue Clay); and b) a high plasticity insensitive clay (Empire Clay):

1. The stiffness (compressibility) in the overconsolidated range is principally controlled by the parameter ξ_v (or ξ), and is, by and large, independent of the current effective stress, σ'_v (or σ').
2. For an overconsolidated soil, the secant compliance or stiffness (relative to the reversal point), κ, is equal in unloading and reloading at the same ratio, ξ_v (or ξ). This provides experimental evidence of symmetry of the hysteresis loop.
3. For reloading, as the preconsolidation pressure (Virgin Consolidation Line) is approached, the reloading and unloading responses diverge as plastic strains occur.

The volumetric response is described by a tangential bulk modulus:

$$K = \frac{1+e}{\kappa_0 (1+\delta)} \sigma' \qquad (24)$$

$$\delta = Cn (\log_e \xi)^{n-1} \qquad (25)$$

where e is the void ratio, κ_0 defines the initial unloading slope in e-$\log_e\sigma'$ space, and C, n are material constants.

Equations 24 and 25 incorporate the following features:

1. The swelling behaviour is normalisable with respect to the Virgin Consolidation Line (i.e. swelling lines from any value of σ' are parallel in the e-$\log_e\sigma'$).
2. When δ=0, $K = (1+e)\sigma' / \kappa_0$, which describes a linear swelling behaviour in e-$\log_e\sigma'$ space and is identical to the swelling behaviour used in the MCC model.
3. The value of κ_0 defines the stiffness immediately at reversal of loading (i.e. the small strain moduli K_{max} and G_{max}). The value of κ_0 is determined from laboratory or field tests used to establish the velocity of elastic wave propagation in the soil (Hardin & Black, 1968).

The main role of the material constants C and n is to provide a flexible function (eqn. 25) which is capable of describing a wide range of swelling behaviour (figure 5). The values of C and n are determined from the swelling behaviour observed in oedometer or CRS tests.

In the perfectly hysteretic formulation, the shear behaviour can be considered from the behaviour in unloading and reloading during an undrained shear test. Using the parameter ξ_s, symmetry of the hysteretic stress-strain behaviour is obtained when the data are plotted in terms of the stress ratio, η. The general variation of

tangential moduli for the perfectly hysteretic model is then written:

$$\delta = Cn\left(\log_e \xi + \omega \xi_s \right)^{n-1} \qquad (26)$$

where ω is a material constant used to describe the small strain non-linearity in shear tests at constant mean effective stress.

The major assumption of the perfectly hysteretic model is that strains are only recovered in a stress cycle if the cycle begins from a stress reversal point. In this sense, the perfectly hysteretic model may be classed as a para-elastic constitutive law (Hueckel & Nova, 1979). In the proposed model, the moduli are described relative to the most recent stress reversal point. After stress reversal, the soil becomes very stiff, with moduli K_{max} and G_{max}. Thus there is a strong similarity between the stress reversal point and the concept of unloading in plasticity. However, for the perfectly hysteretic model, the effective stress and strain rates are proportional and it is only possible to define the stress reversal point from the sign of either the effective stress or strain rates. The model defines the stress reversal point from the direction of the strain rates. This is based on the original suggestion by Hardin & Drnevich (1972) that the non-linearity of soil is most appropriately described in terms of the strain history. Hight et al. (1983) present data which further suggest that the initiation of undrained shearing always involves high stiffness at small strain levels irrespective of the past consolidation (or strain) history. This implies that it may be more useful to separate the loading criterion into volumetric and deviatoric components and take advantage of the lack of coupling between volumetric and shear behaviour in the perfectly hysteretic model. The definition of the load reversal point is achieved by introducing a scalar strain amplitude parameter which describes the strain history relative to (the strain state at) the most recent stress reversal point as follows:

$$\chi = \begin{cases} {}^{\Delta l}\varepsilon & \text{for } \dot{\varepsilon} \neq 0 \\ \left\{ {}^{\Delta l}\underset{\sim}{e} : {}^{\Delta l}\underset{\sim}{e} \right\}^{1/2} & \text{for } \dot{\varepsilon} = 0 \end{cases} \qquad (27)$$

where, $${}^{\Delta l}\underset{\sim}{\varepsilon} = \int_{rev} d\varepsilon = \underset{\sim}{\varepsilon} - \underset{\sim}{\varepsilon}_{rev}$$

The implication of equation 27 is that volumetric strains are predominantly important in determining the non-linearity of soil. 'Loading' is then defined from the sign of the rate of the strain amplitude; $(\dot{\chi} = {}^{t+\Delta t}\chi - {}^{t}\chi)$:

$$\dot{\chi} = \begin{cases} >0 & \text{loading} \\ \leq 0 & \text{unloading} \end{cases} \qquad (28)$$

Bounding Surface Model

In the modelling of overconsolidated clays, the development of plastic strains plays a crucial role for three main reasons. Firstly, plastic strains introduce coupling between volumetric and shear behaviour, so that shear induced pore pressures are obtained for undrained (monotonic and cyclic) shearing. Secondly, within the MIT-E3 formulation, plastic strains enable the incorporation of anisotropic response for overconsolidated clays; and provide a smooth transition to the normally consolidated behaviour. The bounding surface model (first proposed by Dafalias & Popov, 1977) relates the plastic strains of overconsolidated clays to the plastic behaviour previously defined for the normally consolidated material (using the MIT-E1 model). Difficulties lie in the formulation of these mapping relations and the physical meaning of material constants to describe them.

In the proposed model, the bounding surface of normally consolidated clay behaviour is described by the yield function of the MIT-E1 model (equation 9). For overconsolidated stress states, a radial mapping rule is used to define a unique image point on the bounding surface (figure 2). Plastic behaviour at the current (overconsolidated) stress state, P, is linked to the plastic behaviour at the image point, I.

The bounding surface for the MIT-E3 model is developed from observations of the volumetric behaviour of soil. Figure 1b illustrates hydrostatic unloading and reloading for a soil which is initially in a normally consolidated stress state on the isotropic virgin consolidation line (I-VCL) at A. For unloading from A to B, it is assumed that the behaviour does not involve plastic strains as the stress point retreats from the Virgin Consolidation Line. For reloading, the stress state approaches the VCL and plastic strains occur. At B, an image stress B' can be defined on the VCL at the same void ratio such that the incremental plastic strains at B are related to the plastic strains at B' by a measure of the distance between B and B'. Based on this simple model, the bounding surface formulation may be generalized as shown in figure 2. For a stress state, P, lying within the bounding surface, a radial mapping rule is used to define the image point I ($\underset{\sim}{\sigma}'_I$). Implicitly,

this defines a load surface, f_0 passing through P, homothetic to the bounding surface f, with size ratio, α'_0/α'. The occurrence of plastic strains at P is contingent on the loading condition defined as:

$$K Q_I \dot{\varepsilon} + 2G \left(\underset{\sim}{Q'_I} : \underset{\sim}{\dot{e}} \right) \begin{cases} \geq 0 & \text{loading} \\ < 0 & \text{unloading} \end{cases} \qquad (29)$$

where, Q_I and $\underset{\sim}{Q'_I}$ are the volumetric and deviatoric components of the gradient of the bounding surface at the image point, I.

Hardening of the bounding surface for loading at stress state P is assumed to occur as if the stress state were located at its image point. This generalizes the hydrostatic case described above and dictates that the behaviour at the 'normally consolidated' image stress (equivalent pressure) acts as a limit for the behaviour of the overconsolidated clay.

For stress states within the bounding surface, plastic strains are defined by specifying the elasto-plastic modulus, H, and flow direction, $\underset{\sim}{P}$, for loading at the current stress state. In the bounding surface formulation, functions are developed to relate H and $\underset{\sim}{P}$ to the corresponding values at the current image point, H_I and $\underset{\sim}{P_I}$. The MIT-E3 model introduces separate mapping rules for the elasto-plastic modulus and the flow direction which can be expressed in general form:

$$\underset{\sim}{P} = \underset{\sim}{P_I} + \underset{\sim}{P_0}\, g_1 \qquad (30)$$

$$H = H_I + H_0\, g_2 \qquad (31)$$

where $\underset{\sim}{P_0}$, H_0 are the values of $\underset{\sim}{P}$ and H at first yield (i.e. at first loading for stress states within the bounding surface); and g_1, g_2 are mapping functions described by the relative position of the current stress and image stress states.

The selection of suitable expressions for H_0, $\underset{\sim}{P_0}$, g_1 and g_2 is a difficult process, especially in view of the joint effects of the two mapping functions. However, this task can be achieved by observing clay behaviour in a) hydrostatic unloading and reloading, and b) undrained triaxial shearing of overconsolidated clays.

The undrained shear behaviour is particularly relevant as the development of shear induced pore pressures within the bounding surface is described solely by the bounding surface plasticity. In general, positive shear induced pore pressures are generated during undrained shearing of hydrostatically consolidated clays at small OCR's. Negative shear induced pore pressures (tendency to dilate during shearing)

are found for more highly overconsolidated clays and for clays with low OCR's after K_0-consolidation histories. Within the context of an incremental elasto-plastic model, these results are controlled by the sign of the volumetric component of the flow direction, P.

After a number of iterations, a consistent set of equations is proposed for equations 30, 31:

$$P_0 = - \left\{ 2c^2 \alpha' r_c + \left(\underset{\sim}{\eta}_I : \underset{\sim}{Q'}_I \right) \right\} \tag{32a}$$

$$\underset{\sim}{P'}_0 = \underset{\sim}{0} \tag{32b}$$

$$g_1 = \{ (\alpha' - \alpha'_0) / (\alpha' - \alpha'_{0i}) \}^{\gamma} \tag{33}$$

$$H_0 = \frac{1}{\kappa_0} (1 + e) \{ (\alpha' - \alpha'_0) h | Q_I | | P_I | \} \tag{34}$$

$$g_2 = \{ (\alpha' - \alpha'_0) / (\alpha'_0 - \alpha'_{0i}) \} \tag{35}$$

In these equations; h, γ are dimensionless material constants which are established from parametric studies; α'_{0i} is the size of the load surface at first yield.

Equations 32, 33, 34 and 35 incorporate many observations of soil behaviour, including:

1. At first yielding, $\alpha'_0 = \alpha'_{0i}$ and $H \rightarrow \infty$ so that there is a smooth matching of the perfectly hysteretic and bounding surface models.
2. As the stress state approaches the bounding surface, ($\alpha'_0 \rightarrow \alpha'$), both H and $\underset{\sim}{P}$ tend to the value at the image point. This describes a smooth transition in behaviour to the normally consolidated state.
3. The mapping rule for the volumetric component of the flow direction, P, is established from observations of the effective stress paths of overconsolidated clays in undrained shearing.

EVALUATION OF MODEL INPUT PARAMETERS

MIT-E3 is a synthesis of three components each of which contributes material constants and state variables in the overall formulation as shown in Table 1. The model is structured such that the components are nested together and individual parts of the formulation can be added individually to assess their importance for the study of a particular problem. Thus the effects of properties such as anisotropic failure criterion, anisotropic hardening, strain softening, small strain

non-linearity and bounding surface plasticity can be considered separately within the model formulation.

The most general form of the MIT-E3 model uses 15 input parameters which are evaluated, for a given clay, using a strict hierarchy in which some of the constants are determined from predefined parametric studies. The parameters which can be directly measured from standard laboratory tests can be summarized as follows:

1. K_{0NC}, the coefficient of lateral earth pressure at rest for normally consolidated clay can either be estimated from empirical formulae (e.g. Mayne & Kulhawy, 1982) or measured during K_0-consolidation in either a triaxial test (with no lateral straining) or an oedometer with lateral stress measurement.
2. λ, e_0 describe the slope and location of the virgin consolidation line in an e-$\log_e\sigma'$ space, and can also be determined directly from an oedometer test (plotted in e-$\log_{10}\sigma'_v$ space). The reference void ratio, e_0, is defined as the void ratio at unit stress level on the VCL.
3. 2G/K is the ratio of the tangential elastic shear modulus to the bulk modulus, which is related to the Poisson's ratio, v, of the soil skeleton:

$$\frac{2G}{K} = \frac{3\,(1-2v)}{(1+v)} \qquad (36)$$

For one-dimensional (K_0) swelling, it is assumed that the effective stress path is initially linear (i.e. assuming there are no plastic strains). If the OCR at $K_0=1$ is known (OCR_1), then (2G/K) can be determined from the expression:

$$\frac{2G}{K} = \frac{(1 - K_{0NC})\,OCR_1}{1/3\,(1 + 2\,K_{0NC})\,OCR_1 - 1} \qquad (37)$$

4. κ_0 determines the elastic bulk modulus at small strain levels (i.e., those which occur immediately following a stress reversal). In concept, κ_0 can be estimated from the modulus measured immediately after reversal of loading in an oedometer or triaxial test. However, practical difficulties, due to inaccuracy of small strain measurements and secondary compression of clays, invalidate this approach. Instead, it is recommended that κ_0 be estimated from the results of either resonant column tests or from measurements of the in-situ elastic shear wave velocity using techniques such as crosshole or downhole techniques.
5. ϕ'_{TC} and ϕ'_{TE} are friction angles at the critical state condition measured in K_0-consolidated triaxial compression and extension modes of shearing. Critical state conditions are approached asymptotically at large strain levels and can be

obscured by non-uniformities associated with end effects and/or strain localization of the test specimen (Germaine & Ladd, 1988). For most practical purposes, the friction angles can be estimated at $\varepsilon_a \approx 10\%$ in undrained triaxial shear tests.

The remaining input constants must be determined from parametric studies:

1. C, n are the parameters used to describe the non-linearity in the volumetric response for the perfectly hysteretic formulation. Values of C, n are selected to match the swelling behaviour in an oedometer (or CRS test) as shown in figure 5.
2. ψ_0 is a dimensionless constant which controls the rate of change of anisotropy (i.e. the rate of evolution of anisotropic directions) caused by the imposed strain (or stress) history. The most useful tests with which to evaluate ψ_0 are those in which a controlled rotation of the yield surface is expected. For example, figure 6 illustrates the effect of ψ_0 on predictions of drained strain controlled tests in triaxial space. In the first case, (type A), the sample, initially normally consolidated under hydrostatic stress conditions (i.e. $b_1 = 0$ initially), is subjected to a 1-dimensional strain path by applying increments of vertical strain only (i.e.$\Delta\varepsilon_h$=0). The effective stress paths during this test (fig. 6a) approach the K_{0NC} conditions and there is also a rotation of the yield surface towards this direction (i.e. $b_1 = \sqrt{6}\,(1 - K_{0NC}) / (1 + 2K_{0NC})$, at large strains). An inverse test (type B, fig. 6b), considers the application of hydrostatic strain increments ($\Delta\varepsilon_v = \Delta\varepsilon_h$) to a sample which is initially K_0-normally consolidated. In this case, the model predicts a gradual return of the stress path towards the hydrostatic axis. The results in figure 6 show that the magnitude of ψ_0 affects the development of the effective stress path during these tests as well as the juxtaposition of the consolidation lines for hydrostatic and K_0 conditions. Limited laboratory data (e.g. Gens, 1982) suggest that for soft, low plasticity clays, the memory of a previous consolidation history can be erased by increases in stress level corresponding to 2 to 3 times the consolidation stress. Based on this rough estimate, the results in figure 6 suggest values of ψ_0 between 75 and 200 will provide reasonable predictions of yield surface rotation.
3. S_t and c are established from the undrained shear behaviour of a K_0-normally

consolidated clay, for which data are available for at least two different modes of shearing (for example triaxial compression, CK_0UC, and extension CK_0UE). Figure 7 shows the effects of S_t and c on model simulations of CK_0UC and CK_0UE tests (with a fixed value, c=0.866). It can be seen that increases in the value of S_t lead to significant changes in the strain softening for the triaxial compression mode of shearing but have relatively minor influence on undrained shear strength, pre-peak behaviour or behaviour in triaxial extension. In contrast, c controls the undrained strength for both triaxial compression and extension modes of shearing. For example, the peak strength in compression increases by about 10% as c increases from 0.75 to 1.0, while there is a 50% increase in the extension strength over the same range. Changes in c have a secondary influence on the strain softening.

4. ω controls the non-linear behaviour during undrained shearing at small strain levels and/or when the stress state is far from the bounding surface. The magnitude of ω is estimated from the undrained shear behaviour of a lightly overconsolidated clay (OCR=1.5-2.0). Model calculations of the variation of secant shear modulus with strain level are first developed for different values of ω, assuming that there are no plastic strains at small strain levels (figure 8). Values of ω are estimated by comparison with measured data in the small strain range ε_a=0.001-0.05% at which plastic strains are negligible.
5. h and γ are used to specify the mapping laws for the bounding surface plasticity. The parameter h controls the amount of residual plastic strain Δ^p (fig. 1b) observed in hydrostatic unload-reload cycles. Figure 9a shows typical model predictions of the unload-reload behaviour for three different values of h for an unload cycle of one magnitude (OCR_m =3.3). It can be seen that as h decreases, there is a marked increase in the residual plastic strains. Figure 9b shows predictions of residual strains, Δ^p, as a function of the total amount of unloading (OCR_m) for h=1. The value of h can be selected for a given clay, by comparing the calculated values of Δ^p with measured data from CRS (or oedometer) test for at least two different magnitudes of unload-reload cycle (OCR_m).
6. The parameter γ controls the development of shear induced pore pressures during undrained shearing of overconsolidated clays. Figure 10 shows predictions of

shear induced pore pressures for an undrained triaxial compression test of a sample at small OCR. Figure 10 shows that γ controls the magnitude of the maximum shear induced pore pressure (Δu_{max}) and the pore pressures at large strain levels (Δu_{cs}). The change in sign of the shear induced pore pressure is typical of lightly overconsolidated clays. The value of γ is then obtained by parametric study using data from a CK_0UC test at OCR=1.5 to 2.

In order to make predictions using the MIT-E3 model, initial values of the state variables must also be specified. These include:

1. The initial effective stress tensor, $\underset{\sim}{\sigma}'$ and void ratio, e.
2. The size and orientation of the bounding surface, α' and $\underset{\sim}{b}$
3. The effective stresses at the stress reversal point (SRP), $\underset{\sim}{\sigma}'_{rev}$.
4. The strains developed since the last stress reversal state, $^{\Delta 1}\underset{\sim}{\varepsilon}$.
5. The size of the load surface at first yield, α'_{0i}.

For a virgin normally consolidated clay, the stress state is assumed to be located at the tip of the yield surface (eqn. 10), hence initial values of α' and $\underset{\sim}{b}$ are obtained directly. No previous stress reversal has occurred (so that the current stress state is the stress reversal state).

However, for overconsolidated clays, the additional state variables play an important role in the MIT-E3 model. For example, figure 11 considers two samples which are subjected to different hydrostatic stress histories, resulting in the same overconsolidated stress state, D. Sample 1 is normally consolidated to stress B, swelled to C and reloaded to D; while sample 2 is loaded to A and then swelled directly to the stress state D. There is a small difference in the OCR at D for the two samples (but having the same void ratio). For sample 1, the most recent stress reversal point is C, the accumulated volumetric strains are $^{D}\varepsilon$-$^{C}\varepsilon$ and the first yielding occurs at state C (i.e $\alpha'_{0i}=0.5\sigma'_{C}$). For sample 2, the stress reversal point is A, and the soil has state variables listed in figure 11. The differences in the most recent load history experienced by the soil elements lead to significant differences in behaviour especially in the stiffness at small strain levels. These differences are predicted by the MIT-E3 model as a result of the differences in the state variables at D.

Figure 11 indicates that the state of an overconsolidated clay can only be

determined if the recent loading history is known. For predicting simple laboratory tests using SHANSEP consolidation procedures, (Ladd & Foott, 1974) the load history can be established by simulation of the soil behaviour from a virgin normally consolidated stress state. However, for more general classes of boundary value problems, the recent load history of an overconsolidated clay may be difficult to estimate reliably. In these situations, analyses using MIT-E3 should initially be performed assuming that the current stress state is also a stress reversal state.

Conclusions

This paper has presented the formulation of a new effective stress soil model, MIT-E3, for describing the behaviour of overconsolidated clays which obey normalized behaviour and are rate independent. The model incorporates observations of overconsolidated clay behaviour including; a) small strain non-linearity, b) hysteretic stress-strain response, c) coupling of volumetric and shear deformations, and d) transitional yielding as the normally consolidated stress state is approached. For normally consolidated clays, the model describes anisotropic stress-strain-strength for K_0-consolidated clays, as well as strain softening which occurs in certain modes of deformation.

The formulation of MIT-E3 is based on the theory of incrementally linearized elasto-plasticity and consists of three distinct components: a) a plasticity model for normally consolidated clays (MIT-E1); b) a perfectly hysteretic formulation and c) bounding surface plasticity.

The model, in its most general form, uses 15 input parameters to characterize a given clay. These parameters are either directly measured in standard types of laboratory tests, or are obtained from well defined parametric studies which identify clear roles for each of the input parameters. A complete evaluation of input parameters and evaluation of model predictions is described in the following section.

REFERENCES

Anandarajah, A.M. & Dafalias, Y. F. (1986) Bounding Surface Plasticity III: Application to Anisotropic Cohesive Soils, *J. Engrg Mechs Div. Am. Soc. Civ. Engrs.*, Vol. 112, No. EM12, pp. 1292-1318.

Azzouz, A.S., Malek, A.M. & Baligh, M.M. (1989) Cyclic Behaviour of Clays in Undrained Simple Shear, *J. Geotech Engrg Div. Am. Soc. Civ. Engrs.*, Vol. 115, No. GT5, pp. 637-657.

Dafalias, Y.F. & Popov, E.P. (1977) Cyclic Loading for Materials with a Vanishing Elastic Region, *Nuclear Engineering and Design*, Vol. 41, No. 2, pp. 293-302.

Dafalias, Y. & Herrmann, G.R. (1982) Bounding Surface Formulation of Soil Plasticity,Chapter 10 in *Soil Mechanics, Transient and Cyclic Loads*, eds. G.N. Pande & O.C. Zienkiewicz, Wiley and Sons.

Drucker, D.C., Gibson, R.E. & Henkel, D.J. (1957) Soil Mechanics and Work Hardening Theories of Plasticity, *Transactions Am Soc Civ. Engrs*, Vol. 122, pp. 338-346.

Gens, A. (1982) *Stress-Strain and Strength of a Low Plasticity Clay*, PhD Thesis, Imperial College, London University.

Germaine, J.T. & Ladd, C.C. (1988) Triaxial Testing of Saturated Cohesive Soils-State-of-the-Art Paper, *Advanced Triaxial Testing of Soil and Rock*, eds. R.T. Donaghe, R.C. Chaney & M.L. Silver, Am. Soc. Test. & Matls., STP 977, pp. 421-460.

Graham, J. and Houlsby, G.T. (1983) Anisotropic Elasticity of a Natural Clay, *Géotechnique*, Vol. 33, No. 2, pp. 165-180.

Gudehus, G. (1976) On Constitutive Laws for Soils and Rocks, *Proc., Ist International Conference on Numerical Methods in Geomechanics*, Blacksburg, VA., Vol. 3, pp. 1306-1319.

Hardin, B.O. & Black, W.L. (1969) Vibration Modulus of Normally Consolidated Clay, *J. Soil Mech. Fdns Div. Am. Soc. Civ. Engrs*, Vol. 94, No.SM2, pp. 353-368.

Hardin, B.O. & Drnevich, V.P. (1972) Shear Modulus and Damping in Soils: Design Equations and Curves, *J. Soil Mech. Fdns Div. Am. Soc. Civ. Engrs*, Vol. 98, SM6, pp. 667-692.

Hashiguchi, K. (1977) An Expression of Anisotropy in a Plastic Constitutive Equation of Soils, (Discussion to H. Sekiguchi & H. Ohta's Paper) *Proc., 9th Int. Conf. Soil Mech. Fdn. Engrg.*, Tokyo, pp. 302-305.

Hashiguchi, K. (1980) Constitutive Equations of Elasto-Plastic Materials with Anisotropic Hardening and Elastic-Plastic Transition, *Journal of Applied Mechanics*, Vol. 48, pp. 297-301.

Hashiguchi, K. (1985) Constitutive Laws for Soils: II Macrometric Approaches-Static Intrinsically Time Independent, *Proc., XIth Int. Conf. Soil Mech. Fdn. Engrg.*, San Fransisco, pp. 25-65.

Hight, D.W. , Gens, A. & Jardine, R.J. (1983) Evaluation of Geotechnical Parameters from Triaxial Tests on Offshore Clay, *Proc. Soc. for Underwater Tech. Conf. on Offshore Site Investigation*, London, pp. 253-268.

Hueckel, T. (1976) Coupling of Elastic and Plastic Deformations in Bulk Solids, *Meccanica*, Vol. 4, pp. 227-235.

Hueckel T. & Nova, R. (1979) Some Hysteresis Effects of the Behaviour of Geological Media, *Int. J. of Soilds and Structures*, Vol. 15, pp. 625-642.

Jardine, R.J., Symes, M.J.P.R. & Burland, J.B. (1984) The Measurement of Soil Stiffness in the Triaxial Apparatus, *Géotechnique*, Vol. 34, No. 3, pp. 323-340.

Jardine, R.J., Potts, D.M., Fourie, A.B. & Burland, J.B. (1986) Studies of the Influence of Non-Linear Stress-Strain Characteristics in Soil-Structure Interaction, *Géotechnique*, Vol. 36, No. 3, pp. 377-397.

Kavvadas, M. (1982), *Non-Linear Consolidation Around Driven Piles in Clays*, ScD Thesis, MIT, Cambridge, MA.

Kavvadas, M.J. (1983) A Constitutive Model for Clays Based on Non-Associated Anisotropic Elasto-Plasticity, *Proc., Int. Conf. on Mechs. of Engng. Matls.*, Tucson, AZ. pp. 263-270.

Ladd, C.C. & Foott, R. (1974) New Design Procedure for Stability of Soft Clays, *J. Geotech Engrg Div. Am. Soc. Civ. Engrs.*, Vol. 100, No. GT7, pp. 763-786.

Leroueil, S. & Vaughn, P.R. (1989) *The Important and Conguent Effects of Structure in Natural Soils and Weak Rocks*, Université Laval Research Report GCT-89-18.

Mayne, P.W. & Kulhawy, F.T. (1982) K_0-OCR Relationship in Soil, *J. Geotech Engrg Div. Am. Soc. Civ. Engrs.*, Vol. 108, No. GT6, pp. 851-872.

Mróz, Z. (1967) On the Description of Anisotropic Work Hardening, *J. Mechs. Physics and Solids*, Vol. 15, pp. 163-175.

Mróz, Z., Norris, V.A. & Zienkiewicz, O.C. (1978) An Anisotropic Hardening Model for Soils and its Application to Cyclic Loading, *Int. J. for Numer. Analyt. Meth. Geomech.*, Vol. 2, pp. 203-221.

Mróz, Z., Norris, V.A. & Zienkiewicz, O.C. (1981) An Anisotropic, Critical State Model for Soils subject to Cyclic Loading, *Géotechnique*, Vol. 31, No. 4, pp. 451-469.

Prager, W. (1956) A New Method for Analysing Stresses and Strains in Work Hardening Plastic Solids, *J. Appl. Mech*, Vol. 23, Series E, pp. 493-496.

Prevost, J.H. (1977) Mathematical Modelling of Monotonic and Cyclic Undrained Clay Behaviour, *Int. J. for Numer. Analyt. Meth. Geomech.*, Vol. 1, pp. 196-216.

Prevost, J.H. (1978) Plasticity Theory for Soil Stress-Strain Behaviour, *J. Engrg Mechs Div. Am. Soc. Civ. Engrs.*, Vol. 104, No. EM5, pp. 1177-1194.

Roscoe, K.H. & Burland, J.B. (1968) On the Generalized Stress-Strain Behavior of 'Wet' Clay, in *Engineering Plasticity*, ed. J. Heyman & F.A.Leckie, Cambridge University Press, pp. 535-609.

Schofield, A.N. & Wroth, C.P. (1968) *Critical State Soil Mechanics*, McGraw-Hill, London, 310p.

Tavenas, F., Des Rosiers, J-P., Leroueil, S., La Rochelle, P. & Roy, M. (1979) The Use of Strain Energy as a Yield and Creep Criterion for Lightly Overconsolidated Clays, *Géotechnique*, Vol. 29, No. 3, pp. 285-303.

Whittle, A.J. (1987) *A Constitutive Model for Overconsolidated Clays with Application to the Cyclic Loading of Friction Piles*, ScD Thesis, MIT, Cambridge, MA., 641p.

Whittle, A.J. (1990a) A Model for Predicting the Behaviour of Overconsolidated Clays: II Evaluation, submitted to *Géotechnique*.

Whittle, A.J. (1990b) Evaluation of a Constitutive Model for describing Clays subject to Cyclic Loading, submitted to *J. Geotech Engrg Div. Am. Soc. Civ. Engrs.*

Whittle, A.J. & Baligh, M.M. (1990) Analysis of Pile Shaft Behaviour in Normally and Lightly Overconsolidated Clays, submitted to *J. Geotech Engrg Div. Am. Soc. Civ. Engrs.*

Appendix A: Transformed Tensorial Measures used in MIT-E3

Effective Stress	Strain	Yield Surface Gradient	Plastic Flow Direction	Anisotropy
$(\sigma', \underset{\sim}{s})$	$(\varepsilon, \underset{\sim}{e})$	$(Q, \underset{\sim}{Q}')$	$(P, \underset{\sim}{P}')$	$(1, \underset{\sim}{b})$
$\sigma' \equiv \frac{1}{3}(\sigma'_{xx}+\sigma'_{yy}+\sigma'_{zz})$	$\varepsilon \equiv \varepsilon_{xx} + \varepsilon_{yy} + \varepsilon_{zz}$	$Q \equiv Q_{xx} + Q_{yy} + Q_{zz}$	$P \equiv P_{xx} + P_{yy} + P_{zz}$	1
$s_1 \equiv \frac{1}{\sqrt{6}}(2\sigma'_{yy}-\sigma'_{xx}-\sigma'_{zz})$	$E_1 \equiv \frac{1}{\sqrt{6}}(2\varepsilon_{yy}-\varepsilon_{xx}-\varepsilon_{zz})$	$Q_1 \equiv \frac{1}{\sqrt{6}}(2Q_{yy}-Q_{xx}-Q_{zz})$	$P_1 \equiv \frac{1}{\sqrt{6}}(2P_{yy}-P_{xx}-P_{zz})$	$b_1 \equiv \frac{1}{\sqrt{6}}(2b_{yy}-b_{xx}-b_{zz})$
$s_2 \equiv \frac{1}{\sqrt{2}}(\sigma'_{zz}-\sigma'_{xx})$	$E_2 \equiv \frac{1}{\sqrt{2}}(\varepsilon_{zz}-\varepsilon_{xx})$	$Q_2 \equiv \frac{1}{\sqrt{2}}(Q_{zz}-Q_{xx})$	$P_2 \equiv \frac{1}{\sqrt{2}}(P_{zz}-P_{xx})$	$b_2 \equiv \frac{1}{\sqrt{2}}(b_{zz}-b_{xx})$
$s_3 \equiv \sqrt{2}\ \sigma'_{xy}$	$E_3 \equiv \sqrt{2}\ \varepsilon_{xy}$	$Q_3 \equiv \sqrt{2}\ Q_{xy}$	$P_3 \equiv \sqrt{2}\ P_{xy}$	$b_3 \equiv \sqrt{2}\ b_{xy}$
$s_4 \equiv \sqrt{2}\ \sigma'_{yz}$	$E_4 \equiv \sqrt{2}\ \varepsilon_{yz}$	$Q_4 \equiv \sqrt{2}\ Q_{yz}$	$P_4 \equiv \sqrt{2}\ P_{yz}$	$b_4 \equiv \sqrt{2}\ b_{yz}$
$s_5 \equiv \sqrt{2}\ \sigma'_{zx}$	$E_5 \equiv \sqrt{2}\ \varepsilon_{zx}$	$Q_5 \equiv \sqrt{2}\ Q_{zx}$	$P_5 \equiv \sqrt{2}\ P_{zx}$	$b_5 \equiv \sqrt{2}\ b_{zx}$

Appendix B: List of Symbols

$\underset{\sim}{b}$	orientation tensor for bounding surface
c	ratio of major/minor semi-axes of bounding surface ellipse
C	material constant, perfectly hysteretic model
e	void ratio
e_0	void ratio at σ'=1 unit, used to define the location of the VCL
$\underset{\sim}{e}$	tensor of deviatoric strains
$f(\underset{\sim}{\sigma}', a', \underset{\sim}{b})$	bounding surface for normally consolidated clay
g_1, g_2	mapping functions for plasticity of overconsolidated clay
G	elastic shear modulus
G_{max}	maximum elastic shear modulus at small strain levels
$h(\underset{\sim}{\sigma}', \underset{\sim}{\xi})$	failure criterion for critical state conditions
h	material constant for bounding surface plasticity
H	elasto-plastic modulus
H_0	elasto-plastic modulus of OC clay at first yield
$\underset{\sim}{I}$	identity tensor
k	magnitude of critical state failure cone
K	elastic bulk modulus
K_{max}	maximum elastic bulk modulus at small strain levels
K_0	lateral earth pressure coefficient for no lateral strain
K_{0NC}	K_0 value for virgin normally consolidated clay
n	material constant for perfectly hysteretic model
OCR	overconsolidation ratio
OCR_1	overconsolidation ratio at K_0=1
OCR_m	maximum OCR experienced during an unload-reload cycle
$\underset{\sim}{P} = \frac{1}{3} P \underset{\sim}{I} + \underset{\sim}{P}'$	direction of plastic strain increments (flow direction tensor)
$\underset{\sim}{P_0}$	direction of plastic flow at first yield for OC clays
$\underset{\sim}{Q} = \frac{1}{3} Q \underset{\sim}{I} + \underset{\sim}{Q}'$	gradient of bounding surface
r_c	scalar distance mapping for flow rule
r_x	scalar distance mapping for hardening rule of bounding surface rotation
S_t	material constant, related to strain softening of NC clay

$\underset{\sim}{s}$	tensor of deviatoric stress
α'	size of bounding surface
α'_0	size of load surface OC clay
α'_{0i}	size of load surface at first yield
γ	material constant for bounding surface mapping of flow direction
Δ^p	residual plastic strain at the end of hydrostatic unload-reload cycle
$\underset{\sim}{\varepsilon} = \frac{1}{3}\varepsilon \underset{\sim}{I} + \underset{\sim}{e}$	infinitesimal strain tensor
$\Delta I_{\underset{\sim}{\varepsilon}}$	accumulated strain since last stress reversal point
ε_a	axial strain
ϕ'_{TC}	friction angle at large strain, triaxial compression test
ϕ'_{TE}	friction angle at large strain, triaxial extension test
$\underset{\sim}{\eta} = \underset{\sim}{s}/\sigma'$	stress ratio tensor
$\underset{\sim}{\eta}_{rev}$	stress ratio tensor at stress reversal point
κ_0	compressibility parameter at load reversal
λ	compressibility of virgin normally consolidated clay
$\dot{\Lambda}$	scalar controlling magnitude of plastic strain increments
ν	Poissons ratio
σ'	mean effective stress
σ'_m	maximum value of mean effective stress
σ'_p	preconsolidation pressure
σ'_v	vertical effective stress
$\underset{\sim}{\sigma'} = \frac{1}{3}\sigma' \underset{\sim}{I} + \underset{\sim}{s}$	effective stress tensor
ξ, ξ_s	scalar distance parameters used in perfectly hysteretic model
ω	material constant, controlling non-linear shear behaviour
χ	strain amplitude parameter
$\underset{\sim}{\xi}$	orientation (anisotropy) tensor for critical state failure criterion
ψ_0	material constant controlling rate of rotation of bounding surface (i.e., evolving anisotropy)
ζ	density hardening variable determined from consistency

List of Tables:

List of Figures

TEST TYPE	OCR	TEST DETAILS AND MEASUREMENTS	Input Parameters	
			Direct	Indirect
Oedometer or CRS	--	- measure void ratio, e_0 - swelling at two stress levels - include 2 unload-reload cycles	e_0, λ	C, n, h
K_0-oedometer or K_0-triaxial	1 - 4	- measure effective stress path during consolidation and swelling	K_{0NC}, 2G/K	
Undrained Shear Tests	1, 2	- 2 tests in different modes (e.g. CK_0UC and CK_0UE) - 1 CK_0UC test at OCR=2	ϕ'_{TC}, ϕ'_{TE}	s_t, c ω, γ
Resonant Column or In-situ cross hole	--	- direct measurement of elastic shear wave velocity	κ_0	
Special Tests	1	- drained strain path tests in triaxial cell		Ψ_0

Table 1. Input Parameters for the MIT-E3 Model

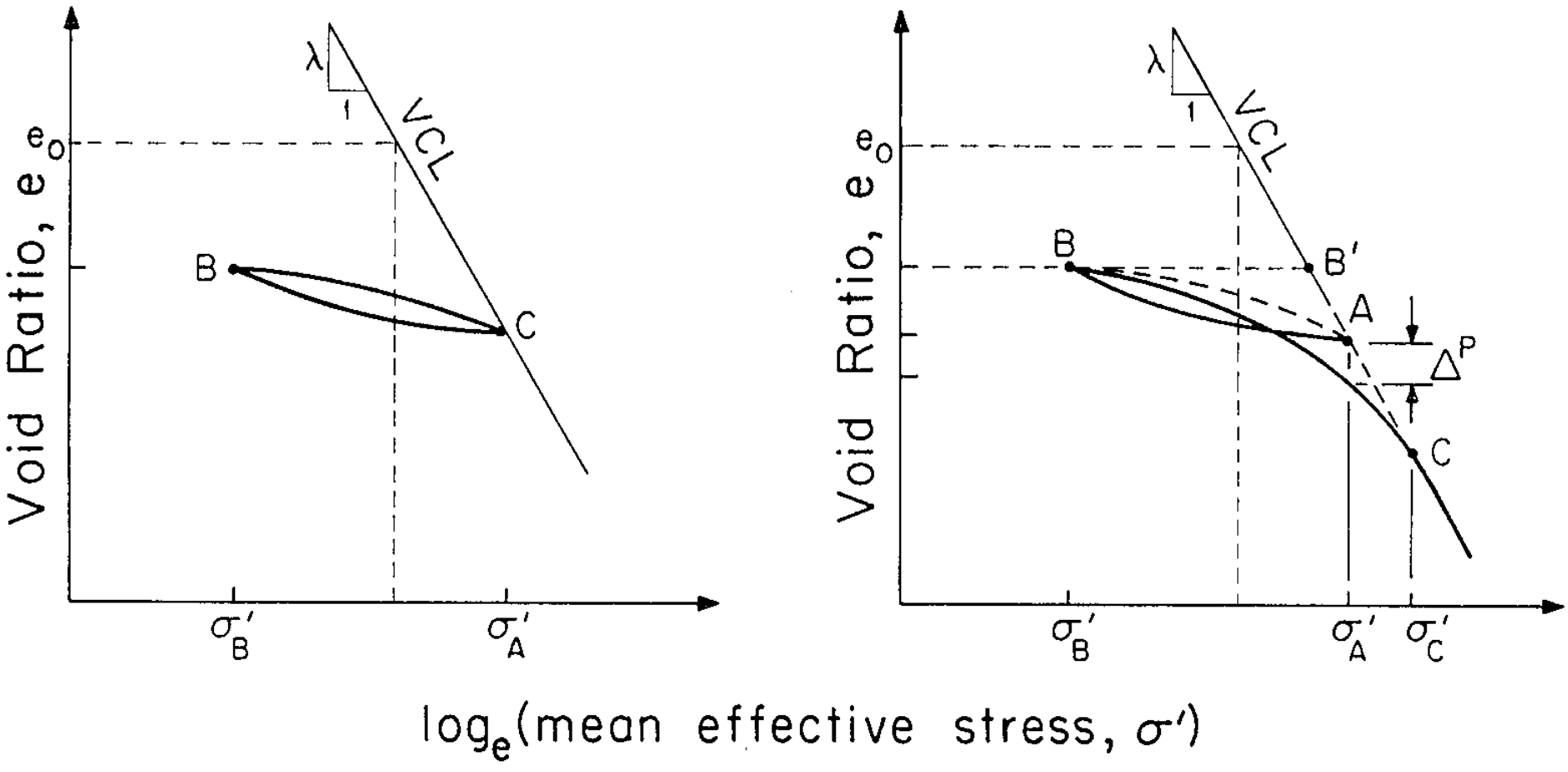

a) 'Perfect Hysteresis'

b) Hysteresis and Bounding Surface Plasticity

1. Conceptual Model of Unload-Reload Used by MIT-E3 for Hydrostatic Compression

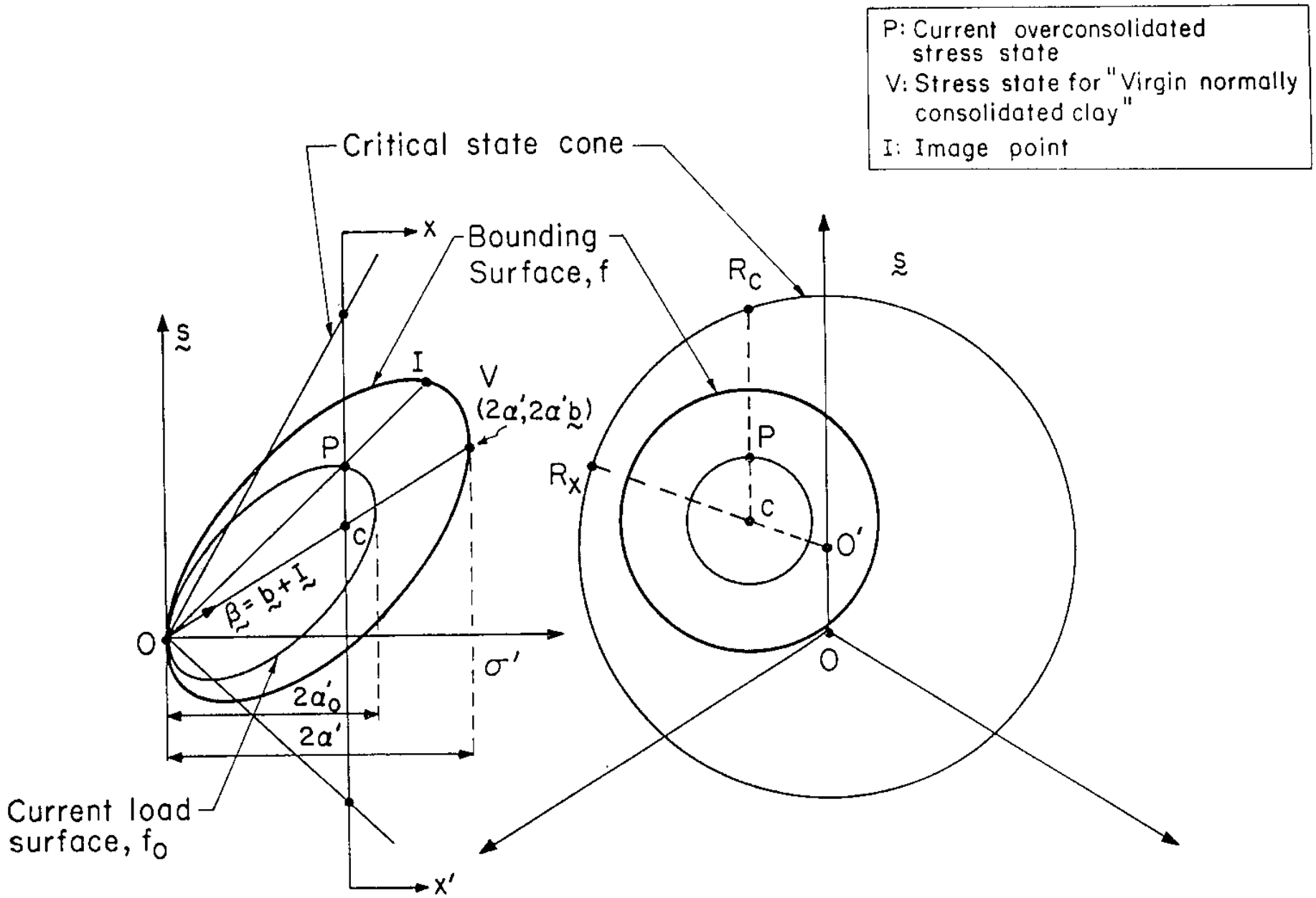

2. Yield and Failure Surfaces for Normally Consolidated Clay

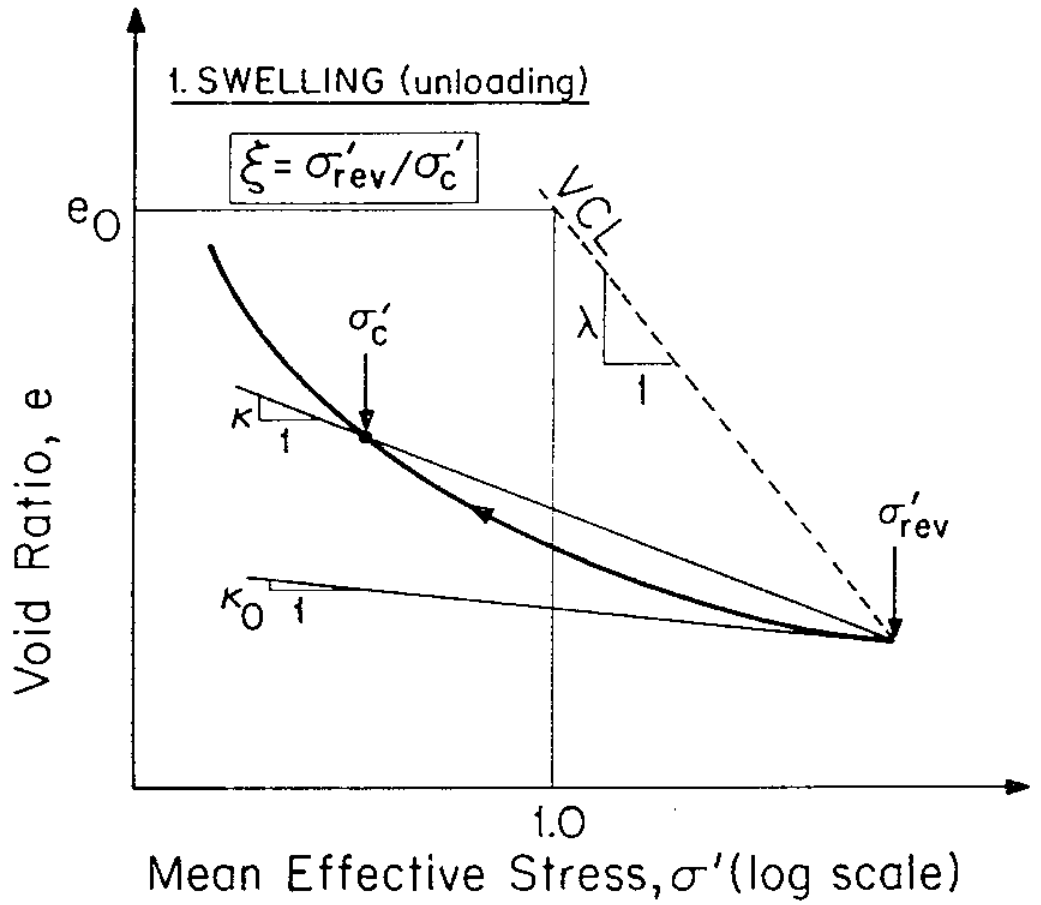

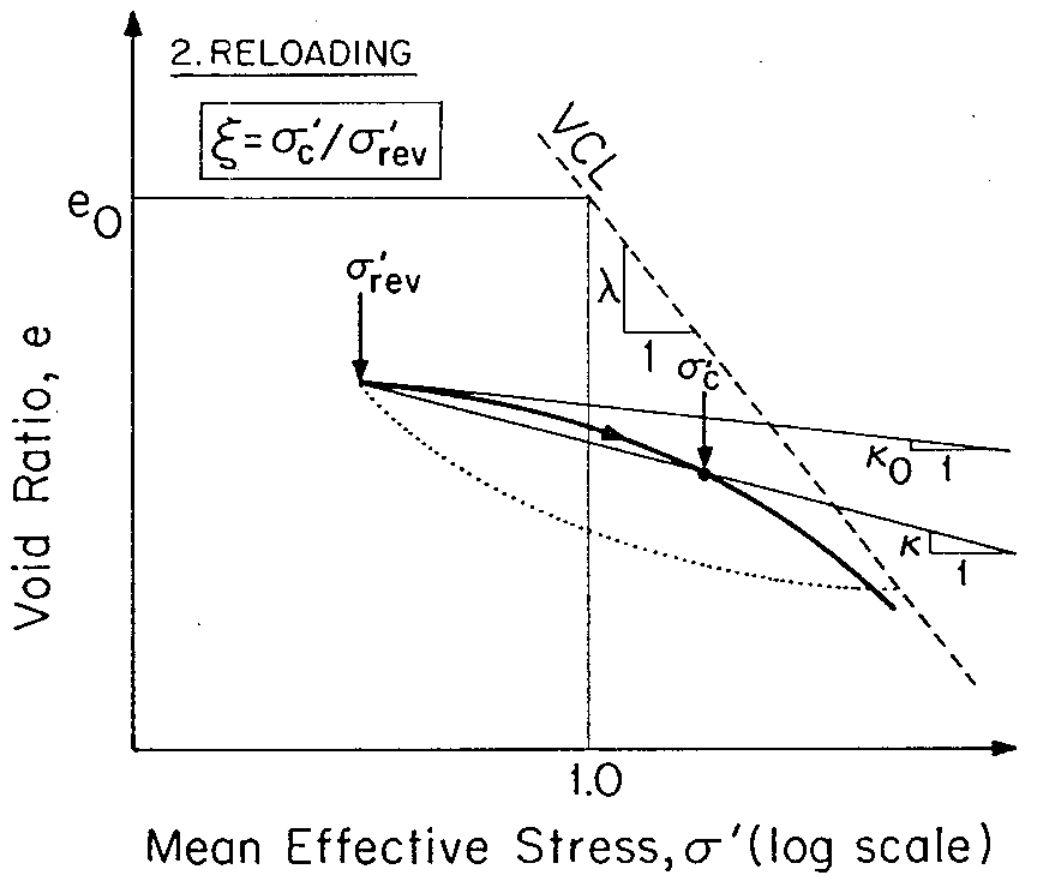

3. Definition of Parameter, ξ

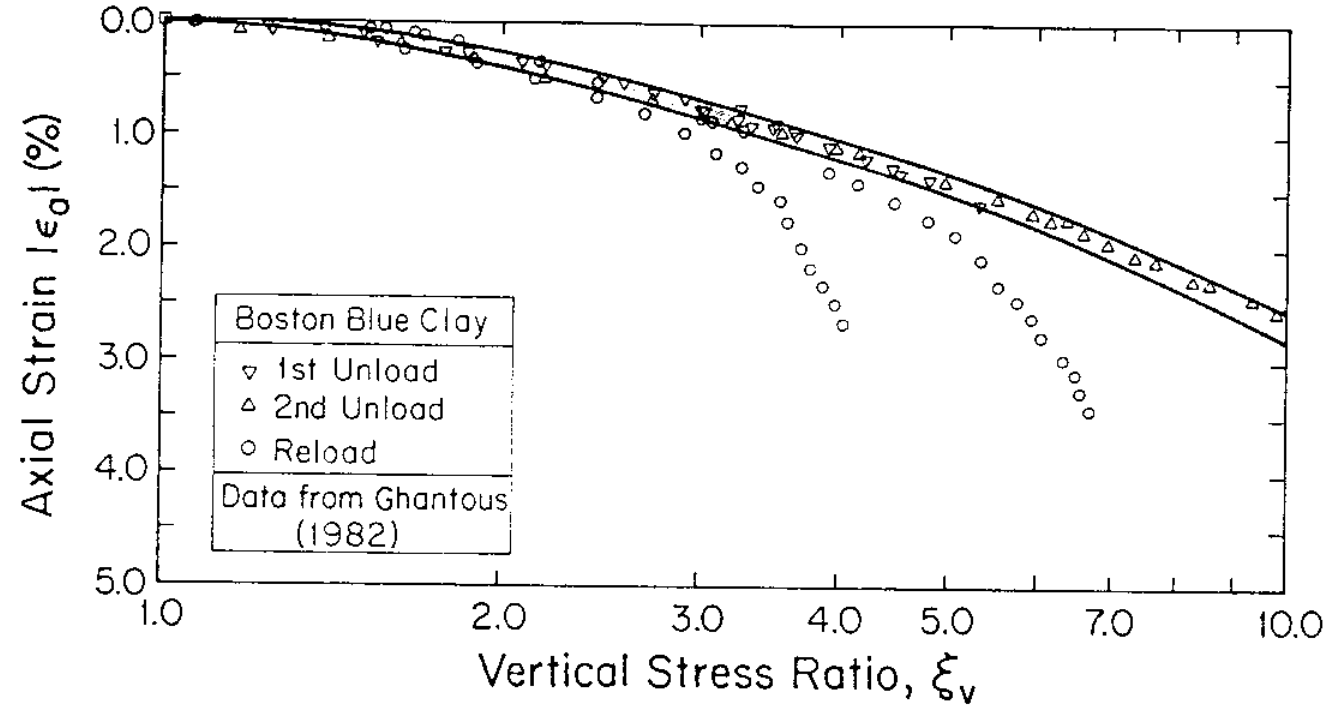

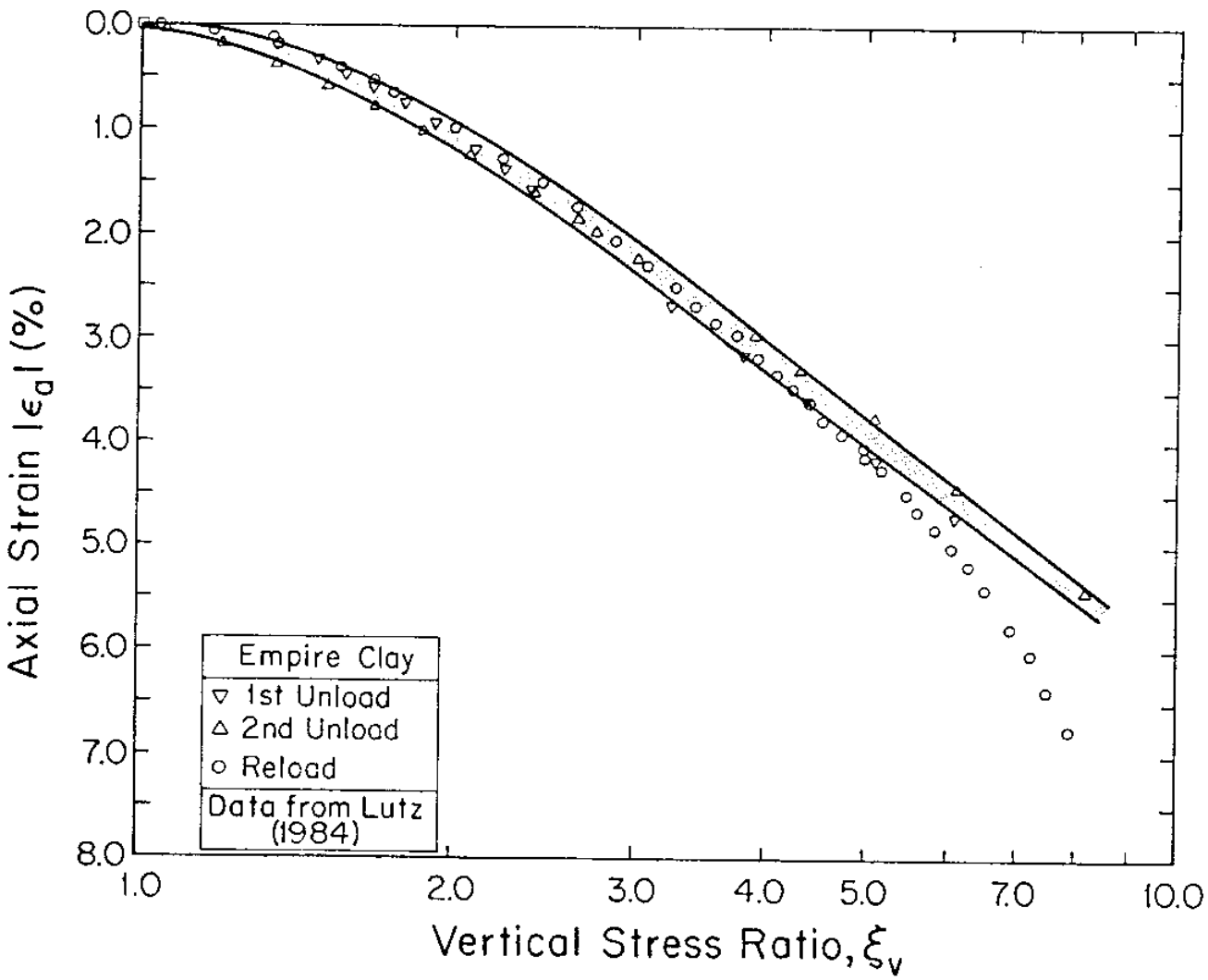

4. Unload-Reload Behaviour of Clay in 1-D Compression a) Boston Blue Clay, b) Empire Clay

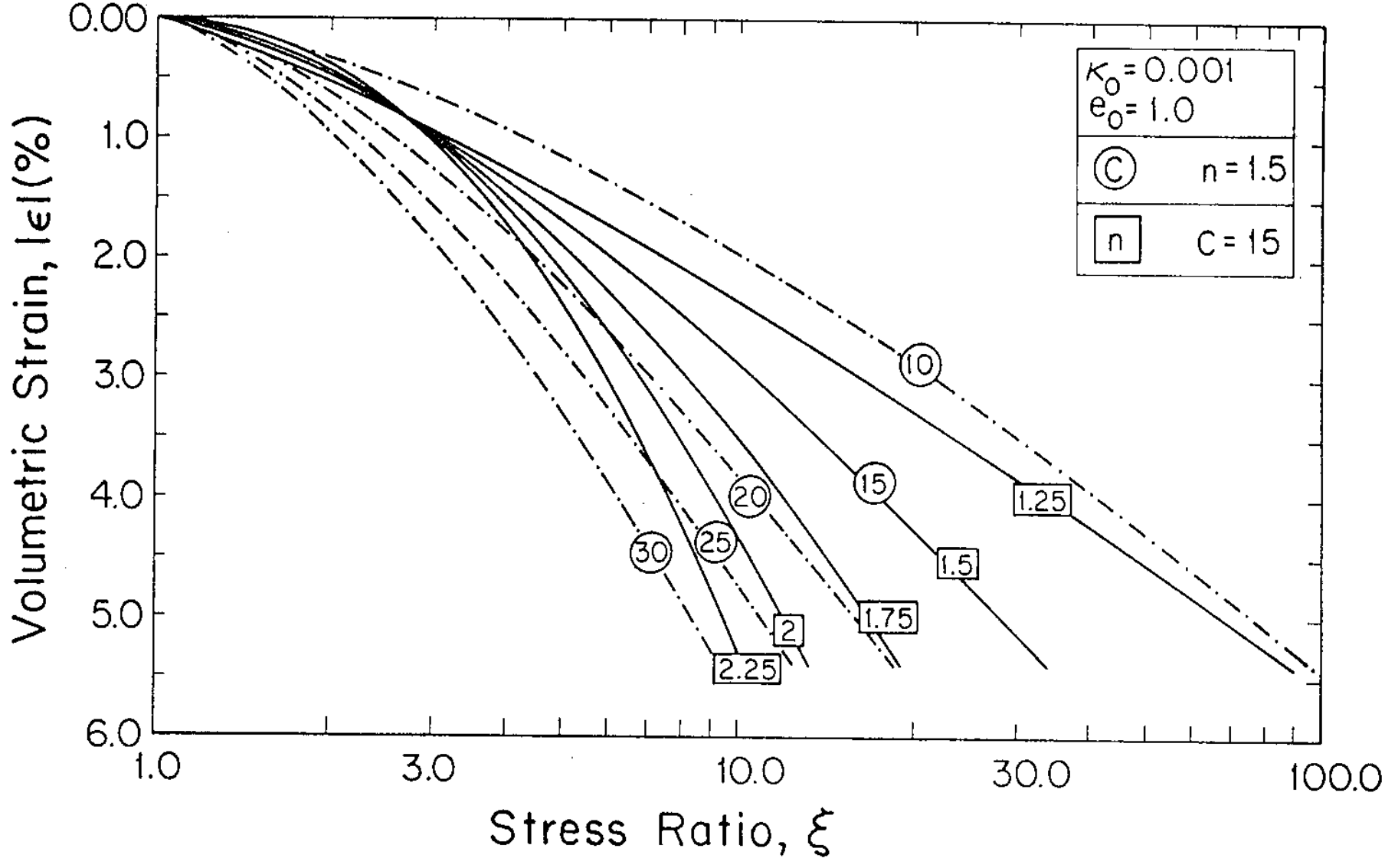

5. Evaluation of Model Parameters C, n

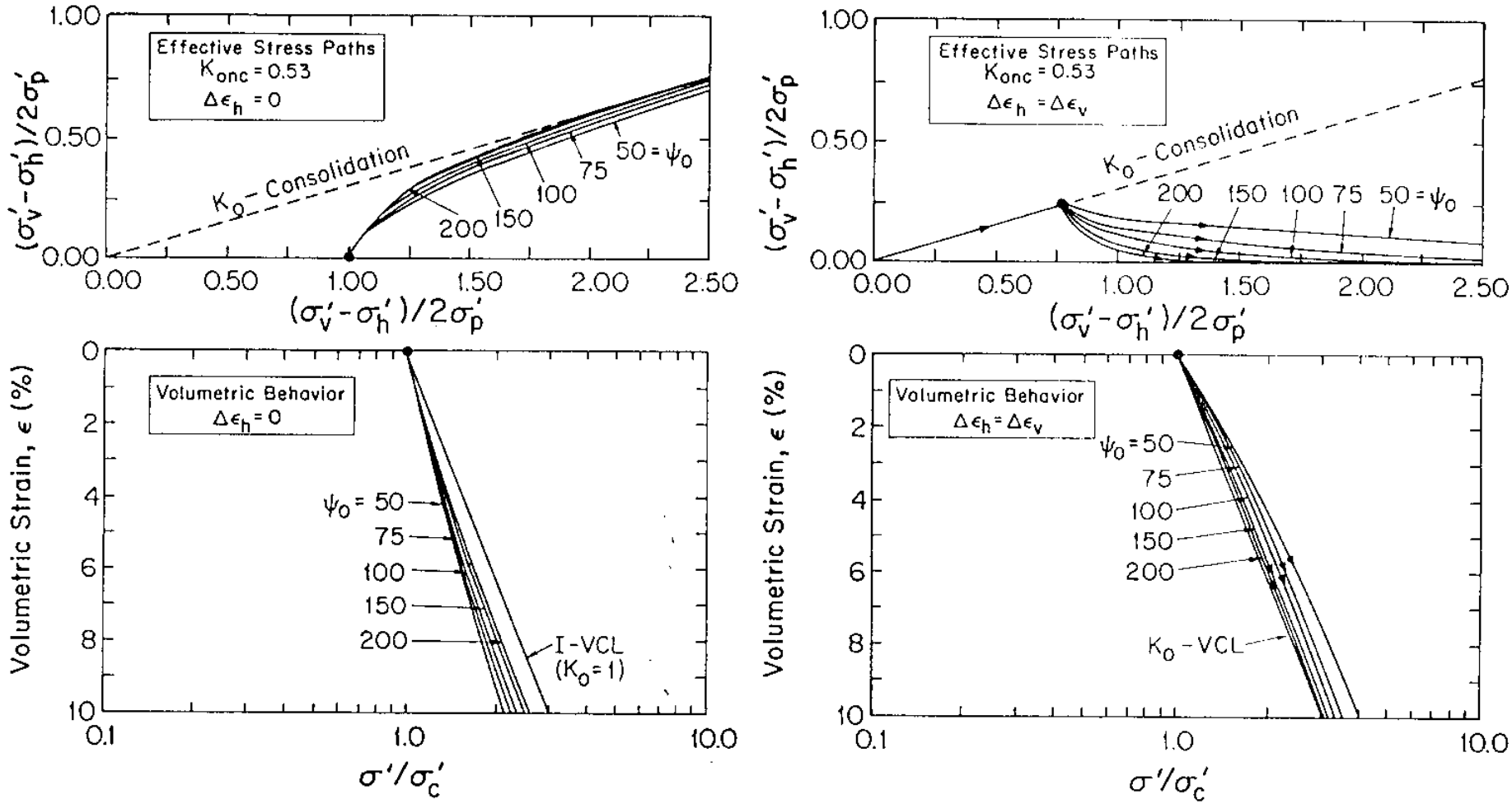

a) Hydrostatic consolidation followed by K_o-straining

b) K_o-consolidation followed by hydrostatic straining

6. The Effects of Parameter ψ_o for Drained Strain Controlled Tests

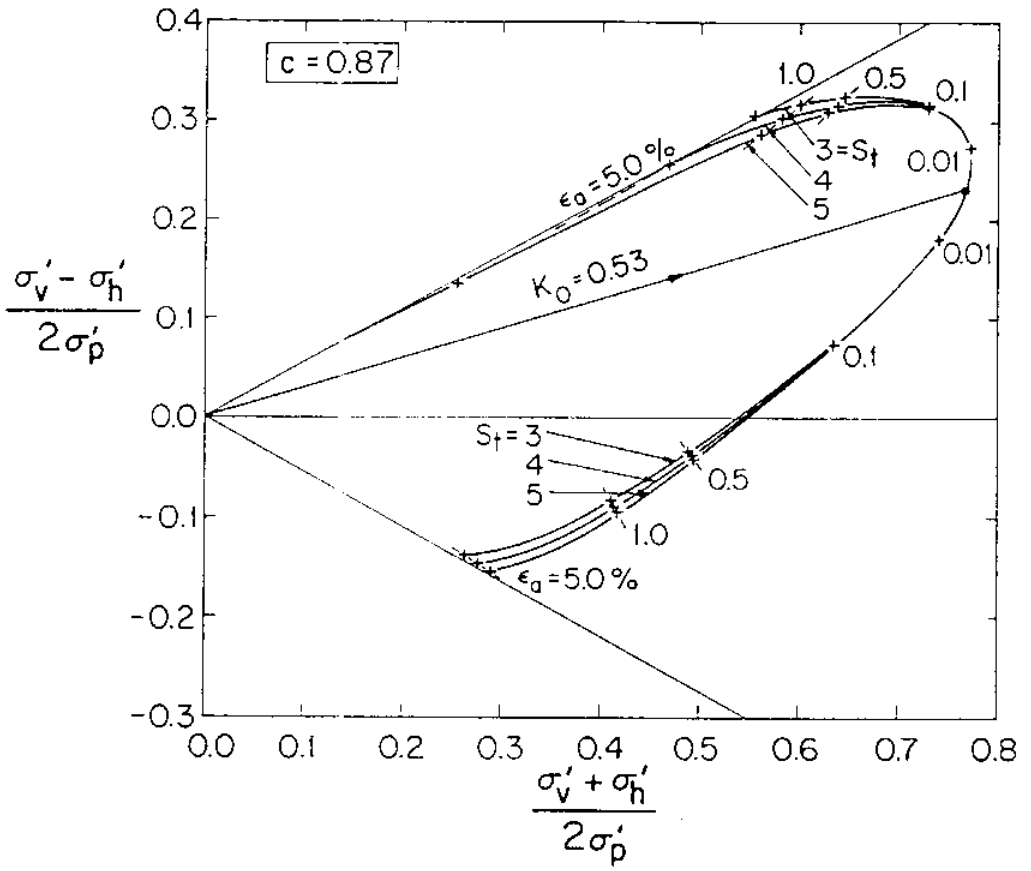

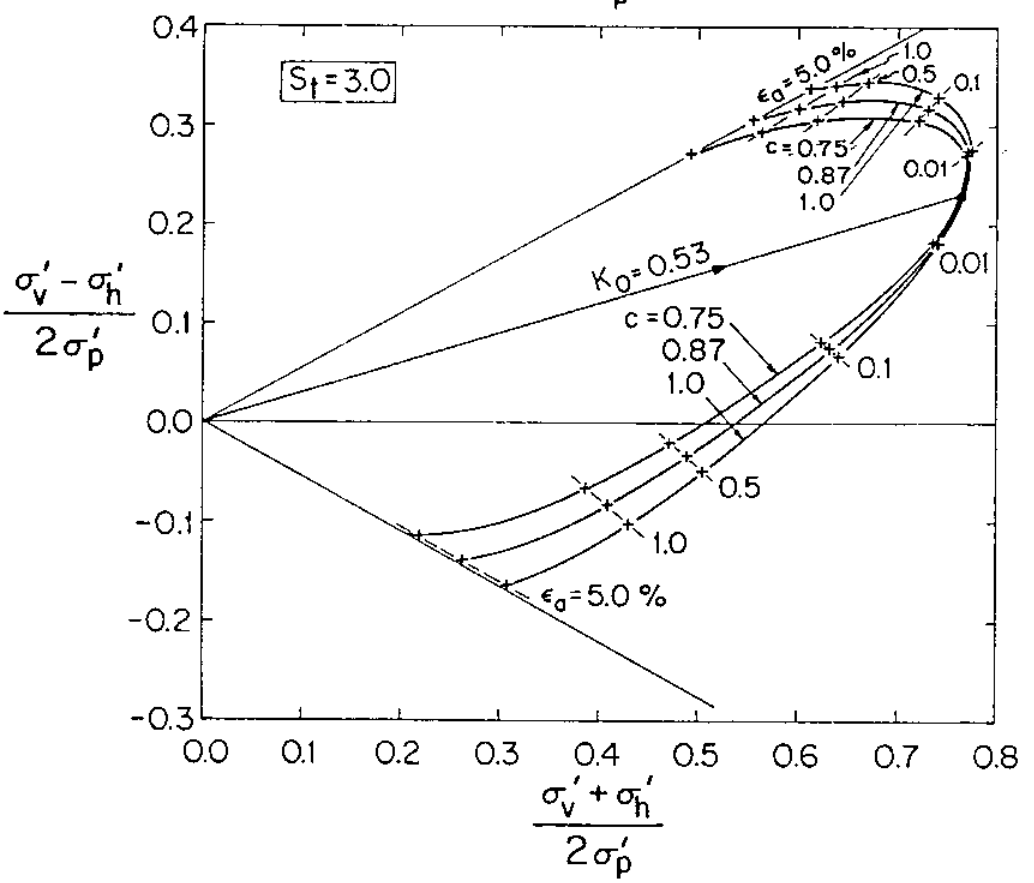

7. Evaluation of Model Parameters S_t and c

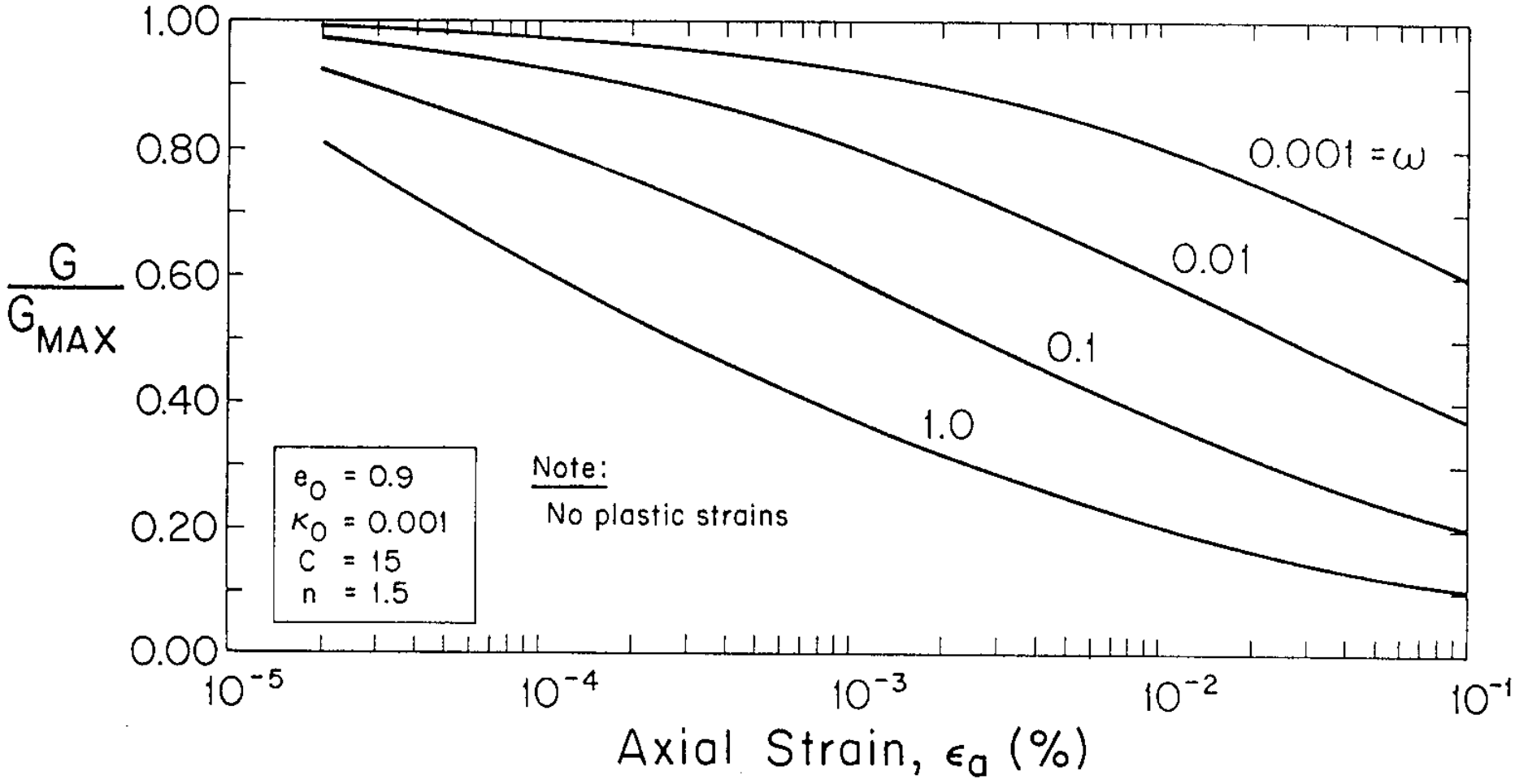

8. Evaluation of ω from CK_0UC Test at OCR=2

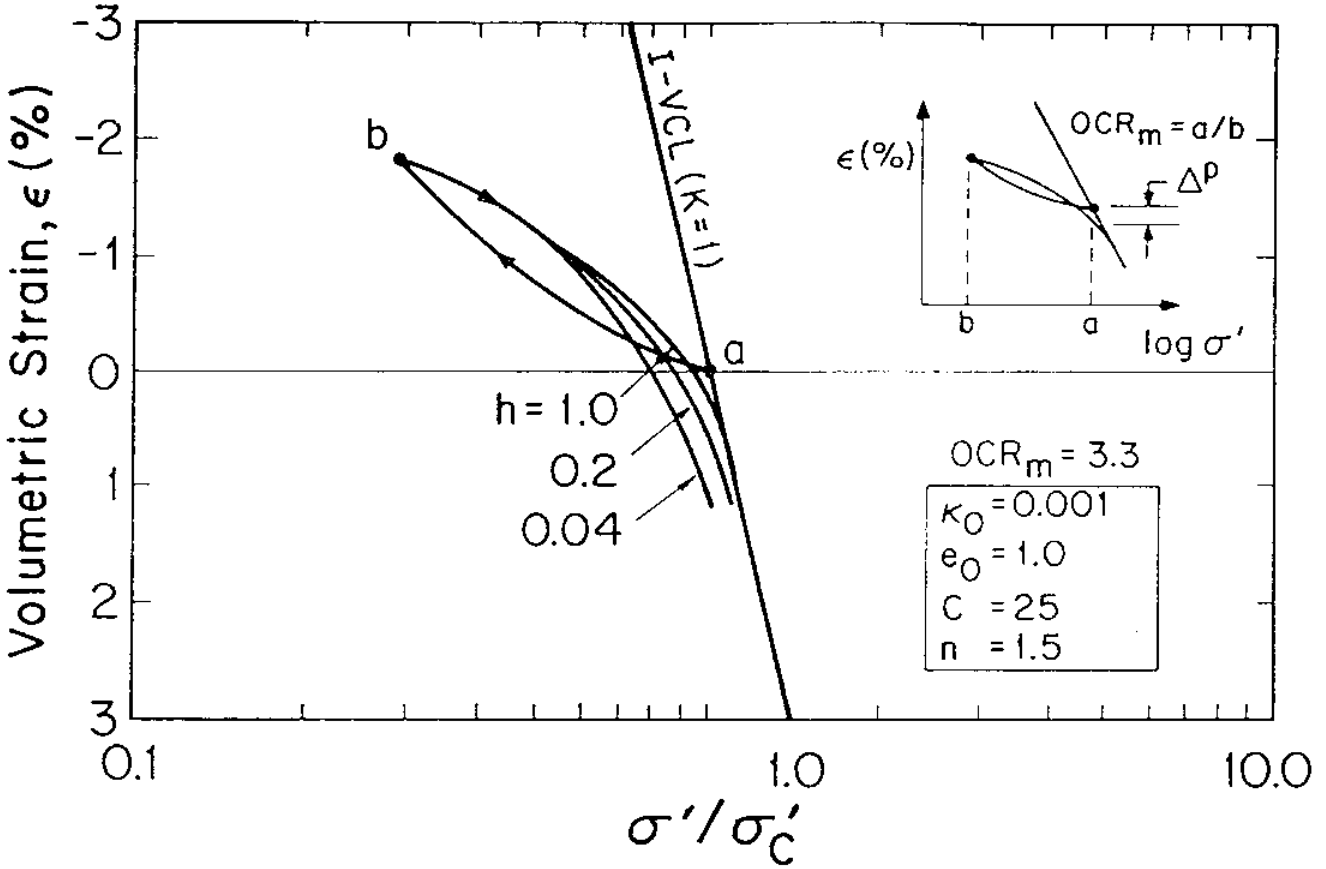

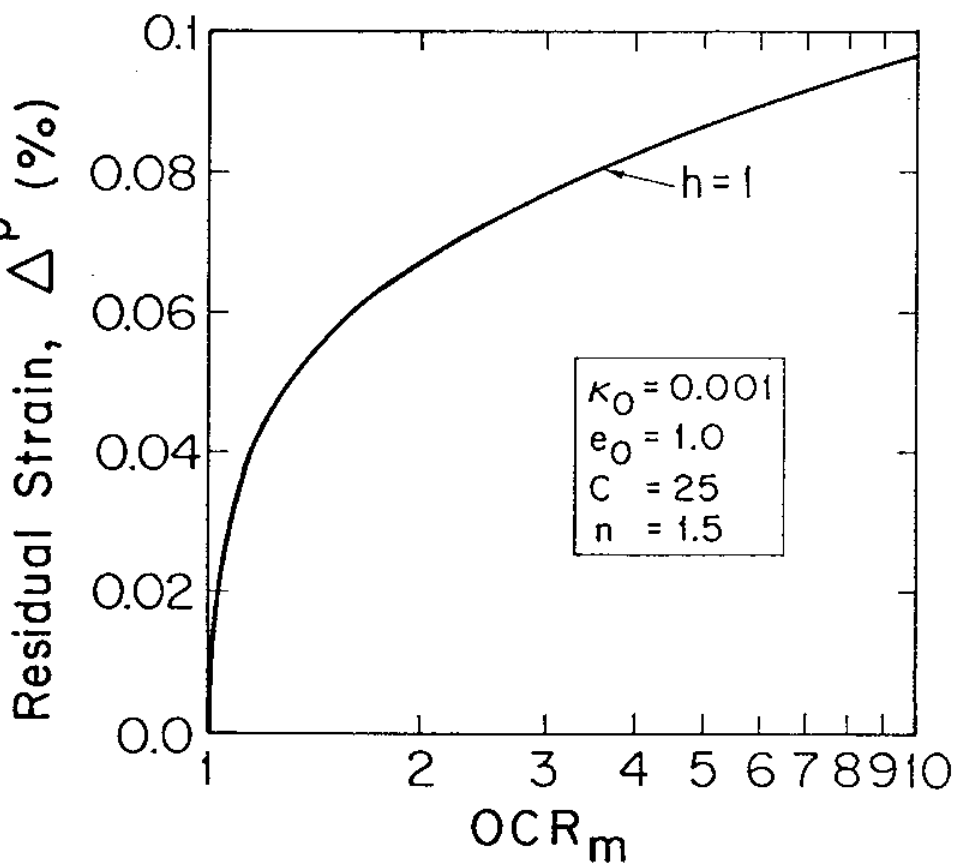

9. Evaluation of h

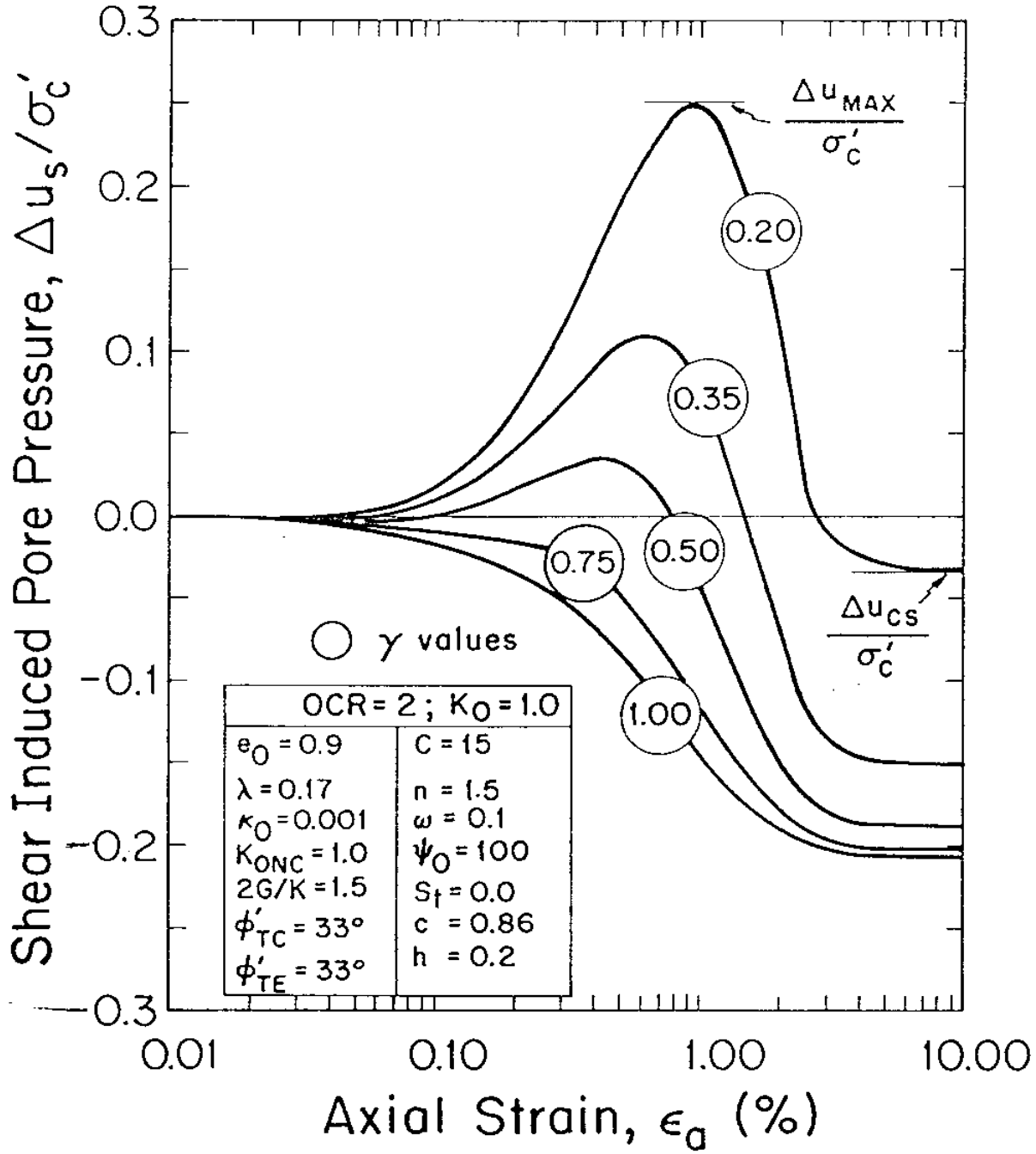

10. Evaluation of γ from CK_0UC Test

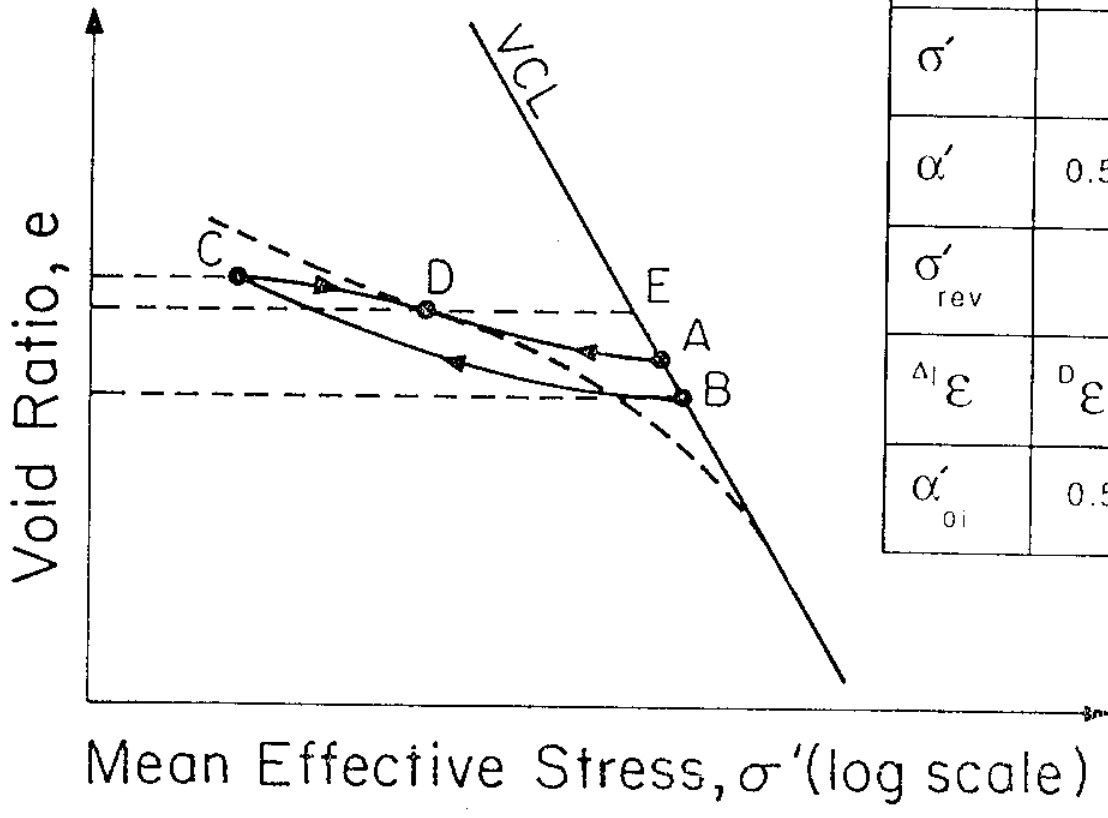

State Variables at D		
Case	B-C-D	A-D
σ'	σ'_D	σ'_D
α'	$0.5\,\sigma'_E$	$0.5\,\sigma'_E$
σ'_{rev}	σ'_C	σ'_D
${}^{\Delta l}\varepsilon$	${}^{D}\varepsilon - {}^{C}\varepsilon$	${}^{D}\varepsilon - {}^{A}\varepsilon$
α'_{0i}	$0.5\,\sigma'_C$	$0.5\,\sigma'_D$

Fig. 11. The Effects of Load History on Initial Values of State Variables

Part 2: Model Evaluation

INTRODUCTION

The formulation of the MIT-E3 model, described in a companion paper (Whittle, 1989a), is based on the theory of rate-independent, incrementally linearized, elasto-plasticity. The model comprises three components; a) an elasto-plastic model for normally consolidated clay including anisotropic and strain softening behaviour, b) equations to describe the small strain nonlinearity and hysteretic response in unloading and reloading, and c) bounding surface plasticity for irrecoverable, anisotropic and path dependent behaviour of overconsolidated clays. Input parameters for the model are obtained either directly from standard (types of) laboratory tests or using pre-defined parametric studies.

In this paper, the predictive capabilities and limitations of MIT-E3 are evaluated using results of laboratory tests. The first step in the evaluation is to select input parameters for a given clay and to assess how these constants are affected by variability in test data, and by different types of clays. Model predictions are then compared with reliable experimental data from undrained shear tests in different modes of shearing (triaxial, plane strain and simple shear) and for overconsolidation ratios, $1 \leq OCR \leq 8$. These data illustrate key features of model's predictive capabilities and limitations. Comparisons of model predictions with experimental data from two unique laboratory devices, the directional shear cell (DSC, Germaine, 1982), and the multi-directional direct simple shear apparatus (MDSS, DeGroot, 1989) are used to demonstrate the importance of anisotropic stress-strain-strength properties due to consolidation stress history. Further evaluations of the proposed model for clay behaviour under cyclic loading are described elsewhere (Whittle, 1990b).

DETERMINATION OF INPUT PARAMETERS

Whittle (1990a) proposes a standard procedure for determining the 15 input material constants used by the MIT-E3 model. The parameters are all estimated from standard types of laboratory test and include 7 constants measured directly in the laboratory tests and 8 'properties' which are established from a pre-defined set of parametric studies. In this section, parameters are selected for Boston Blue Clay (BBC), a low plasticity ($I_p \approx 21\%$), marine clay of moderate sensitivity ($s_t \approx 3$ to

7). This material was deposited after the Pleistocene glaciation (ca. 14,000 years ago) and underlies much of the Boston Basin with thicknesses up to 40 m and in-situ OCR varying from 4 or more in the desiccated crust to nearly 1 at depth (Baligh et al., 1980). The physical and engineering properties of BBC have been extensively studied at MIT in conjunction with a variety of projects including embankment construction on soft foundations (MIT, 1975) and the development of in-situ test devices (Baligh et al., 1981). In addition, fundamental studies of soil behaviour have been conducted using resedimented BBC which is consolidated from a slurry (with I_l>3.5) in a large scale consolidometer (Germaine, 1982). Fayad (1986) summarizes the measured properties of BBC as measured for both natural and resedimented clay. Differences in the average properties of the intact and resedimented clay are not considered in the current discussion. The following tests are used to define input parameters for the model:

1. Constant rate of strain (CRS) consolidation tests on samples of intact clay from the MIT test site (Ghantous, 1982) and oedometer tests on resedimented clay (Fayad, 1986). In these tests, the void ratio is accurately measured and the load sequence includes at least one cycle of unloading and reloading. A total of about 10 tests were used in order to establish reliable average properties.
2. Oedometer test with lateral stress (K_0) measurement (Germaine, 1986) which include variations in K_0 for unloading and reloading.
3. Undrained shear tests on K_0-consolidated (resedimented) clay including: a) one test in triaxial compression (CK_0UC) at OCR=1; b) one test in triaxial extension (CK_0UE) at OCR=1; and c) one CK_0UC test at OCR≈2. These tests were conducted using SHANSEP consolidation procedures in order to ameliorate the effects of sample disturbance on the measured soil behaviour (Ladd and Foott, 1974). Using the standard triaxial equipment, these tests provide reliable data for axial strains in the range, $0.05 \leq \varepsilon_a \leq 10.0\%$.
4. Cross-hole shear wave velocity tests (Trudeau et al., 1974) in order to estimate the small strain shear modulus (there is a scarcity of small strain data for samples of resedimented BBC).

Tables 1 and 2 show the average index properties for BBC and the input parameters selected for BBC (based on the above tests) respectively:

1. The value of K_{0NC}[2] has been variously reported for BBC between 0.41 and 0.53 depending on testing conditions. Recent studies on resedimented clay report K_{0NC}≈0.48 which is used in all subsequent predictions unless otherwise stated[3].
2. The slope of the virgin consolidation line for intact BBC, $\lambda = 0.18 \pm 0.07$, is reported by Ghantous (1982) from a comprehensive set of CRS tests on natural BBC. For natural clays, λ decreases with increasing confining stress, reflecting greater sensitivity of this material as compared to the resedimented clay. An average value, λ=0.184 is used for MIT-E3 predictions.
3. The friction angles, ϕ'_{TC} and ϕ'_{TE}, which describe the critical state failure locus, are estimated from undrained triaxial shear tests (CK_0UC and CK_0UE) at OCR=1. In practice, these angles are difficult to determine at large strains due to geometric non-uniformities (especially necking in triaxial extension) which develop during testing. The parameters are reported at ε_a≈10% corresponding to the assumed limit of reliable test data[4].
4. For BBC, the variation of K_0 during swelling is well described by the empirical relation (Schmidt, 1966):

$$K_0/K_{0NC} = (OCR)^m \qquad (1)$$

where, m=0.4 for BBC. This expression leads to a Poisson's ratio, v=0.277 (2G/K=1.05) from the procedure described by Whittle (1989a).

5. The parameter κ_0 is estimated from the small strain shear modulus, G_{max}, measured at a known void ratio, e, and stress state (σ'_{v0}, K_0), together with the selected value of 2G/K.
6. The values of C, n are estimated from a parametric study of the stress-strain behaviour during unloading in CRS tests. Figure 1 compares the measured data with model calculations of swelling for different combinations of C, n; and identifies best fit values, C=1.6, n=22.
7. Using the selected values of κ_0, C and n; ω is obtained from the measurements of small strain stiffness (ε_a<0.05%) in a CK_0UC test at OCR=2 as shown in figure

[2]For definitions of notation, please refer to Whittle (1990a).

[3]K_{0NC} is adjusted to match initial consolidation stress conditions where measured.

[4]Recent data on resedimented BBC (Germaine, 1989) suggest, ϕ'_{TE}≈40°, which is lower than the value selected in table 2.

2. More reliable measurements of soil stiffness in the range, $0.005 \leq \varepsilon_a \leq 0.05\%$, can be achieved using local strain measurements (e.g. Jardine et al., 1984).

8. The parameters c and S_t are obtained from a parametric study comparing the effective stress paths from CK_0UC and CK_0UE tests on K_0-normally consolidated clay. The constant c has most influence on the magnitude of the peak undrained shear strengths (c_{utc} and c_{ute}) while S_t affects the strain softening behaviour (Whittle, 1990a). Using the selected values, c=0.87 and S_t=4.5, the model matches closely the observed effective stress paths and stress-strain behaviour measured for K_0-normally consolidated BBC as shown in figure 5 and dicussed in more detail in the next section.

9. The constant h controls the magnitude of residual plastic strains, Δ^p, obtained from unload-reload cycles in hydrostatic (or 1-dimensional) compression as a function of the magnitude of the unloading, OCR_m. Figure 3 compares values of Δ^p measured by Ghantous (1982) with predictions of the model for different values of h. Given the scatter in the experimental data, the value of h can be estimated as, h=0.2±0.1.

10. The parameter γ is obtained by comparing the shear induced pore pressure, Δu_s, with measured data for the CK_0UC test at OCR=2. The value of γ is then selected by comparing the effective stress paths calculated by the model with the measured data. For the selected value γ=0.5, figure 5a shows good agreement between the calculated and measured effective stress paths, including a characteristic reversal in the sign of the shear induced pore pressures beyond peak shear strength.

The above suite of tests enable all of the MIT-E3 input parameters to be determined for BBC with the exception of ψ_0, which controls the description of evolving anisotropy. There is currently very little reliable test data with which to evaluate ψ_0. Instead, a value ψ_0=100 is assumed throughout the current evaluations based on arguments presented by Whittle (1990a). Figure 4 compares the model predictions using ψ_0=100 with measured data for a drained, $1/K_0$, strain controlled triaxial test (i.e. $\Delta\varepsilon_v$=0, $\Delta\varepsilon_h \neq 0$) on K_0-normally consolidated BBC[5]. The figure shows that both the effective stress path and volumetric behaviour are well

[5]Note that K_{0NC}=0.53 and λ=0.125 were measured in this test (Bensari, 1984).

described by the model with the selected value of ψ_0. More extensive studies of the type proposed by Whittle (1990a) are required to provide a more complete evaluation of ψ_0.

UNDRAINED TRIAXIAL SHEAR TESTS

Figure 5 compares MIT-E3 predictions of undrained triaxial compression (CK_0UC) tests with measured data for resedimented Boston Blue Clay with initial overconsolidation ratios, OCR=1, 2, 4 and 8. The laboratory samples were re-consolidated following SHANSEP procedures (Ladd & Foott, 1974) and then rebounded to the required OCR. Model predictions are obtained by simulating swelling from a virgin normally consolidated condition (i.e., one in which the principal directions of stress and anisotropy coincide for K_0-normal consolidation). Hence differences in the stress state prior to undrained shearing (fig. 5) reflect the differences in the measured and predicted swelling behaviour. From the preceding discussion it is clear that the test data at OCR=1, 2 are part of the database used to determine model input parameters. Thus, good agreement between the model calculations and measured data is to be expected. However, the results at OCR's=4, 8 can be properly classified as model predictions. The model describes a number of characteristic features which are also measured in the laboratory tests:

1. For normally consolidated and lightly overconsolidated clay, the peak undrained strength conditions (maximum shear stress) are mobilized at small strain levels and at stress obliquities which are lower than critical state conditions.
2. The stress strain behaviour of BBC is nonlinear at all strain levels measured in the tests, for both normally consolidated and overconsolidated samples. There is no well defined 'yield point' in the tests.
3. Shear induced pore pressures develop at early stages of the tests for all OCR's (observed by changes in mean effective stress). Negative shear induced pore pressures ($\Delta\sigma'>0$) indicate the tendency of the overconsolidated clays to dilate during shearing.

At OCR's=4, 8 it can be seen that the model predictions are generally in very good agreement with the measured data. Figure 6 summarizes the predicted and measured conditions at peak shear strength as described by the undrained strength

ratio (c_u/σ'_{vc}) and Skempton's pore pressure parameter at failure, A_f [= $(\Delta u - \Delta\sigma_3)/(\Delta\sigma_1 - \Delta\sigma_3)$]. The stress strain behaviour is examined in more detail in figure 5c in which the strains have been replotted on a logarithmic scale in order to illustrate, a) the small strain non-linearity, and b) the strain required to mobilize the peak shear strength. It can be seen that the MIT-E3 model provides good descriptions of the small strain non-linearity of the soil but slightly overpredicts the strain at failure for all OCR's. Further comparison of the secant shear modulus confirms in the tests (fig. 5d) shows that MIT-E3 gives excellent agreement with the measurements for strain levels, $\varepsilon_a \geq 0.1\%$, but tends to underpredict the measured data at smaller strain levels.

Based on the results in figures 5 and 6, it can also be seen that there are certain consistent discrepancies between the model predictions and measured data:

1. The model overestimates the undrained shear strength (by approximately 5%) for undrained shear at OCR's=4, 8, but matches closely the pre-peak stress-strain behaviour. This discrepency can be explained, in part, by the development of slip planes observed in the samples (Fayad, 1986). This localization of deformation is commonly observed in laboratory tests on overconsolidated clays and has been linked to the high rates of dilation at stress ratios which are larger than critical conditions (Parry & Amerasinghe, 1973) and to local volume changes which occur in the rupture zone (Atkinson & Richardson, 1987). Localization has been investigated theoretically as an instability in the constitutive description of homogeneous deformation (Rudnicki & Rice, 1975; Vardoulakis et al., 1979), while laboratory ring shear tests have been used to study residual friction along pre-existing slip surfaces (e.g. Lupini et al., 1981). These studies all demonstrate the complexity of the shear strength for overconsolidated clays and reflect limitations of the simple critical state failure criterion as used by the MIT-E3 model.
2. The model overestimates the maximum stress obliquity $[(\sigma'_1 - \sigma'_3)/(\sigma'_1 + \sigma'_3)]$ mobilized at OCR's=4, 8. This is due to the assumed shape of the bounding surface used by MIT-E3. Modified shapes of the yield/bounding surface, on the dry side of critical, have been proposed in the literature (e.g., Dafalias & Herrmann, 1982; St. Pietruszak & Mróz, 1982, and Hashiguchi, 1979). However,

such modifications inevitably require additional input parameters.

Figure 5 also shows the measured data (Ladd & Varallyay, 1965; Fayad, 1986) for undrained triaxial extension tests (CK_0UE) on BBC at OCR's=1, 2, and 4. It should be noted that the test data at OCR=1 were used to determine input parameters (c, S_t) for the MIT-E3 model, hence only the results presented for OCR>1 can be classified as predictions. The measured data include much greater scatter than for the analogous set of compression tests. In particular, the friction angles mobilized at large strain levels can vary by up to 10^0 between tests, probably due to necking of the specimens. The measured data are probably unreliable for strains levels ε_a>1-2% and almost certainly unreliable for ε_a>5%. The results show that MIT-E3 gives very good predictions of the stress-strain behaviour prior to necking for all OCR's. Shear induced pore pressures predicted by the model are also in excellent agreement with the measured data at OCR=2 but become progressively less reliable as OCR increases. This result may reflect limitations in the model and/or experimental difficulties in obtaining reliable extension data at higher OCR's.

EFFECT OF CLAY TYPE

Input parameters for the MIT-E3 model have been selected to describe a number of other clays using the procedure described above. Table 1 compares the index properties for resedimented Boston Blue clay with those for two other clays; a) natural Empire Clay (EC; Azzouz & Baligh, 1984; Lutz, 1985), and b) resedimented London Clay (LC; Hight et al., 1983; Jardine, 1985). The three clays describe a wide range of index properties including; a) low to high plasticity index (BBC vs. EC), b) low to high liquidity index (LC vs. BBC), and c) low to moderate sensitivity[6] (EC vs BBC). A comparison of input parameters selected for the MIT-E3 model (table 2) shows the following:

1. Empire clay is significantly less stiff at small strain levels (higher value of κ_0) than either BBC or London clay. London clay and Empire clay are significantly more non-linear, in their undrained shear behaviour at small strain levels, than BBC (higher values of ω).
2. Large differences in the selected values of C, n are due to variations in the

[6]'Sensitivity' here refers to the index property measured using a device such as a torvane.

stress-strain behaviour of the three materials measured in 1-dimensional swelling tests.

3. The values of c and S_t are larger for BBC than for the other clays. These parameters reflect the higher undrained shear strength, c_{utc}, and more pronounced post peak softening for CK_0UC tests on normally consolidated BBC.

Figures 7 and 8 compare the model predictions of undrained triaxial compression and extension tests with the measured data for; a) Empire clay at OCR=1, 1.5 and 2 (Lutz, 1985), and b) London clay with OCR's=1, 1.5, 3, and 7 (Jardine, 1985). Overall, these figures show a similar pattern of agreement between model calculations and measured data as reported above for BBC. The model limitations, observed in these figures, include; a) overestimation of the maximum stress obliquity for samples with OCR>2, and b) underestimation of the shear strength in triaxial extension tests.

PREDICTIONS FOR OTHER MODES OF SHEARING

Test data from other laboratory tests in modes of shearing other than triaxial tests provides the first independent assessment of model predictive capabilities and limitations. Figure 9 compares model predictions with measured data for plane strain compression (active, CK_0UPSA) and extension (passive, CK_0UPSP) tests at OCR's=1, 2 and 4 (Ladd et al., 1971):

1. For normally consolidated clay, the predicted peak shear strength in plane strain compression, $c_u/\sigma'_{vc}=0.34$, occurs at a small strain levels, $\varepsilon_a \approx 0.2\%$ and is in excellent agreement with the measured data. Significant post-peak strain softening in conjunction with positive shear induced pore pressures are also well described by the model. In plane strain extension, the shear strength is mobilized at larger strain levels ($\varepsilon_a > 3\%$) and positive shear induced pore pressures develop throughout the test. The extension data are not considered reliable for $\varepsilon_a > 5\%$ (Ladd et al, 1971).
2. For compression tests at OCR=2, the undrained shear strength is also mobilized at small strain levels and is characterized by a reversal from negative to positive shear induced pore pressures as predicted by the model. The undrained shear strengths predicted by the model are approximately 5% higher and 10%

lower than the measured data in compression and extension, respectively.

3. At OCR=4, MIT-E3 significantly overestimates the undrained shear strength (by ca. 20%) and the pre-peak stress obliquity $[(\sigma'_1-\sigma'_3)/(\sigma'_1+\sigma'_3)]$ for plane strain compression. In extension the model tends to underestimates the shear strength[7] and also the undrained shear strength.

Figure 9a also shows a small but consistent difference between the predicted and measured critical state (large strain) failure conditions. For plane strain tests, the critical state failure locus in MIT-E3 is described in a $(S_1/\sigma', S_2/\sigma', S_3/\sigma')$ space as follows:

$$\left(\frac{S_1}{\sigma'} - \xi_1\right)^2 + \left(\frac{S_2}{\sigma'}\right)^2 + \left(\frac{S_3}{\sigma'}\right)^2 - k^2 = 0 \qquad (2)$$

i.e. a sphere with centre, $(\xi_1,0, 0)$ and radius, k.

Equation 2 describes an anisotropic critical state failure criterion using the measured friction angles in triaxial compression and extension tests as input parameters to determine ξ_1 and k. Table 3 shows the calculated friction angles computed by the MIT-E3 model for Boston Blue Clay in different modes of shearing. It can be seen that different values of ϕ' are obtained for plane strain compression, plane strain extension and direct simple shear modes. For BBC, the model predicts that $\phi'_{PSC}>\phi'_{TC}$, while $\phi'_{PSE}<\phi'_{TE}$ and $\phi'_{PSE}<\phi'_{DSS}<\phi'_{PSC}$. Examples for other clays show that the relative magnitudes of these angles depend on the (input) values of ϕ'_{TC} and ϕ'_{TE}. For BBC, MIT-E3 estimates a friction angle in plane strain compression, ϕ'_{PSC}, which is approximately 9^0 larger than ϕ'_{TC}, while the measured data (table 3) report smaller differences, $(\phi'_{PSC}- \phi'_{TC}) = 4^0$. In plane strain extension the results are hard to evaluate due to the scatter in the measured data.

Table 3 also compares friction angles[8] for BBC described by; a) the extended von Mises failure condition (commonly used in soil models), and c) the criterion proposed by Matsuoka & Nakai, (1982). In contrast to the MIT-E3 model, these isotropic failure criteria are characterized by one measured friction angle (usually in triaxial compression) which establishes the ratio, ϕ'_{TC}/ϕ'_{TE}, and generates a

[7]Note that differences in the pre-shear stress state (fig. 9) reflect model predictions of the swelling behaviour as compared to measured swelling.

[8]The Mohr-Coulomb criterion describes ϕ' as a unique material constant for all modes of shearing.

unique value of ϕ' for all plane strain shearing modes:

1. The extended von Mises criterion describes friction angles which are much higher than measured conditions for triaxial extension and plane strain modes.
2. The Matsuoka & Nakai criterion is in good agreement with measured data in both triaxial and plane strain compression but generally underpredicts the friction angles in the corresponding extension tests.
3. By coincidence, both the MIT-E3 and Matsuoka criteria describe similar values of friction angle for DSS shearing. However, as ϕ'_{DSS} is not measured directly, this result cannot be evaluated.

Table 3 also shows the magnitude of the intermediate principal stress at critical state conditions, as described by the b parameter [$b_f = (\sigma_{2f}-\sigma_{3f})/(\sigma_{1f}-\sigma_{3f})$]. The MIT-E3 model predicts b_f values which vary with mode of shearing and range from b_f=0.23 in simple shear to b_f=0.28 in plane strain compression tests. In contrast, the isotropic failure criteria describe unique values of b_f for all plane strain shearing[9]. Ladd et al. (1971) report a large scatter in measured values of b_f for BBC and hence it is difficult to evaluate the model predictions. Recent data for BBC measured in the directional shear cell (Seah, 1990) show b=0.25 for plane strain compression tests.

A large number of undrained direct simple shear tests (CK_0UDSS) have been conducted on resedimented BBC in the Geonor direct simple shear apparatus (Ladd & Edgers, 1972; Malek, 1987). In this device, the sample is confined laterally by a wire reinforced membrane to prevent lateral straining and undrained shearing is simulated by conducting constant volume (height) tests such that the total vertical stress is assumed to be equal to the vertical effective stress. In standard tests[10], the lateral normal traction, σ'_h, is not measured and hence the complete stress state in the sample cannot be defined. In addition, the boundary conditions are not well controlled in the test as complementary shear tractions cannot be imposed on the vertical sides of the sample. As a result, non-uniformities inevitably develop during shearing. Analytical research, devoted to investigating these measurement difficulties (e.g. Lucks et al., 1971; Prevost & Hoeg, 1975), have given no clear

[9] Associated plastic flow is assumed at critical state conditions .

[10] Dyvik and Zimmie (1983) report data for radial stresses using resistance wire within the confining membrane.

picture as to their importance; while experimentalists report highly consistent measurements of engineering properties (Ladd et al., 1977; Vucetic & Lacasse, 1984; Airey & Wood, 1987).

In this work, the measured data are considered reliable for shear strains in the range, $0.1 \leq \gamma \leq 10.0\%$. This reflects measurement limitations at small strain levels and the rotation of the sample at large strains (DeGroot, 1989). Figures 10a, b compare the effective stress paths (acting on horizontal planes in the sample, i.e. σ'_v vs. τ) and the shear stress-strain behaviour for CK_0UDSS tests on resedimented BBC, with MIT-E3 predictions for OCR's=1, 2, 4 and 8:

1. At OCR=1, the model predictions give excellent agreement with the measured data for the undrained shear strength, c_{uDSS}/σ'_{vc}, effective stress paths and stress-strain behaviour over the full range of strain levels considered.
2. At OCR=2, the model overpredicts the undrained shear strength by 10% and is slightly stiffer than the measured data. Predictions do not capture accurately the shear induced pore pressures at small strain levels (fig. 10a).
3. For OCR's 4 and 8 model predictions show much higher stress obliquities (τ/σ'_v) mobilized on horizontal planes. As above, this can be attributed, in large part, to the adopted form of the bounding surface in MIT-E3. The undrained shear strength is approximately 25% higher than measurements at OCR=8.
4. The stress obliquity predicted at large strains, $h(=\tan^{-1}\tau/\sigma'_v)=21^0$, is in good agreement with the measured data for all OCR's.
5. Figure 10c examines the stress-strain behaviour in more detail by replotting the shear strains on a logarithmic scale. It can be seen that although the model tends to predict higher stiffness for the overconsolidated tests, the general variations in stiffness with strain levels are well modelled.

During a CK_0UDSS test, the direction of the applied principal strains is fixed at 45^0 to the vertical, while the direction of the principal stresses rotates during shearing. Although model predictions of the principal stress rotations cannot be evaluated due to the lack of data, the calculated behaviour provides valuable insights into the physical interpretation of failure described by the model. Figure 11 shows the predicted behaviour for K_0-normally consolidated clay in terms of: a) δ, the orientation of the major principal stress to the vertical; b) ϕ', the maximum

obliquity angle in the sample (i.e. the angle of tangency to the Mohr circle of stress at a given stress state); and c) v ($=\tan^{-1}\tau/\sigma'_h$) and h corresponding to the stress obliquity mobilized on vertical and horizontal planes in the sample respectively (see fig. 11a). The results show that at the peak strength condition ($\gamma\approx3\%$, fig. 10b), the stress obliquity acting on vertical planes (v) coincides with the maximum obliquity mobilized in the sample (ϕ'). Principal stresses rotate rapidly up to a value $\delta\approx28^0$ for loading up to peak strength but remain almost constant for continued straining of the sample. Maximum stress obliquity is mobilized at large strain levels ($\phi'\approx38.2^0$) corresponding to critical state conditions and coinciding with the obliquity mobilized along the vertical planes in the sample as shown in figure 11. As the vertical plane is also a zero extension direction, the kinematics of the problem imply that failure is initiated by sliding along vertical planes at large strain levels as suggested by theoretical analyses (Shield,1953; de Josselin de Jong, 1971). Model predictions do not show the large rotations of principal stress directions in the post-peak region described in the analysis of Randolph & Wroth (1981). A more detailed assessment of stress rotations and failure conditions in the direct simple shear test is described elsewhere (Whittle & Baligh, 1990).

Figure 12 summarizes MIT-E3 predictions of undrained shear strength (c_u/σ'_{vc}) for the different modes of shearing with $1 \le OCR \le 8$ compared to the measured data for BBC. The model predicts the highest shear strengths in plane strain active tests and the lowest strengths in triaxial extension. Direct simple shear tests provide average values for undrained shear strength for all OCR's considered. The model predictions are in excellent agreement with the measured data at OCR=1 but are less reliable as OCR increases (overestimate strengths in compression while understimating the measured values in extension tests).

PREDICTIONS OF ANISOTROPIC BEHAVIOUR DUE TO STRESS HISTORY

Directional Shear Cell Tests

Standard laboratory tests are severely limited in the range of stress paths that they can apply to a soil sample. For example, in triaxial and plane strain tests, the principal stress axes coincide with the axes of the devices and remain fixed during the test, while the direction of the major principal stress is either in the vertical

or horizontal directions (i.e., δ is either fixed or undergoes 90^0 rotations for stress paths crossing the hydrostatic axis). In contrast, in the direct simple shear apparatus, principal stresses are free to rotate but the state of stress is not fully defined and the direction of principal stresses is not controlled.

In order to investigate the anisotropic properties of soils and to simulate stress histories that are more representative of field conditions, sophisticated devices have been developed including; a) the Hollow Cylinder Apparatus (HCA; Saada & Zamani, 1969; Hight et al., 1983), and b) the Directional Shear Cell (DSC; Arthur & Menzies, 1972; Arthur et al., 1977). At MIT, the DSC has been developed to conduct undrained shear tests on clays (Germaine, 1982).

The Directional Shear Cell is a plane strain, stress-controlled device which is able to apply both normal and shear forces to four faces of a cubical sample. Hence it is possible to control principal stress directions in the plane of loading. Tests on resedimented BBC have been conducted to evaluate the anisotropic properties of the clay due to a 1-dimensional (K_0) consolidation history. The test procedure is illustrated in figure 13:

1. The sample is K_0-normally consolidated in a large scale consolidometer (i.e. with no lateral strains in the x-z plane). It is then swelled until there is no shear stress acting on the sample (i.e. $\sigma'_{xx}=\sigma'_{yy}=\sigma'_{zz}=\sigma'_c$). This occurs at a nominal OCR≈4.
2. The sample is then transfered to the Directional Shear Cell and reconsolidated to the stress level, σ'_c, and is sheared undrained with a fixed direction of the major principal stress in either the x-z (ψ^0) or the x-y plane (δ^0).

Tests in the x-z plane constitute proof tests of the laboratory equipment as the soil properties are isotropic due to the imposed stress history (i.e. prior to undrained shearing). Hence the direction of the applied major principal stress during undrained shearing (ψ^0) should have no influence on the stress-strain-strength of the clay. This mode of shearing is also of importance in the practical interpretation of in-situ tests (such as the self-boring pressuremeter test) which are based on 'cavity expansion modes' of shearing. Figure 14 compares the measured effective stress paths and stress-strain behaviour (Germaine, 1982; O'Neill, 1985) with MIT-E3 predictions:

1. The undrained strength ratio predicted by MIT-E3, c_u/σ'_p=0.175, compares closely with the measured response, c_u/σ'_p=0.17±0.1.
2. Critical state failure conditions predicted by the model correspond to a friction angle, $\phi'=57^0$ as compared to the measured value of $\phi'=55^0$. In both cases the friction angle is much higher for undrained plane strain shearing in the x-z plane (normal to the direction of deposition) than for any of the modes of shearing described above (table 3).
3. The predicted stress-strain response is stiffer than the measured data leading to a strain level at peak conditions, γ_p≈3% as compared to the measured response in which γ_p>5%. Small positive shear induced pore pressures are measured in the tests, and are also predicted by the MIT-E3 model.

Anisotropic behaviour due to the one-dimensional (K_0) consolidation stress history is examined by undrained shear tests in the x-y plane (fig. 13) conducted at various orientations of the major principal stress (δ^0). Figure 15 shows the measured data and model predictions for these tests. It should be noted that the results for $\delta=0$, 90^0 correspond to standard plane strain tests (cf. fig. 9). The results show that the direction of loading has a pronounced effect on the undrained clay behaviour. Model predictions are in good qualitative agreement with the measured data. A more quantitative assessment shows:

1. As the δ angle increases from 0 to 90^0 the measured undrained shear strength decreases monotonically from c_u/σ'_p=0.25 to 0.14 as compared to model predictions which range from 0.29 to 0.11. MIT-E3 predicts higher strengths for $\delta<45^0$ and lower strengths for $\delta>45^0$ as compared to measured data (fig. 16a).
2. The strain required to mobilize the shear strength of the clay, γ_p, increases from γ_p≈2% at $\delta=0^0$ to γ_p>10% at $\delta=90^0$ for both model predictions and measurements. The model predictions of stress-strain behaviour are in excellent agreement with the measured data at large δ angles but are stiffer than the measurements for $\delta<45^0$.
3. The pore pressures predicted at failure (described by A_f) are compared to the measured values at peak shear strength in figure 16b. Both the predictions and measurements show increasing values of A_f as δ increases from 0 to 90^0. MIT-E3 underpredicts the magnitude of A_f at low δ values. Shear induced pore

pressures, measured at small strain levels, are not well described by the model.

4. The predicted friction angles mobilized at peak shear strength vary from 42.3^0 at $\delta=0^0$ to 35.7^0 at 90^0. These results reflect the anisotropic critical state failure criterion of the model. The measured data show a similar but less pronounced decrease in the friction angle at peak strength.
5. For tests with $\delta<45^0$, the model predicts maximum stress obliquities which are mobilized prior to attaining peak shear strength conditions. The maximum obliquities (fig. 15) are much larger than the measured values. This result is controlled by the shape of the bounding surface in MIT-E3 (as described previously).

Overall, the evaluation of MIT-E3 predictions for DSC tests provides a severe check on model predictive capabilities and limitations. More detailed investigations of the principal stress rotations described by Whittle (1987) have shown that MIT-E3 can describe a state surface for undrained shearing similar to that described for sands by Symes et al. (1984). Further evaluations of model predictions for K_0-normally consolidated BBC are presented by Seah (1990), Whittle et al. (1990).

Multi-directional Direct Simple Shear Device

In order to simulate the complex stress conditions imposed during ice loading of an arctic gravity structure, a new Multi-directional Direct Simple Shear apparatus (MDSS) has recently been built at MIT (DeGroot, 1989). The device comprises the same basic geometry as the standard Geonor direct simple shear (DSS) apparatus but has the additional capability to impose horizontal shear stresses in two independent directions. The first shear stress is used to simulate the shear stress acting on horizontal planes in the soil due to the gravity loading of the structure. Ice loading is then simulated by application of shear in a second direction. The test procedure is illustrated in figure 17:

1. The sample is normally consolidated by applying vertical and shear stresses (direction 1 fig. 17) $(\sigma'_{yy}, \sigma'_{xy}, \sigma'_{yz})_c$ under K_0 conditions (i.e. $\sigma'_{xx} = \sigma'_{zz} = K_{0NC}\sigma'_{yy}$). The total magnitude of the applied consolidation shear stress is described by $||\tau|| = \left\{\sigma^2_{xy} + \sigma^2_{yz}\right\}^{1/2}$.
2. The sample is sheared undrained by applying $\Delta\sigma'_{xy}$ (i.e. acting in direction 2, at

angle θ^0 to the consolidation shear stress direction, fig. 17).

The tests illustrate the development of anisotropic properties due to consolidation under an applied shear stress. MIT-E3 predictions for the normally consolidated clay are obtained by assuming that the stress state at the end of phase 1 corresponds to a 'virgin normally consolidated condition' (i.e. the principal directions of the applied stresses and anisotropy coincide). Figure 18 compares measurements of the maximum shear stress acting on horizontal planes in the sample, $||\tau||_{max}/\sigma'_{vc}$, with MIT-E3 predictions, for K_0-normally consolidated BBC with $(||\tau||/\sigma'_v)_c = 0.2$, and $\theta=0^0$ - 150^0:

1. The maximum shear stress measured in the tests decreases from a maximum, $||\tau||_{max}/\sigma'_{vc}= 0.27$ at $\theta=0^0$ to $||\tau||_{max}/\sigma'_{vc}= 0.21$ at $\theta=150^0$. This decrease in shear resistance reflects the anisotropic shear strength that develops due to the imposed consolidation history.
2. MIT-E3 predictions show similar trends to the measured data, but overpredict the maximum shear stress by 15% at $\theta=0^0$.

A more practically important measurement is the maximum shear strength mobilized in the x-y plane (i.e., in the plane of the simulated ice loading). Figure 19 compares the measured effective stress paths and stress-strain behaviour (in the x-y plane), with MIT-E3 predictions for the same tests:

1. The measured data show a maximum shear strength, $(\sigma'_{yx})_{max}/\sigma'_{vc}=0.27$, at $\theta=0^0$, and a minimum, $(\sigma'_{yx})_{max}/\sigma'_{vc}=0.15$, at $\theta\approx120^0$. MIT-E3 overpredicts the shear strength at small values of θ by up to 15% (at $\theta=0^0$). Figure 18 compares the measured and predicted values of shear strength normalized by the 'reference strength' at $\theta=0^0$, $[\sigma'_{yx}/\sigma'_{yx}(\theta=0^0)]_{max}$. These results confirm that MIT-E3 predicts variations in undrained shear strength which are in excellent agreement with the measured data.
2. For small θ angles, the shear strength of the soil is mobilized at very small shear strains, $\gamma_p\approx0.6\%$, at $\theta=0^0$; while at $\theta=150^0$, peak strength is reached at $\gamma_p>10\%$. The model predictions show similar trends and are in good agreement with the measured data in the range $0.1\% \le \gamma \le \gamma_p$.
3. For all q angles, the model predictions and measurements show similar developments of shear induced pore pressures and mobilized friction $(\sigma'_{yx}/\sigma'_{yy})$

at lareg strain levels.

4. The measured data show significant post-peak strain softening especially for $\theta<60^0$. In contrast, MIT-E3 predicts little or no post-peak softening. These differences may reflect limitations of the model and/or problems of geometric non-linearities associated with the design of the device (as discussed by DeGroot, 1989)

CONCLUSIONS

This paper gives a detailed evaluation of the predictive capabilities and limitations of a new constitutive model, MIT-E3, whose formulation has been described in a companion paper (Whittle, 1990a). Input parameters for the model are obtained from standard types of laboratory tests using a consistent procedure which is detailed for the case of Boston Blue clay, a low plasticity marine clay of moderate sensitivity. Differences in the selected properties for three clays, (Boston Blue clay, Empire clay and resedimented London clay) are used to illustrate typical ranges for the input parameters used by the model (table 2).

Model predictions are compared with measured data for undrained shear tests on K_0-consolidated Boston Blue clay; a) in triaxial, plane strain and direct simple shear modes of shearing, and b) at different overconsolidation ratios ($1\leq OCR\leq 8$). These comparisons show that the model describes accurately many of the observed features of the behaviour of normally and lightly overconsolidated clays, including:

1. Variations in undrained shear strength with mode of shearing (fig. 12), described primarily through the anisotropic yield/bounding surface used in MIT-E3. With increasing OCR (≥ 4), the model tends to overpredict the undrained shear strength in compression modes of shearing, while underpredicting the strength in the extension modes.
2. For shearing at large strain levels, variations in the mobilized friction angle for different modes of shearing are also well predicted by the model using an anisotropic ('critical state') failure criterion (table 3).
3. Small strain non-linearity is generally well described by the model in compression modes of shearing. For the selected input parameters, the model generally overpredicts the secant stiffness at small strain levels for extension

and simple shear modes of shearing.

Other aspects of measured behaviour, are less well described by the model, including:

1. Shear induced pore pressures measured at small strain levels for overconsolidated clays are generally underpredicted due to the assumption of isotropic behaviour at small strain levels.
2. For compression modes of shear at OCR≥4, the model significantly overpredicts the effective stress obliquity mobilized prior to peak shear strength.

Finally, the MIT-E3 model is used to predict measured behaviour for two unique sets of tests which illustrate the important aspects of anisotropic behaviour due to stress history: The first data are undrained shear tests, conducted in the Directional Shear Cell, which show the anisotropic stress-strain strength of overconsolidated BBC (at OCR≈4) for samples sheared in different directions of the major principal stress to the original direction of deposition (δ^0). The second, are undrained simple shear tests, conducted on normally consolidated BBC in the Multi-directional Direct Simple Shear apparatus, which illustrate anisotropic properties generated by shear stresses applied during consolidation. The undrained shear stress is applied at angle (θ^0) to the consolidation shear stress. The MIT-E3 model describes accurately the measured variations of the shear strength and stress-strain behaviour with direction of shearing in both sets of tests. Predictions of shear induced pore pressures are also in reasonable agreement with measured data.

From the above evaluations, it is concluded that MIT-E3 is capable of describing many important aspects of the observed behaviour of clays for OCR's≤8. Limitations of the model are consistently described throughout the evaluation process and can be addressed by further refinement of the model.

ACKNOWLEDGEMENTS

This work was sponsored in part through the MIT Sea Grant College Program through grants NA84AA-D00046 and NA86AA-D-SG-089, and in part by a consortium of oil companies including Amoco Production Company, Chevron Oil Field Research, Exxon Production Research, Marathon Oil Company, Mobil Research and Development, Shell Development Company. The author is indebted to Professor

Mohsen Baligh for his assistance and guidance throughout this work and would also like to extend a special acknowledgement to the numerous former graduate students of the Massachusetts Institute of Technology whose experimental data has contributed so significantly to this work.

REFERENCES

Airey, D.W. & Wood, D.M. (1987) An Evaluation of Direct Simple Shear Tests on Clay, *Géotechnique*,**37**, No. 1, 1-25.

Atkinson, J.H. & Richardson, D. (1987) Effects of Local drainage in Shear Zones on the Undrained Strength of Overconsolidated Clays, *Géotechnique*,**37**, No. 3, 393-403.

Arthur, J.R.F. & Menzies, B.K. (1972) Inherent Anisotropy in a Sand, *Géotechnique*,**22**, No. 1, 115-128.

Arthur, J.R.F. Chua, K.S. & Dunstan, T. (1977) Induced Anisotropy in a Sand, *Géotechnique*,**27**, No. 1, 13-36.

Azzouz, A.S. & Baligh, M.M. (1984) *Behaviour of Friction Piles in Plastic Empire Clays*, Research Report No. R84-14, Department of Civil Engineering, Massachusetts Institute of Technology.

Baligh, M.M., Vivatrat, V., & Ladd, C.C. (1979) *Exploration and Evaluation of Engineering Properties for Foundation Design of Offshore Structures*, MIT Sea Grant Program Report No. 79-8, Massachusetts Institute of Technology, 268p.

Baligh, M.M., Azzouz, A.S., Wissa, A.Z., Martin, R.T. & Morrison, M.J. (1981) The Piezocone Penetrometer, *Proc. ASCE Conf. on Cone Penetration Testing & Experience*, St Louis, MO., 247-263.

Bensari, J. E. (1984) *Stress-Strain Characteristics from Undrained & Drained Tests on Resedimented Boston Blue Clay*, SM Thesis, Massachusetts Institute of Technology.

Dafalias, Y. & Herrmann, L.R. (1982) Bounding Surface Formulation of Soil Plasticity, *Soil Mechanics, Cyclic & Transient Loads*, Eds. G.N. Pande & O.C. Zienkiewicz, Wiley & Sons, New York, 253-282.

de Josselin de Jong, G. (1971) The Double Sliding Free Rotating Model for Granular Assemblies, *Géotechnique*,**21**, No. 2, 155-163.

Degroot, D.J. (1989) *The Multi-directional Direct Simple Shear Apparatus with application to Design of Offshore Arctic Gravity Structure,* PhD Thesis, Massachusetts Institute of Technology.

Dyvik, R. & Zimmie, T.F. (1983) *Lateral Stress Measurements during Static and Cyclic Simple Shear Testing*, NGI Report, No. 149.

Fayad, P. (1986) *Aspects of the Volumetric and Undrained Behaviour of Boston Blue Clay*, SM Thesis, Massachusetts Institute of Technology.

Germaine, J.T. (1982) *Development of the Directional Shear Cell for Measuring Cross-Anisotropic Clay Properties*, ScD Thesis, Massachusetts Institute of Technology.

Germaine, J.T. (1986) Personal Communication.

Ghantous, I.B. (1982) *Prediction of In-Situ Consolidation Parameters of Boston Blue Clay*, Civil Engineer Thesis, Massachusetts Institute of Technology.

Hashiguchi, K. (1979) Constitutive Equations for Granular Media with Anisotropic Hardening, *Proc. 3rd Intl. Conf. on Numerical Methods in Geomechanics*, Aachen, Vol. 3, 435-439.

Hight, D.W. , Gens, A. & Symes, M.J. (1983) The Development of a New Hollow Cylinder Apparatus for Investigating the Effects of Principal Stress Rotation in Soils, *Géotechnique*, **33**, No. 4, 355-383.

Hight, D.W. , Gens, A. & Jardine, R.J. (1983) Evaluation of Geotechnical Parameters from Triaxial Tests on Offshore Clay, *Proc. Soc. for Underwater Tech. Conf. on Offshore Site Investigation*, London, 253-268.

Jardine, R.J. (1985) *Investigations of Pile-Soil Behaviour with Special Reference to the Foundations of Offshore Structures*, PhD Thesis, Imperial College, London University.

Jardine, R.J., Symes, M.J.P.R. & Burland, J.B. (1984) The Measurement of Soil Stiffness in the Triaxial Apparatus, *Géotechnique*,**34**, No. 3, 323-340.

Ladd, C.C. & Varallyay, J. (1965) *The Influence of the Stress System on the Behaviour of Saturated Clays during Undrained Shear*, Research Report R65-11, Department of Civil Engineering, Massachusetts Institute of Technology.

Ladd, C.C. & Edgers, L. (1972) *Consolidated-Undrained Direct Simple Shear Tests on Boston Blue Clay*, Research Report R72-82, Department of Civil Engineering,

Massachusetts Institute of Technology.

Ladd, C.C. & Foott, R. (1974) New Design Procedure for Stability of Soft Clays, *J. Geotech Engrg Div. Am. Soc. Civ. Engrs*, **100**, No. GT7, 763-786.

Ladd, C.C., Bovee, R., Edgers, L. & Rixner, J.J. (1971) *Consolidated-Undrained Plane Strain Tests on Boston Blue Clay*, Research Report R71-13, Department of Civil Engineering, Massachusetts Institute of Technology.

Ladd, C.C., Foott, R., Ishihara, K., Schlosser, F. & Poulos, H.G. (1977) Stress-Deformation & Strength Characteristics, State of the Art Report, *Proc. 9th Intl. Conf. on Soil Mechs. & Fdn. Engrg.*, Tokyo, **2**, 421-494.

Lutz, D.G. (1985) *Predictions of the Axial Capacity of Friction Piles in Empire Clay by Means of the Piezo-Lateral Stress Cell*, SM Thesis, Massachusetts Institute of Technology.

Lucks, A.S., Christian, J.T., Brandow, G.E. & Hoeg, K. (1971) Stress Conditions in NGI Simple Shear Test, *J. Soil Mechs. & Fdn. Engrg Div. Am. Soc. Civ. Engrs.*,**98**, No. SM1,

Lupini, J.F., Skinner, A.E., & Vaughn, P.R. (1981) The Drained Residual Strength of Cohesive Soils, *Géotechnique*, **31**, No. 2, 181-213.

Malek, A.M. (1987) *Cyclic Behaviour of Clays in Direct Simple Shear and Application to Offshore Tension Piles*, ScD Thesis, Massachusetts Institute of Technology.

Matsuoka, H. & Nakai, T. (1982) A New Failure Criterion for Soils in Three Dimensional Stresses, *Proc. IUTAM Conf. on Deformation & Failure of Gran. Matls.*, Delft, 253-263.

MIT (1975) *Proceedings of the Foundation Deformation Prediction Symposium*, US Federal Highway Admin. Report No. FHWA-RD-75-516, 2 vols.

O'Neill, D.A. (1985) *Undrained Strength Anisotropy of an Overconsolidated Thixotropic Clay*, SM Thesis, Massachusetts Institute of Technology.

Parry, G.H.G. & Amerasinghe, S.F. (1973) Components of Deformations in Clays, *Proc. Symp. on Plasticity in Soil Mechs.*, Cambridge, 108-128.

Pietruszak, S. & Mróz, Z. (1982) On-Hardening Anisotropy of K_0-Consolidated Clays, *Intl. J. for Num. & Anal. Meths. in Geomechs.*, **7**, 19-38.

Prevost, J-H. & Hoeg, K. (1975) Re-analysis of Simple Shear Soil Testing, *Canadian*

Geot. J., **25**, No. 2, 279-297.

Randolph, M.F. & Wroth, C.P. (1981) Application of the Failure State in Undrained Simple Shear to the Shaft Capacity of Driven Piles, *Géotechnique*, **31**, No. 1, 143-157.

Rudnicki, J.W. & Rice, J.R. (1975) Conditions for Localization of Deformation in Pressure Sensitive Dilatant Materials, *J. Mech. & Phys. of Solids*, **23**, 371-394.

Saada, A.S. & Zamani, K.K. (1969) The Mechanical Behaviour of Cross-Anisotropic Clays, *Proc. 6th Intl. Conf. on Soil Mechs. & Fdn. Engrg.*, Mexico City, 1, 351-359.

Schmidt, B. (1966) Discussion of Paper by Brooker & Ireland, *Canadian Geot. J.*, **3**, No. 4, 239-242.

Seah, T.H. (1990) Anisotropy of Normally Consolidated Boston Blue Clay, ScD. Thesis, Massachusetts Institute of Technology,

Shield, R.T. (1953) Mixed Boundary Value Problems in Soil Mechanics, *Quart. Applied Math.*, **11**, 61-75.

Symes, M.J., Gens, A. & Hight, D.W. (1984) Undrained Anisotropy and Principal Stress Direction Rotation, *Géotechnique*, **34**, No. 1, 11-27.

Trudeau, P.J., Whitman, R.V. & Christian, J.T. (1974) Shear Wave Velocity & Modulus of a Marine Clay, *J. Boston Soc. Civ. Engnrs.*, 12-25.

Vardoulakis, I. (1979) Bifurcation Analysis of the Triaxial Test on Sand Samples, *Acta Mechanica*, **32**, 35-54.

Vucetic, M. & Lacasse, S. (1984) Specimen Size Effect in Simple Shear Test, *J. Geotech Engrg Div. Am. Soc. Civ. Engrs*, **110**, No. GT3, 439-453.

Whittle, A.J. (1987) *A Constitutive Model for Overconsolidated Clays with Application to the Cyclic Loading of Friction Piles*, ScD Thesis, Massachusetts Institute of Technology.

Whittle, A.J. (1990a) A Model for Predicting the Behaviour of Overconsolidated Clays: I Formulation, submitted to *Géotechnique*.

Whittle, A.J. (1990b) Evaluation of a Constitutive Model for describing Clays subject to Cyclic Loading, submitted to *J. Geotech Engrg Div. Am. Soc. Civ. Engrs.*

Whittle, A.J. & Baligh, M.M. (1990) Analysis of Pile Shaft Behaviour in Normally and

Lightly Overconsolidated Clays, submitted to *J. Geotech Engrg Div. Am. Soc. Civ. Engrs.*

List of Tables

List of Figures

Property	Boston Blue Clay	Empire Clay	London Clay
w_L (%)	42	76	75
w_P (%)	21	26	28
I_P (%)	21	50	47
I_L (%)	95	36	5

Table 1. Average Index Properties of Three Clays

Input Parameter	Boston Blue Clay	Empire Clay	London Clay
e_0	1.12	1.26	1.21
K_{0NC}	0.48	0.62	0.62
κ_0	0.001	0.0035	0.001
λ	0.184	0.274	0.172
2G/K	1.05	0.86	0.99
ϕ'_{TC}	33.4^0	23.6^0	22.5^0
ϕ'_{TE}	45.9^0	21.6^0	22.5^0
c	0.86	0.75	0.80
S_t	4.5	3.0	3.9
C	22.0	24.0	65.0
n	1.60	1.75	1.50
ω	0.07	0.20	0.20
h	0.2	0.2	0.1
γ	0.5	0.5	0.5
Ψ_0	100.0	100.0	100.0

Table 2 Selected Values of Input Parameters for the MIT-E3 Model

FAILURE CRITERION	TRIAXIAL		PLANE STRAIN				DIRECT SIMPLE SHEAR	
			active		passive			
	ϕ'_{TC}	ϕ'_{TE}	ϕ'_{PSA}	b_f	ϕ'_{PSP}	b_f	ϕ'_{DSS}	b_f
VON MISES	33.4^0	60.4^0	51.1^0	0.5	51.1^0	0.5	51.1^0	0.5
MATSUOKA	33.4^0	33.4^0	37.9^0	0.33	37.9^0	0.33	37.9^0	0.33
MIT-E3	33.4^0	45.9^0	42.3^0	0.28	35.7^0	0.25	38.2^0	0.23
MEASURED DATA	33.4^0	45.9 ± 8^0	37 ± 3^0	N/A	49 ± 11^0	N/A	N/A	N/A

Table 3. Predicted and Measured Critical State Failure Conditions for Boston Blue Clay

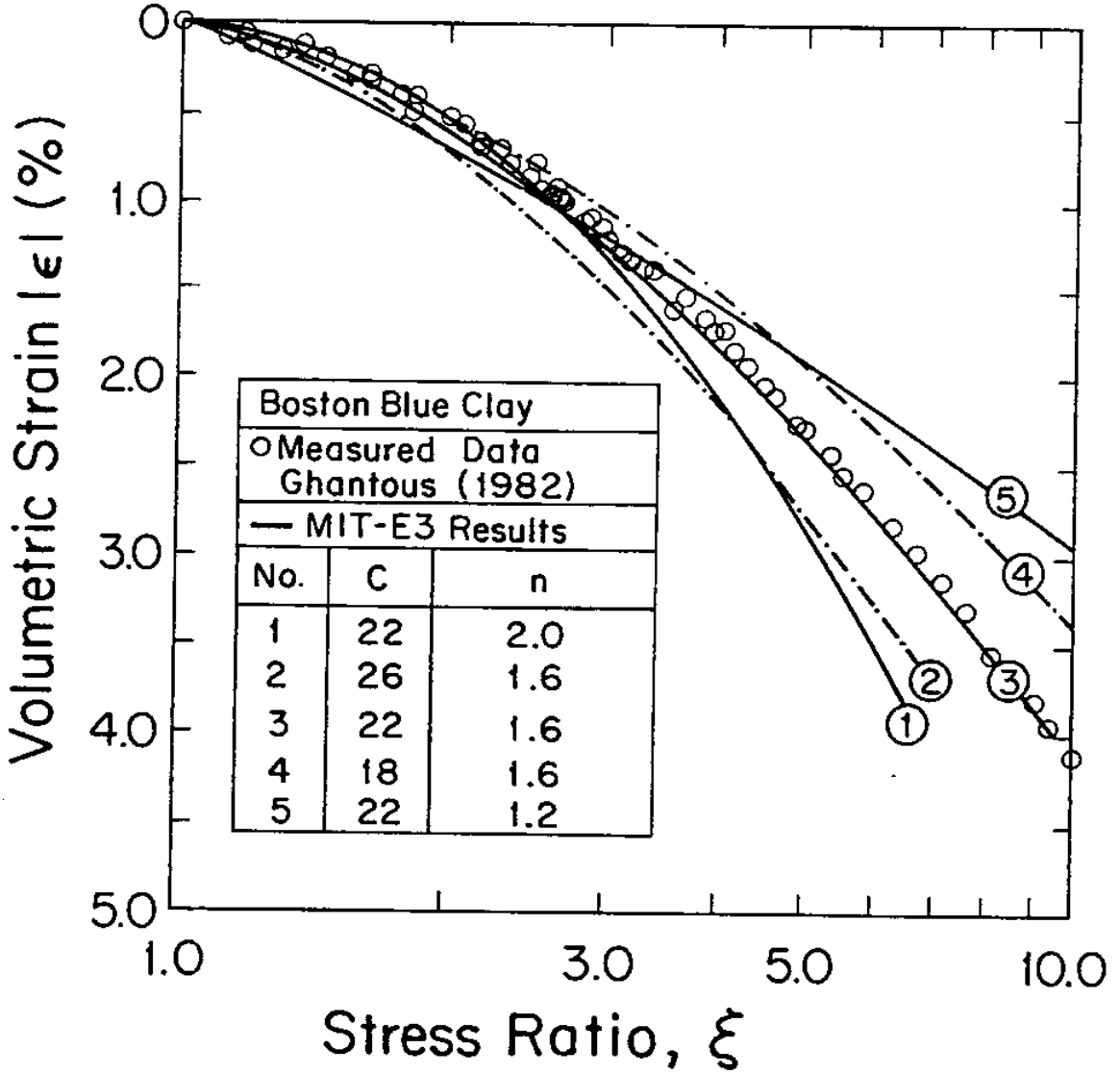

1. Estimation of Input Parameters C,n for Boston Blue Clay

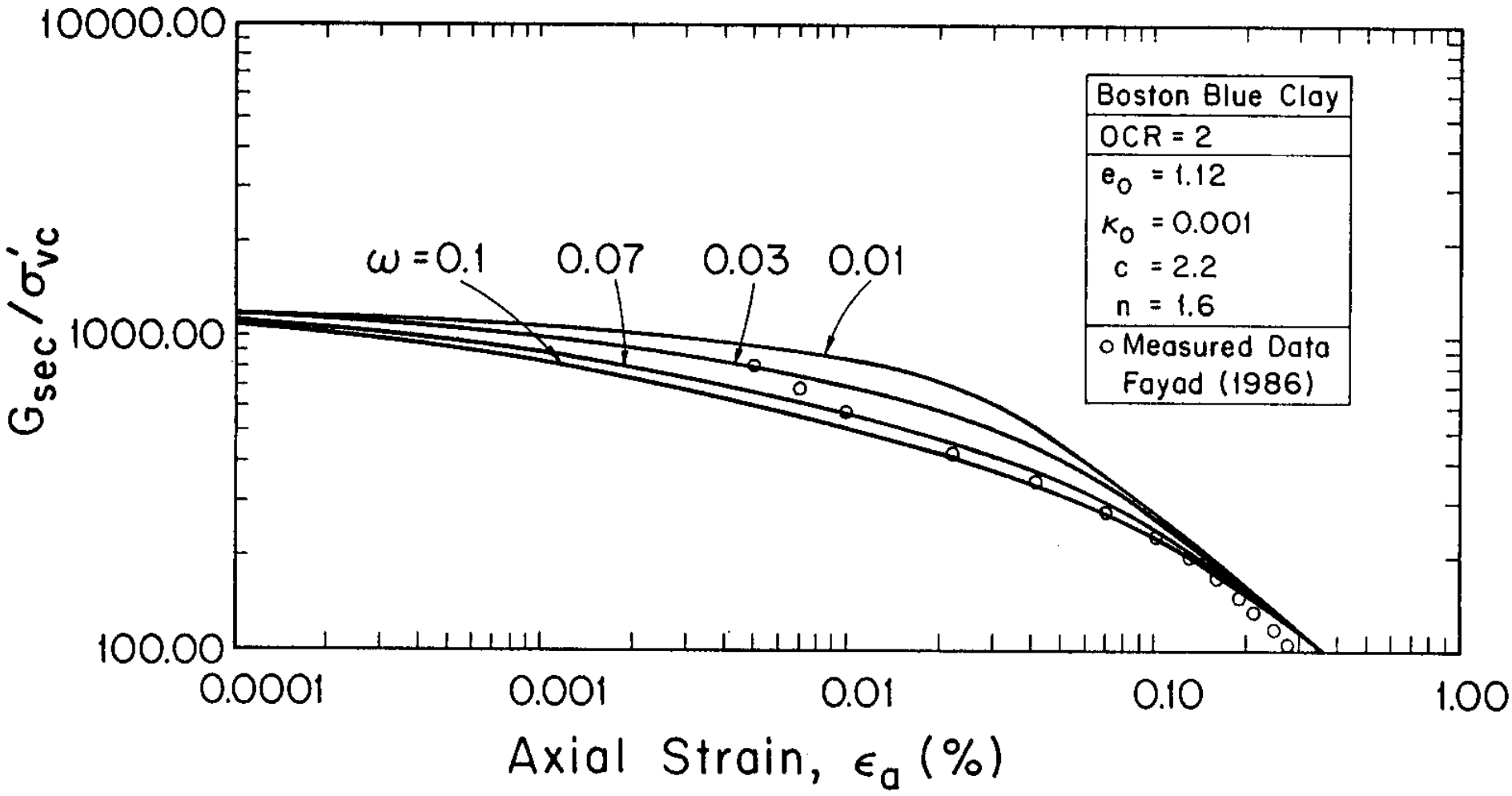

2. Estimation of Input Parameter ω for Boston Blue Clay

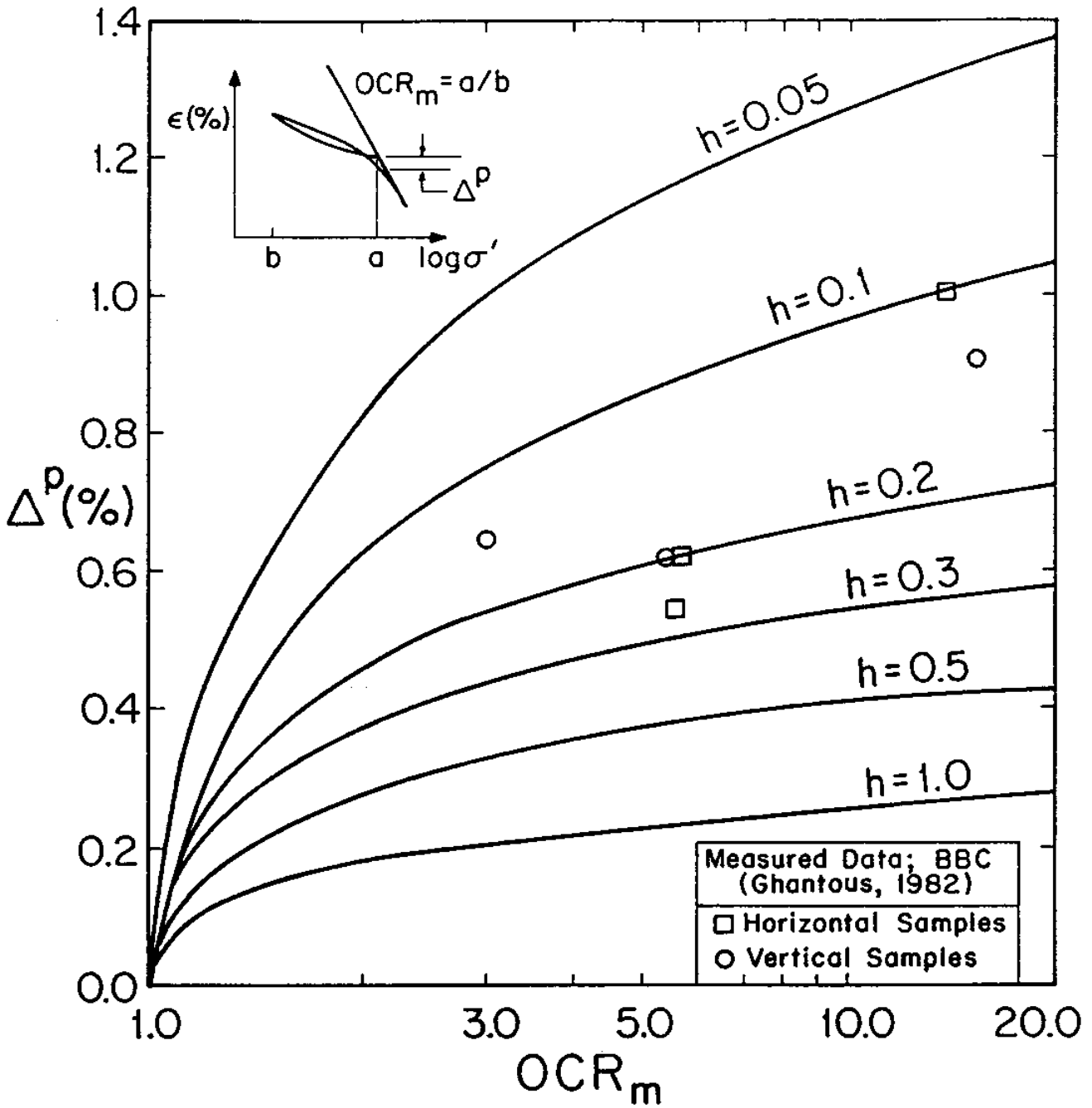

3. Estimation of Input Parameter h for Boston Blue Clay

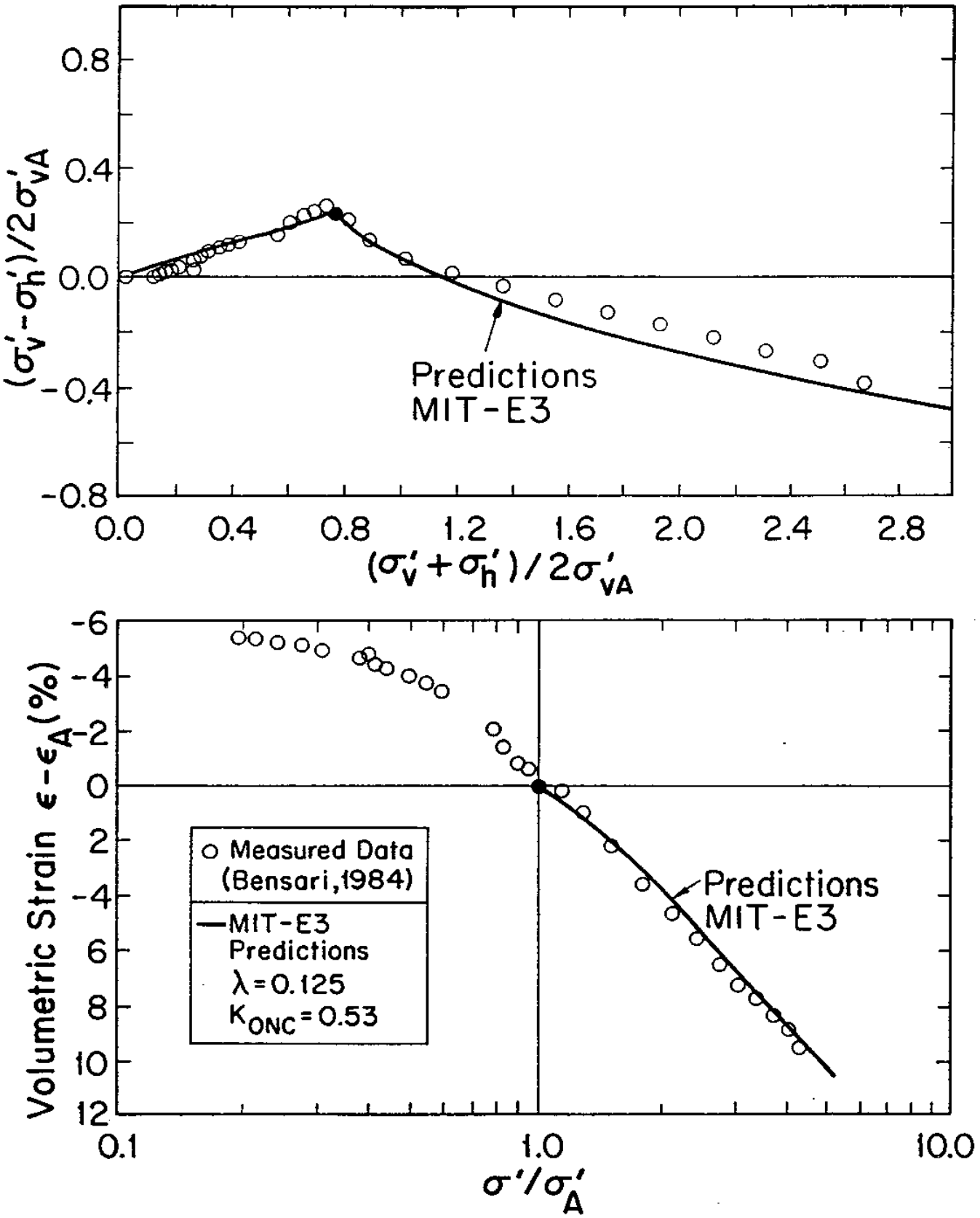

4. Model Predictions of a Drained Strain Controlled Test on Boston Blue Clay

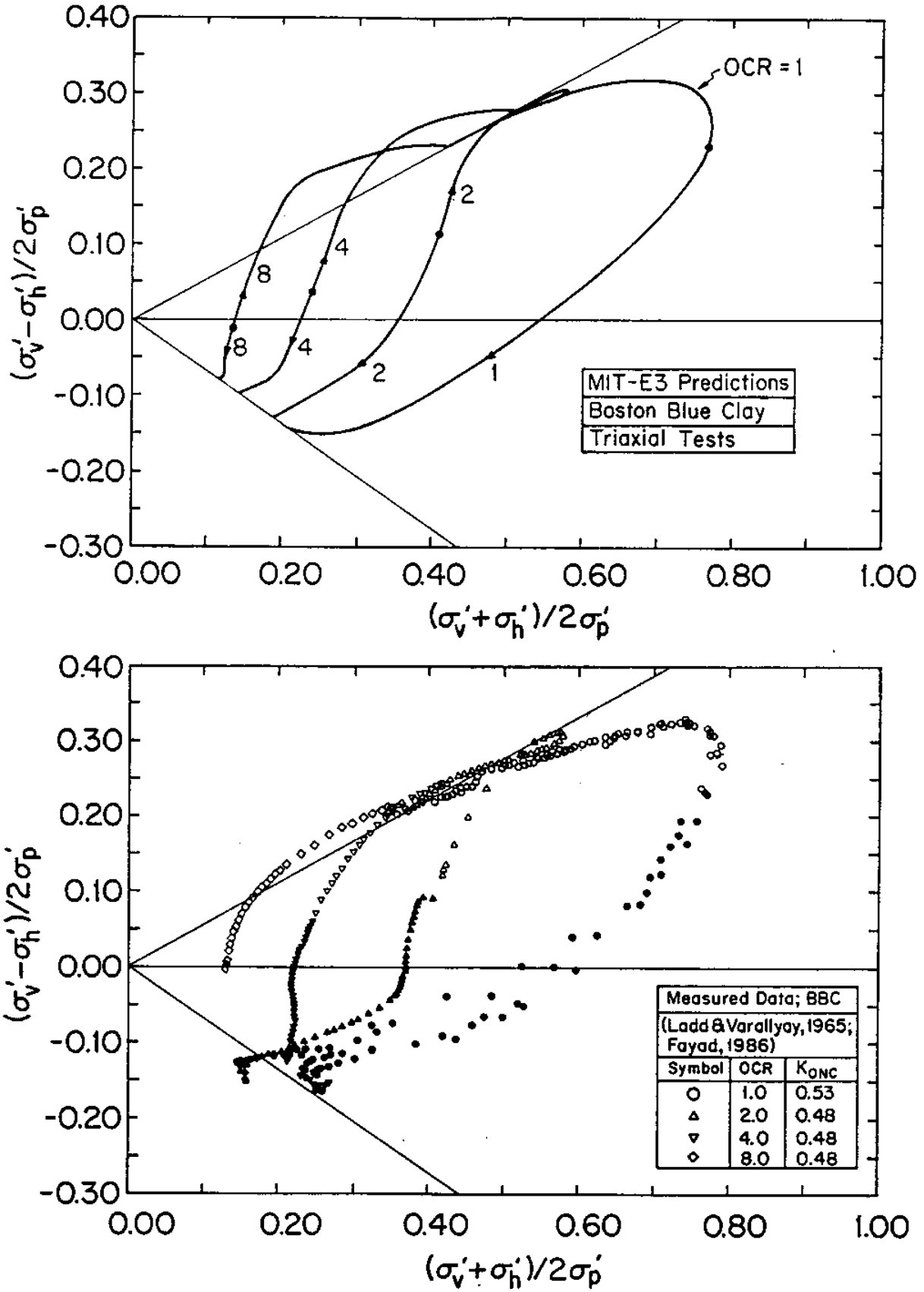

a) Effective Stress Paths

5. Comparison of Model Predictions and Measured Data for K_0-Consolidated, Undrained Triaxial Tests on Resedimented Boston Blue Clay

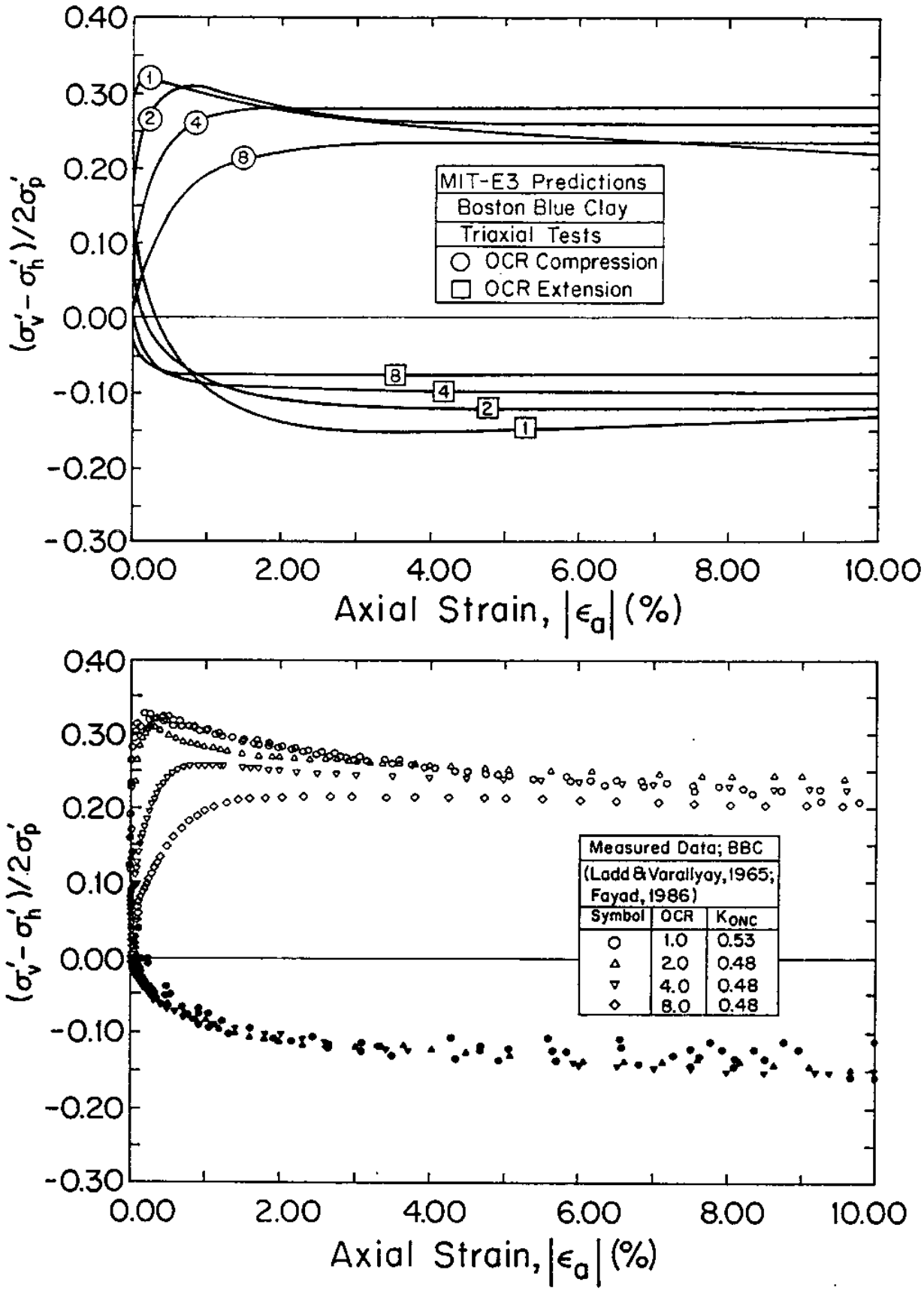

b) Stress-Strain Response

5. Comparison of Model Predictions and Measured Data for K_0-Consolidated, Undrained Triaxial Tests on Resedimented Boston Blue Clay

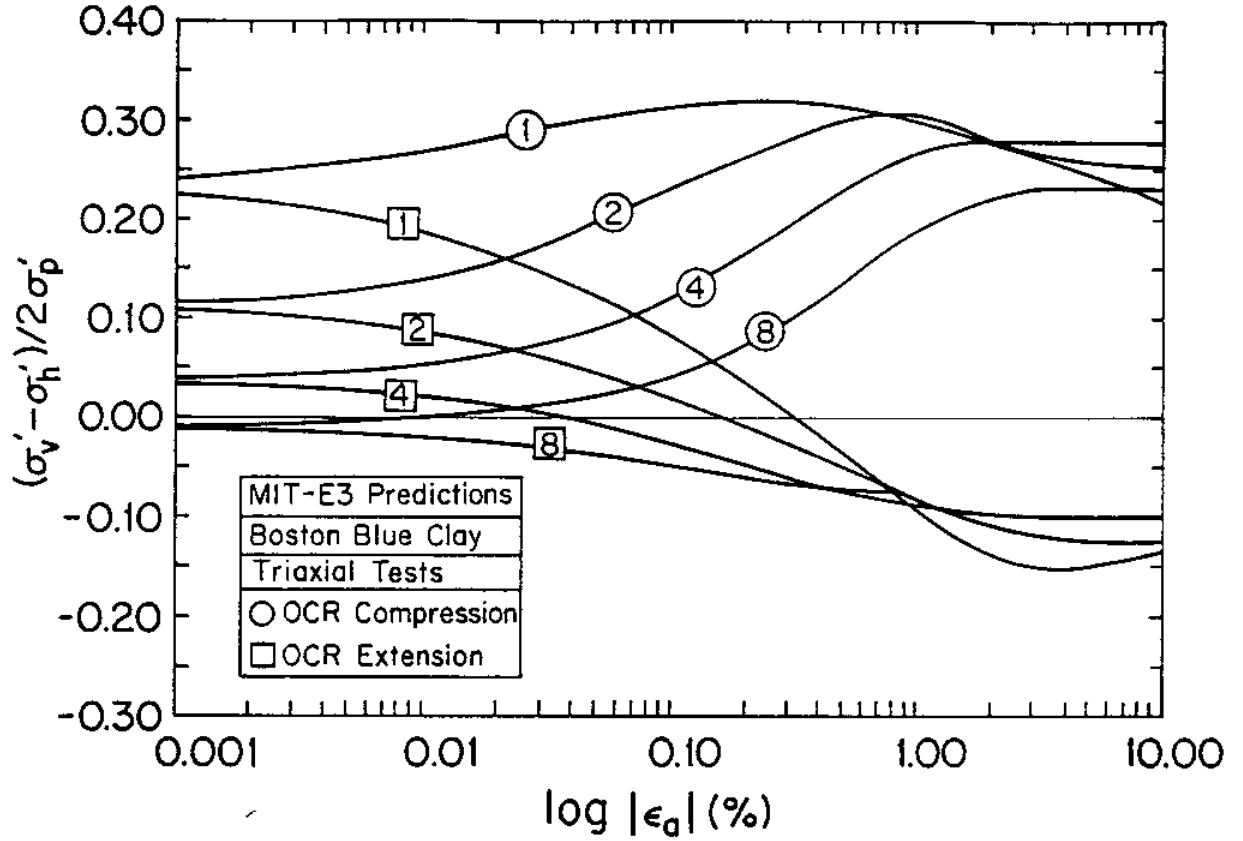

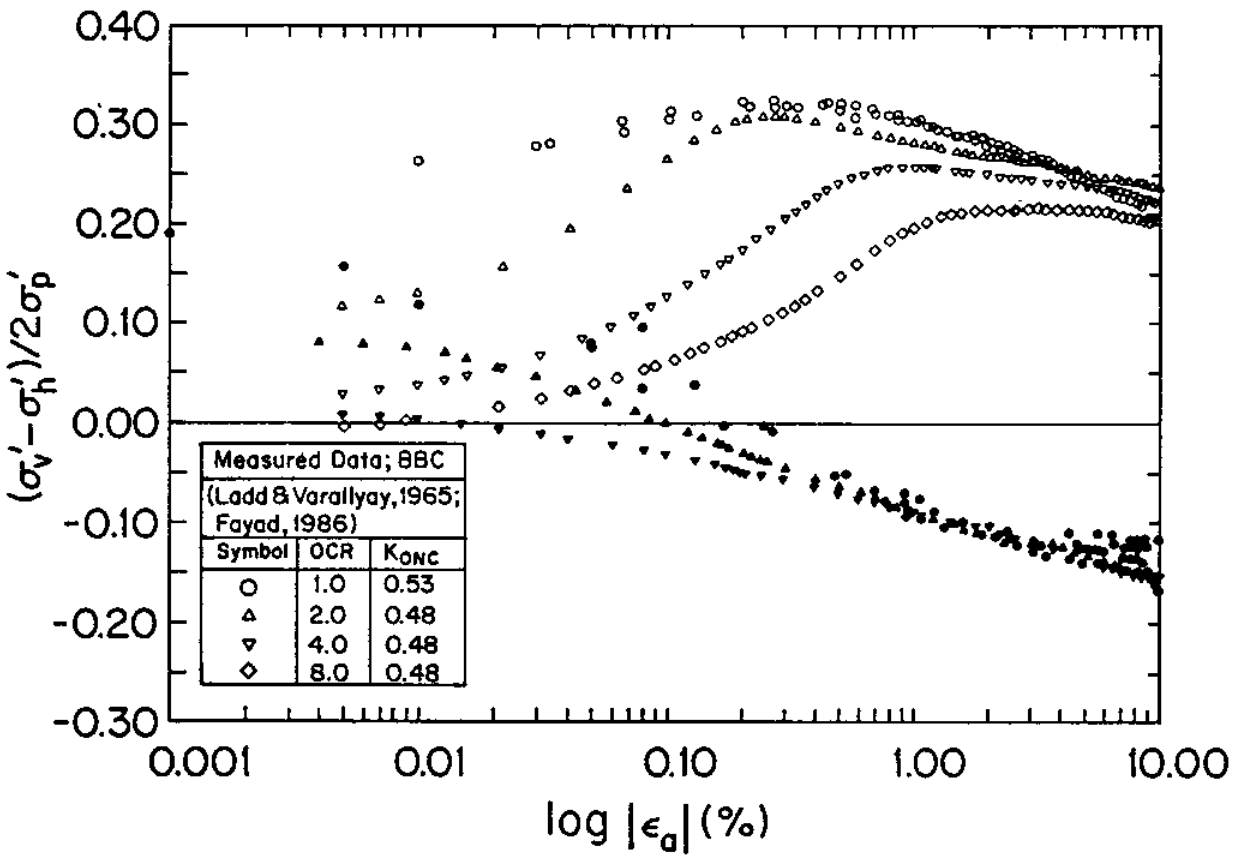

c) Shear Stress versus log Strain

5. Comparison of Model Predictions and Measured Data for K_0-Consolidated, Undrained Triaxial Tests on Resedimented Boston Blue Clay

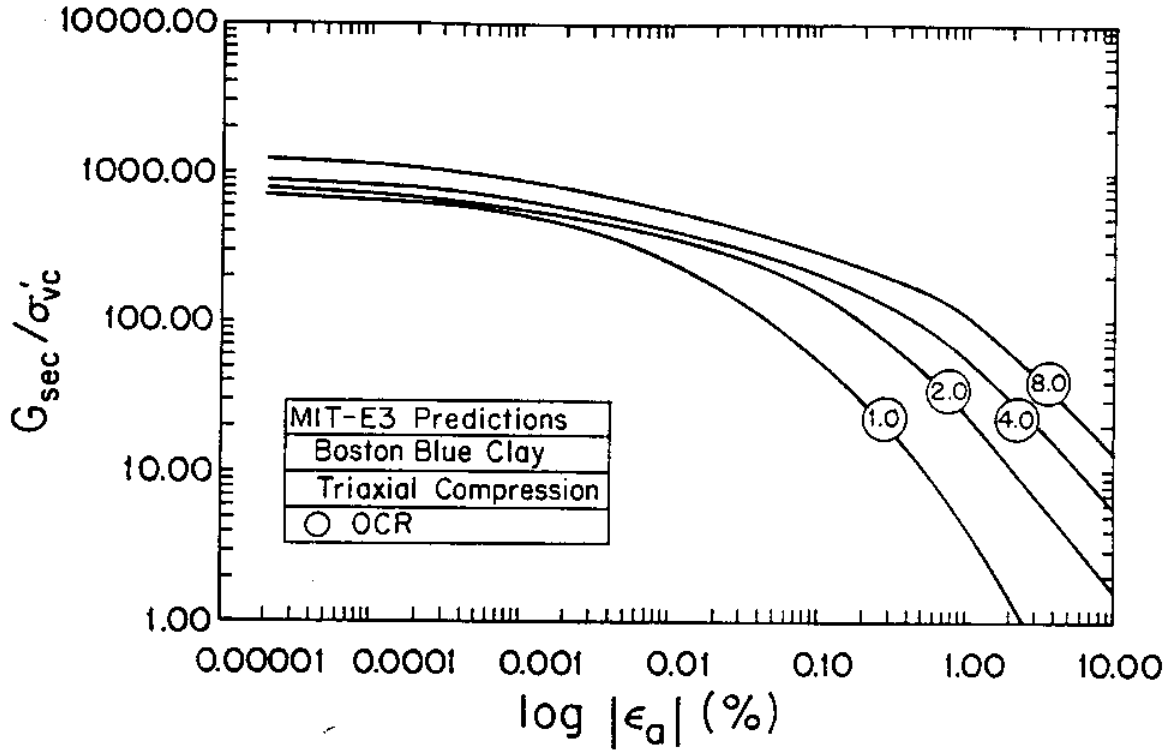

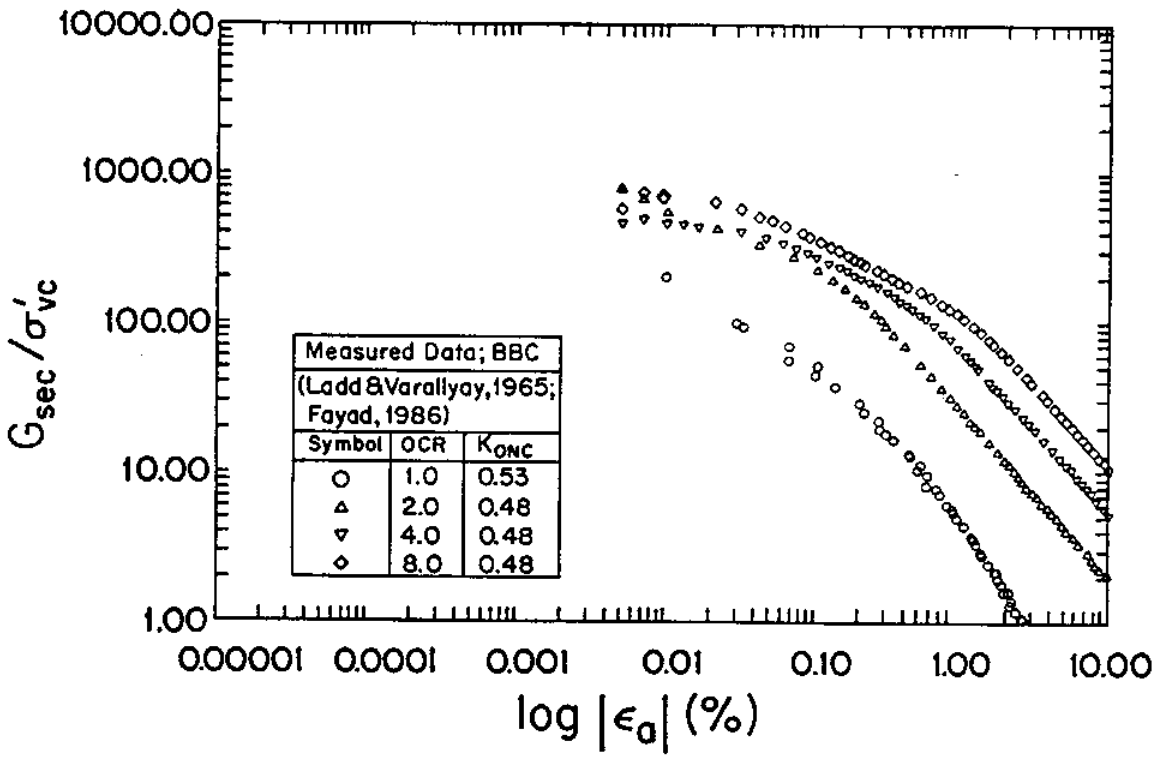

d) Secant Stiffness versus Strain

5. Comparison of Model Predictions and Measured Data for K_0-Consolidated, Undrained Triaxial Tests on Resedimented Boston Blue Clay

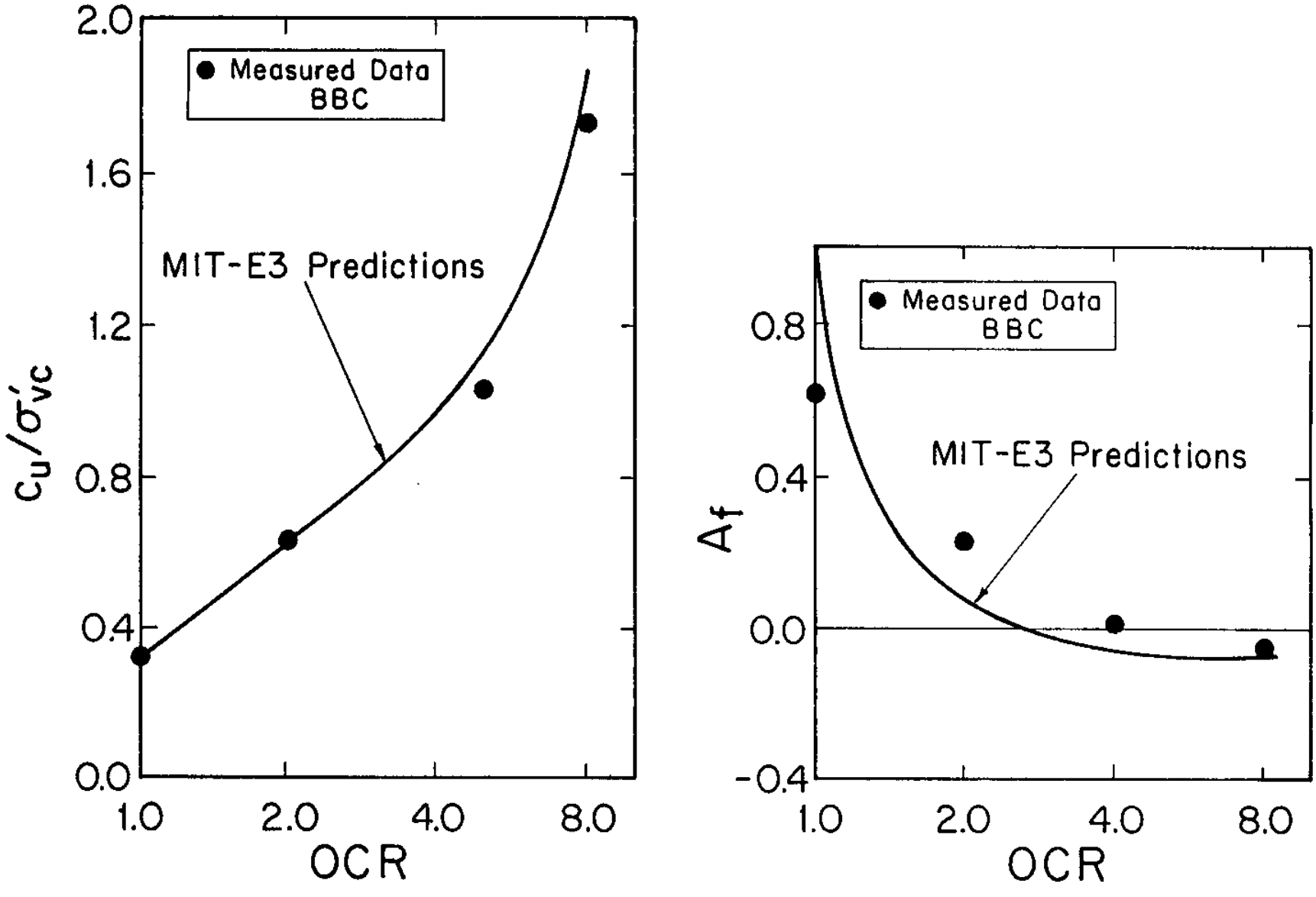

6. Comparison of Measured and Predicted Conditions at Peak Shear Stress in Undrained Triaxial Compression Tests

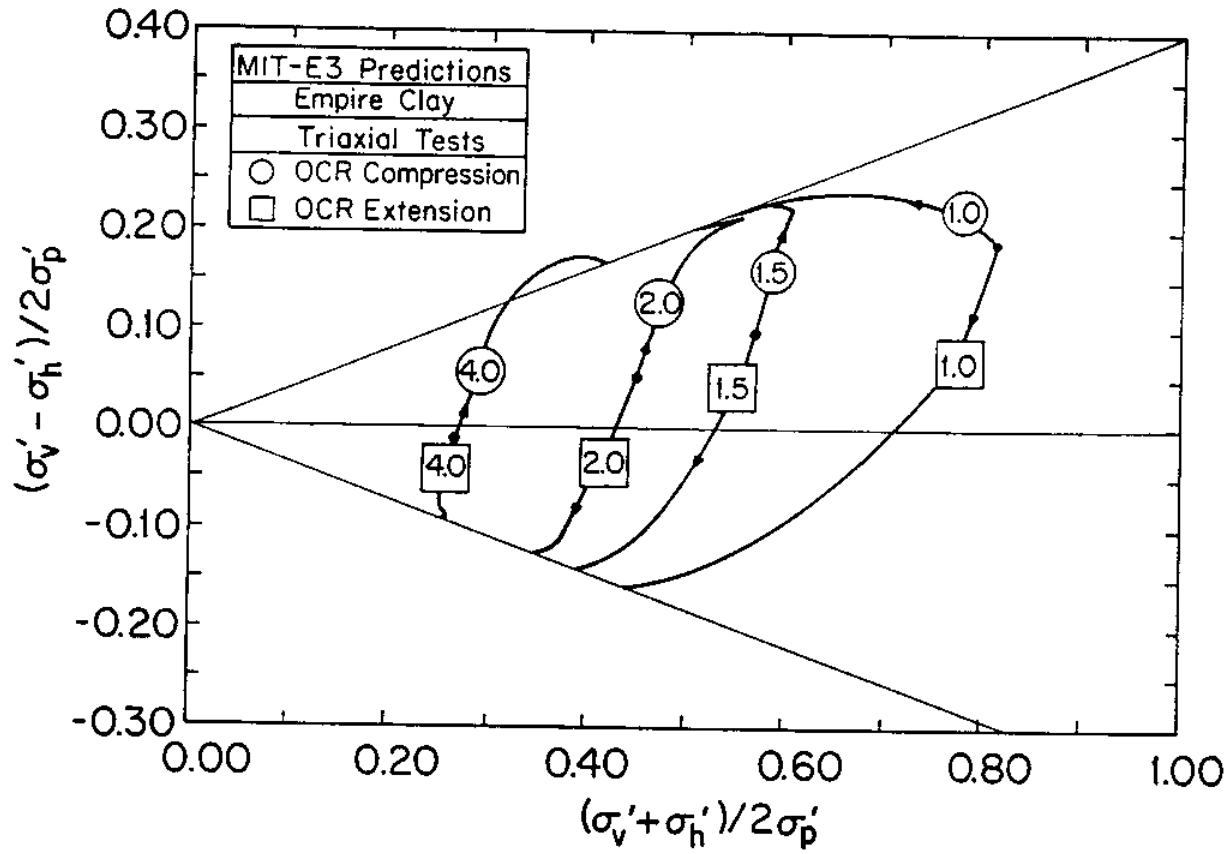

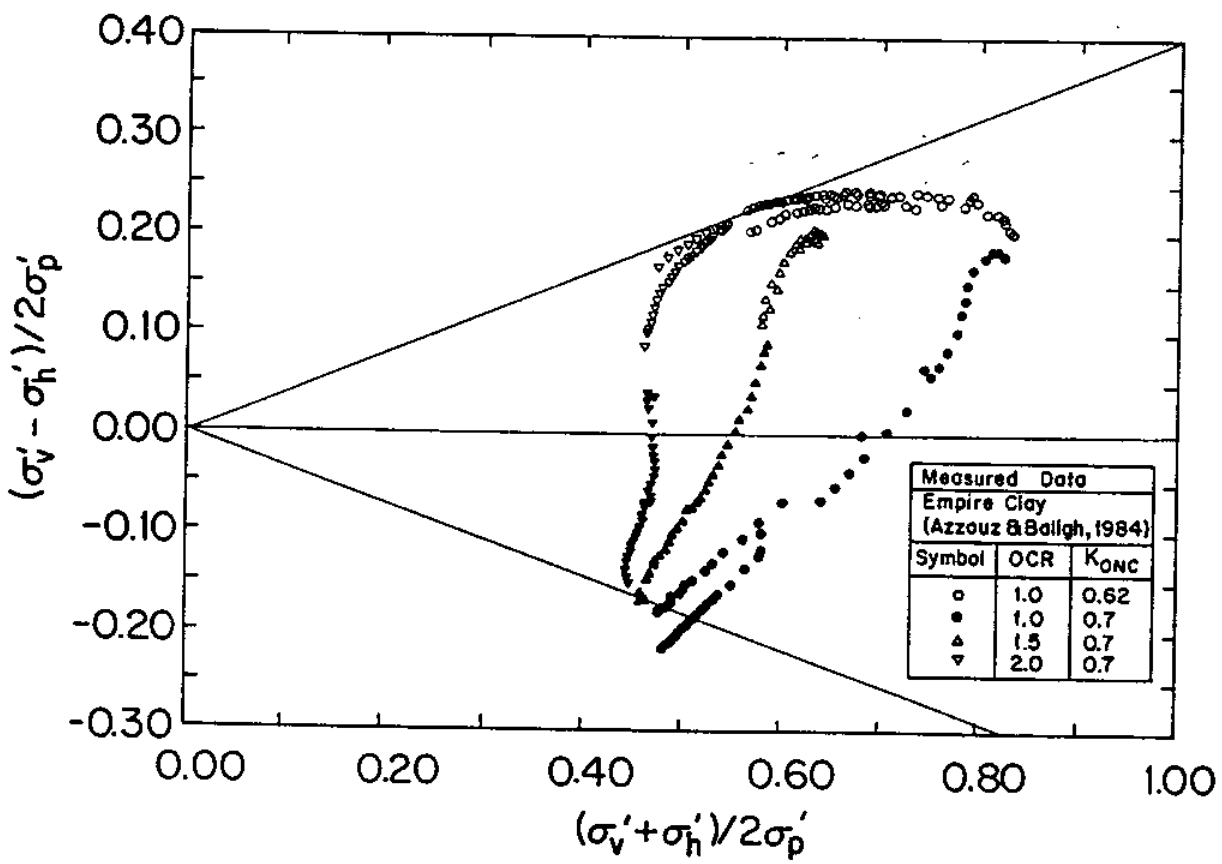

a) Effective Stress Paths

7. Comparison of Model Predictions and Measured Data for K_0-Consolidated, Undrained Triaxial Tests on Empire Clay

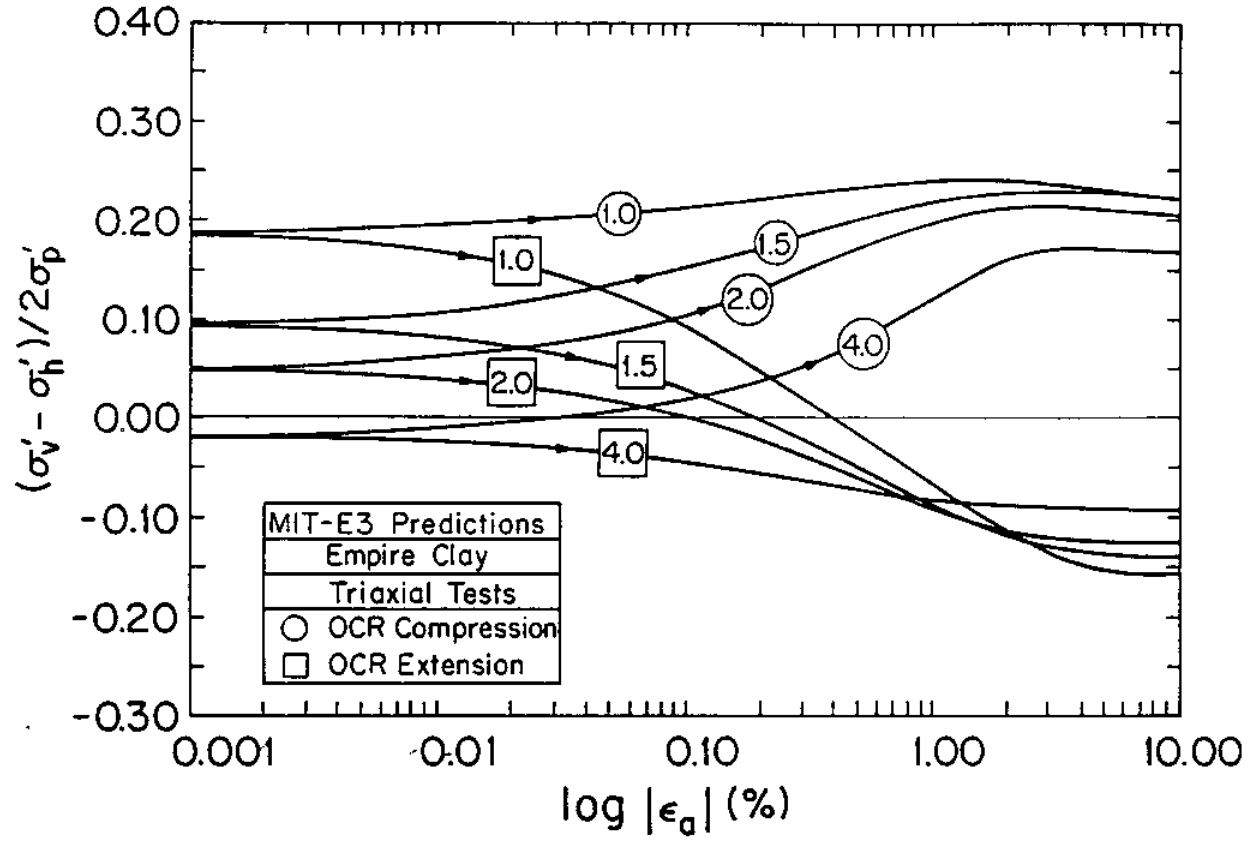

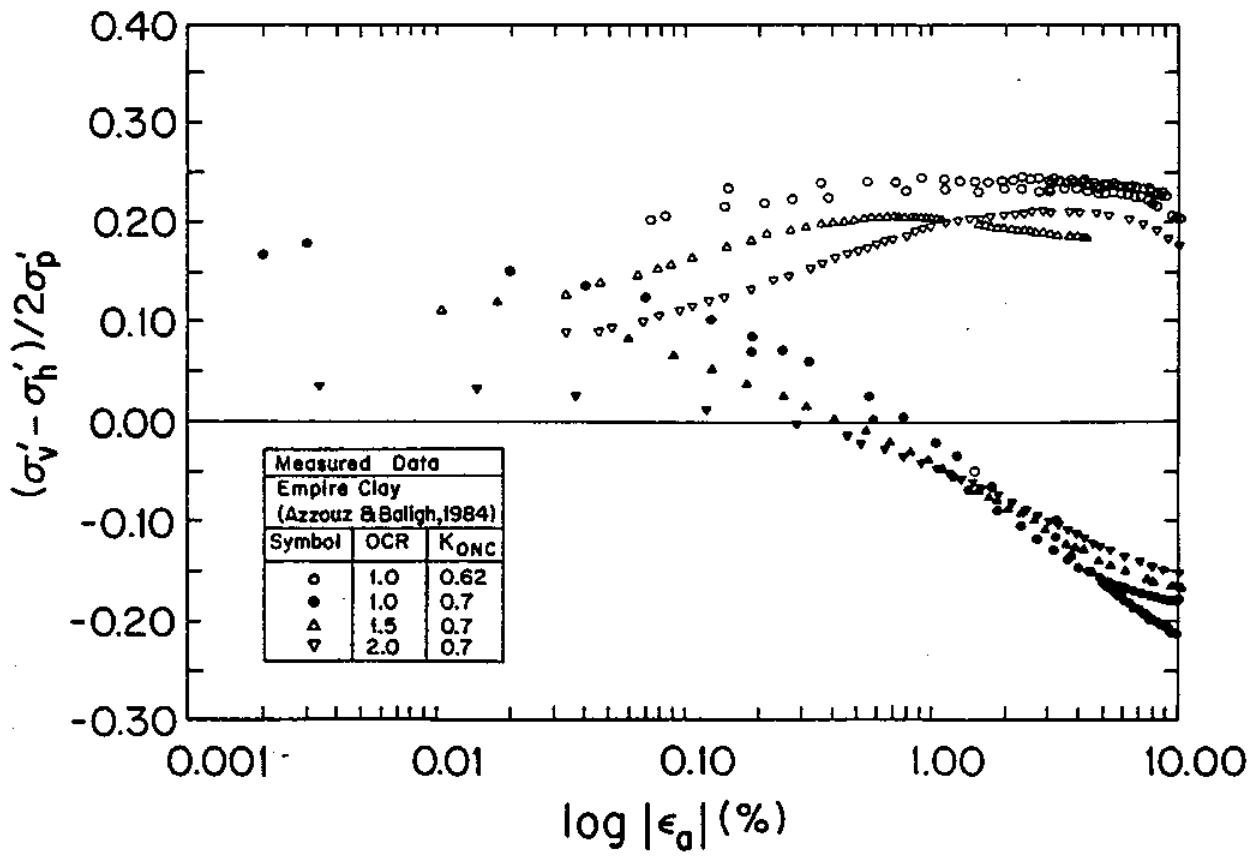

b) Stress-Strain Response

7. Comparison of Model Predictions and Measured Data for K_0-Consolidated, Undrained Triaxial Tests on Empire Clay

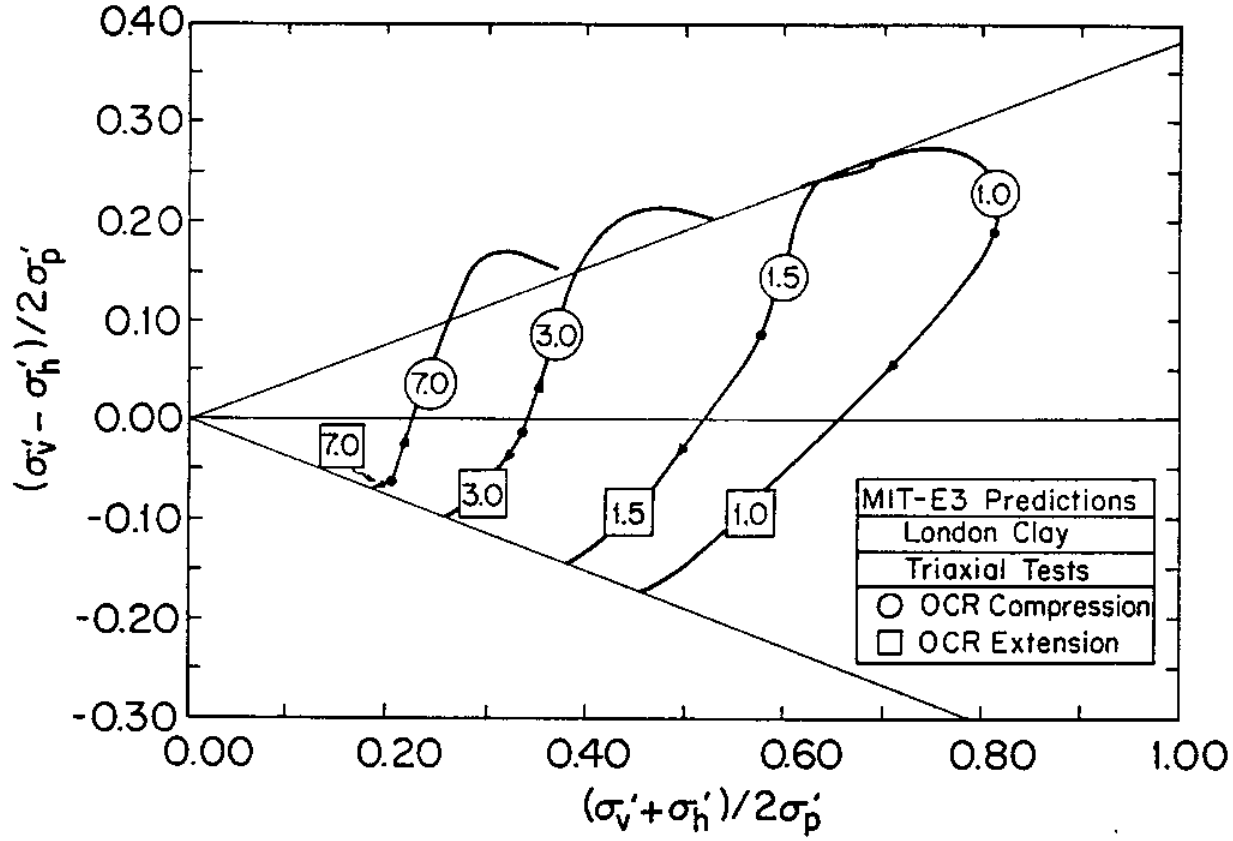

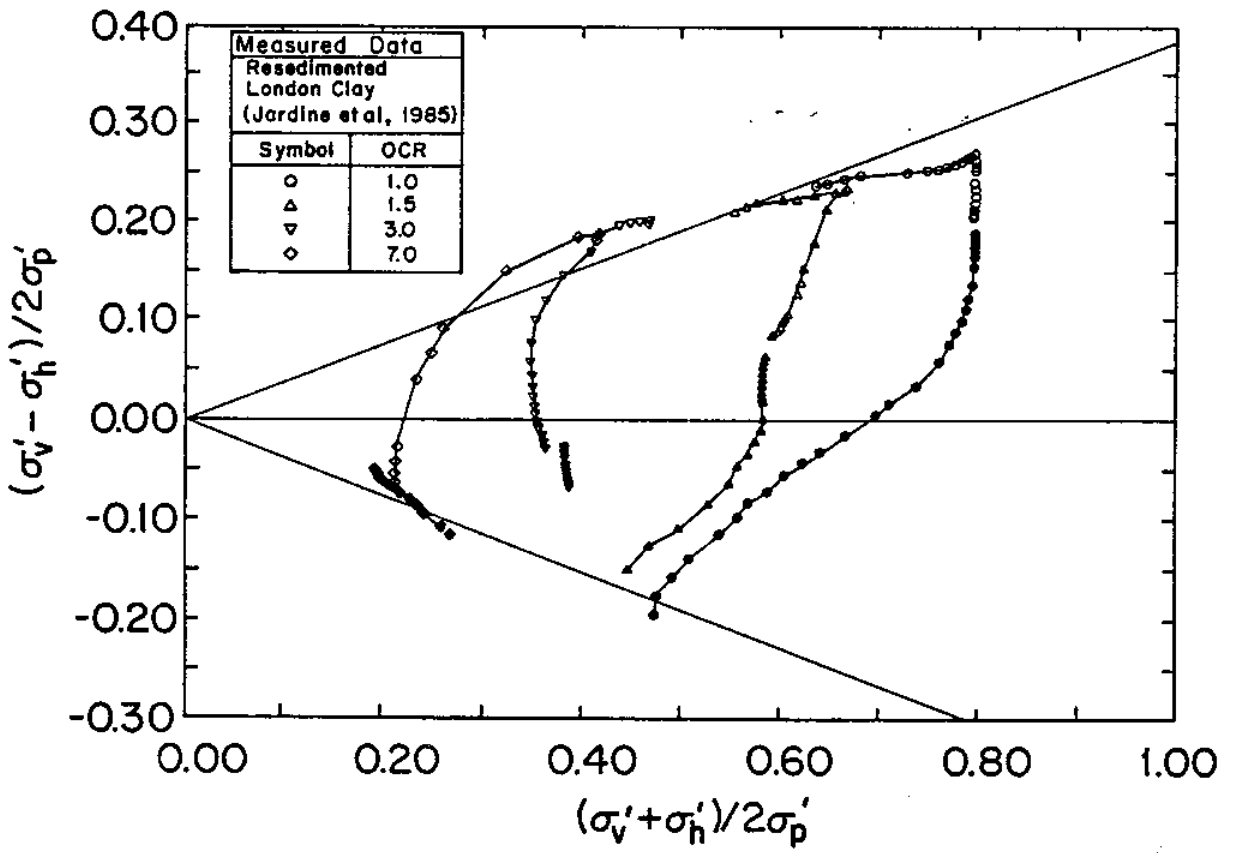

a) Effective Stress Paths

8. Comparison of Model Predictions and Measured Data for K_0-Consolidated, Undrained Triaxial Tests on Resedimented London Clay

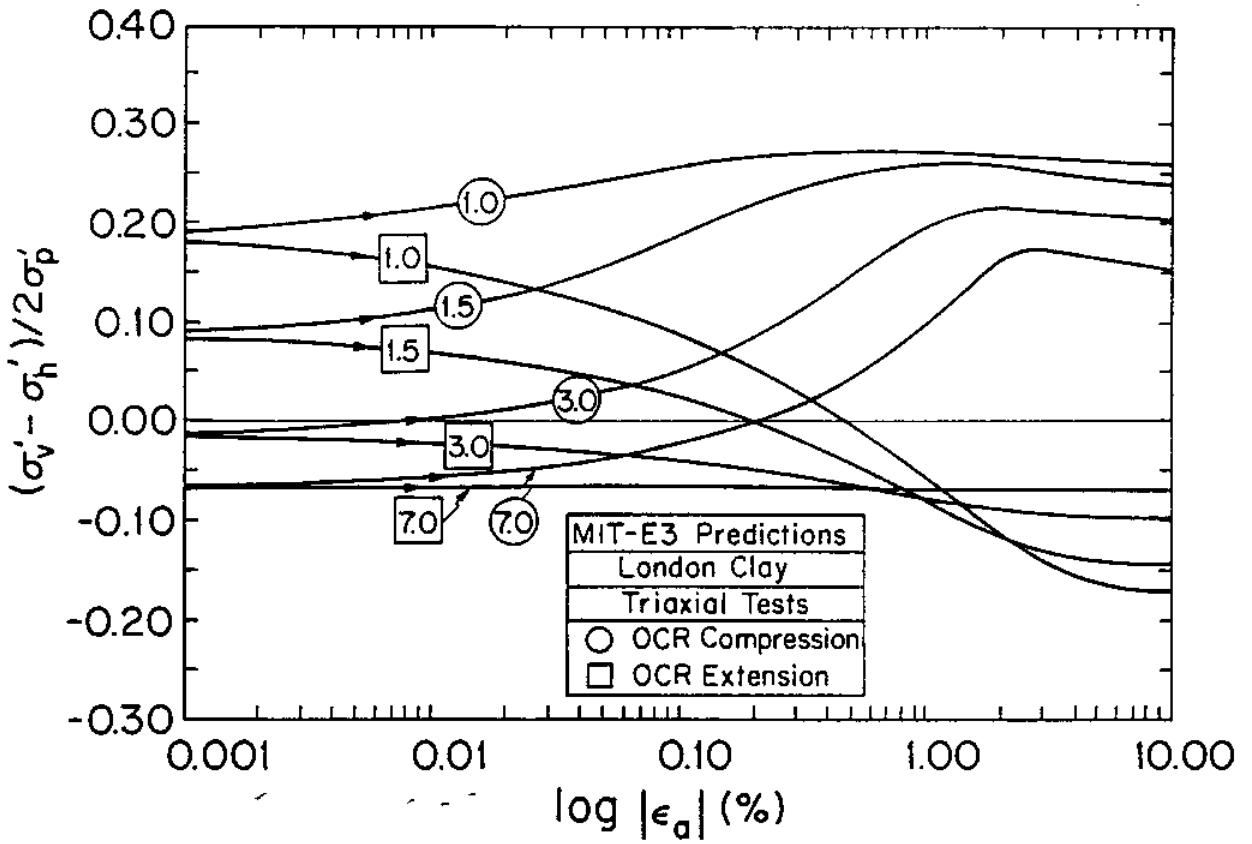

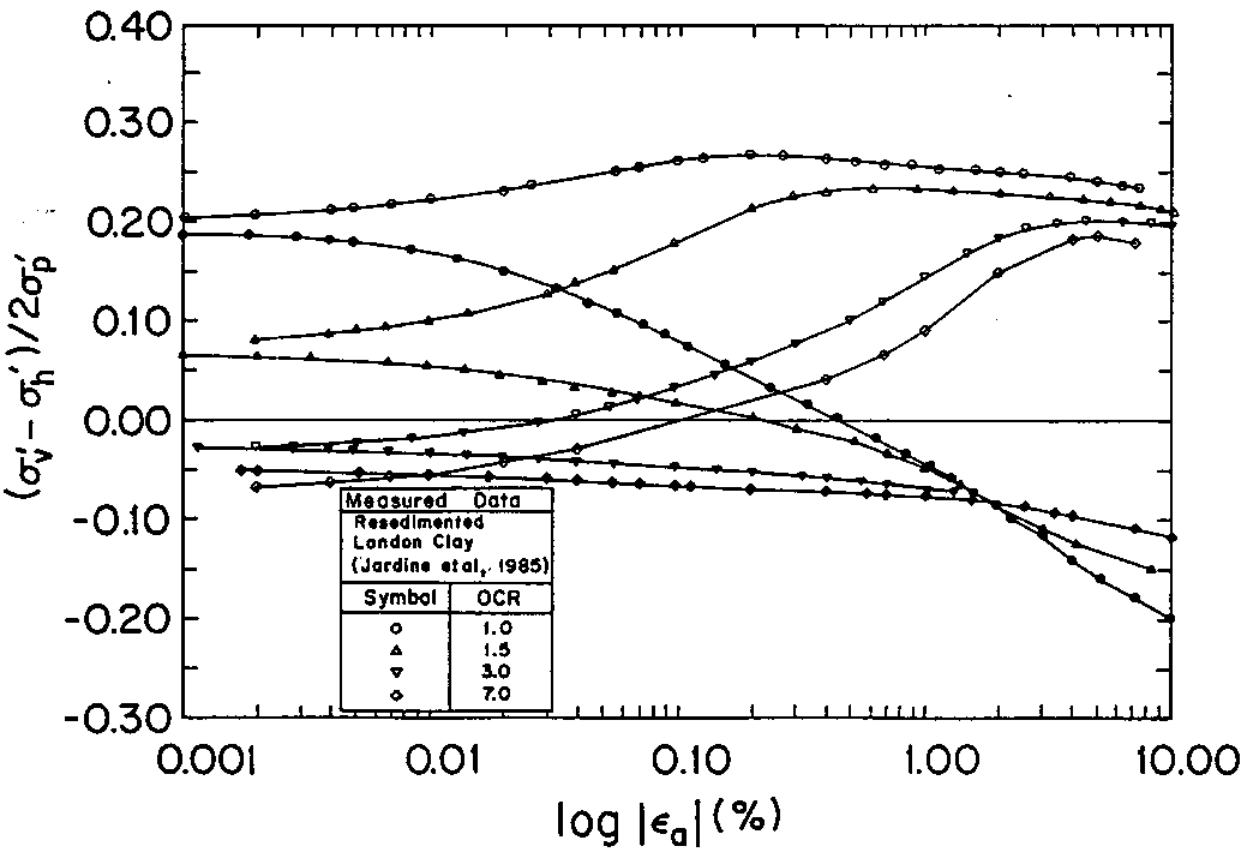

b) Stress-Strain Response

8. Comparison of Model Predictions and Measured Data for K_0-Consolidated, Undrained Triaxial Tests on Resedimented London Clay

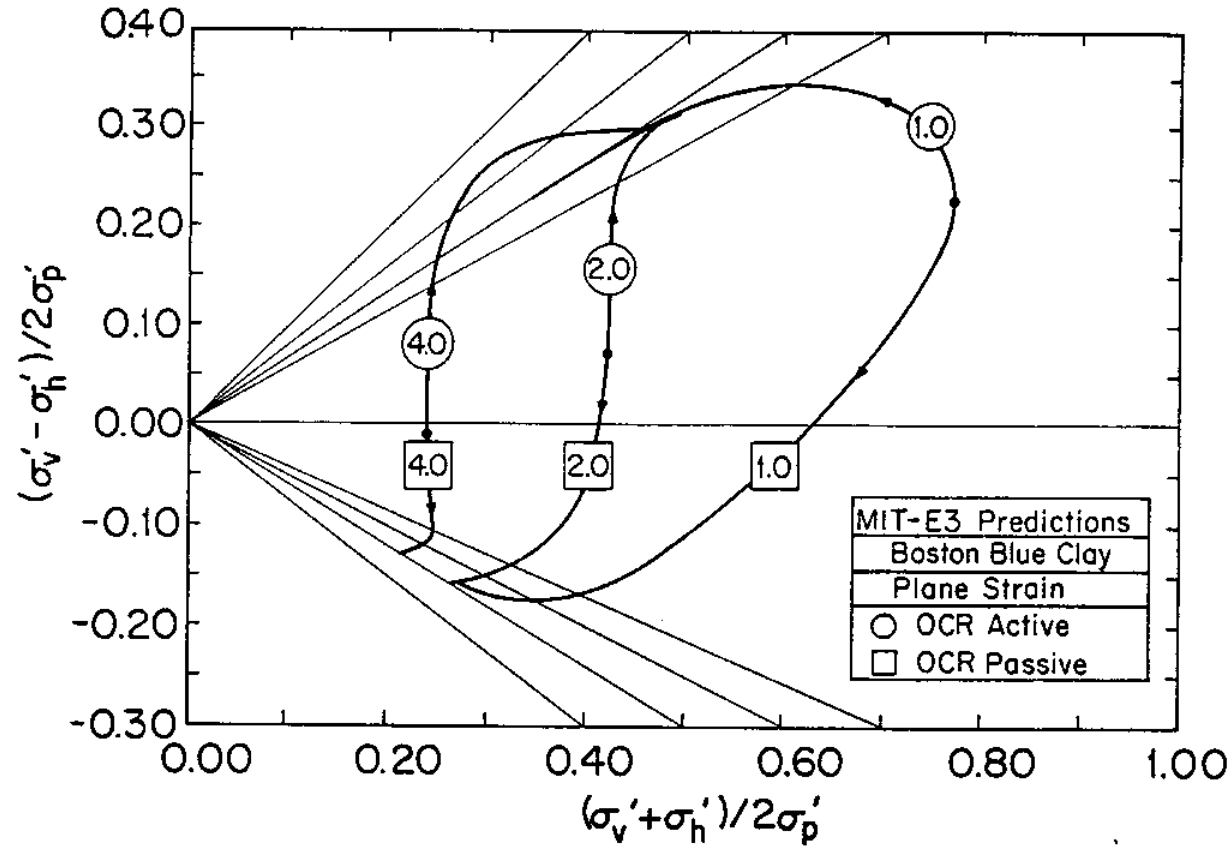

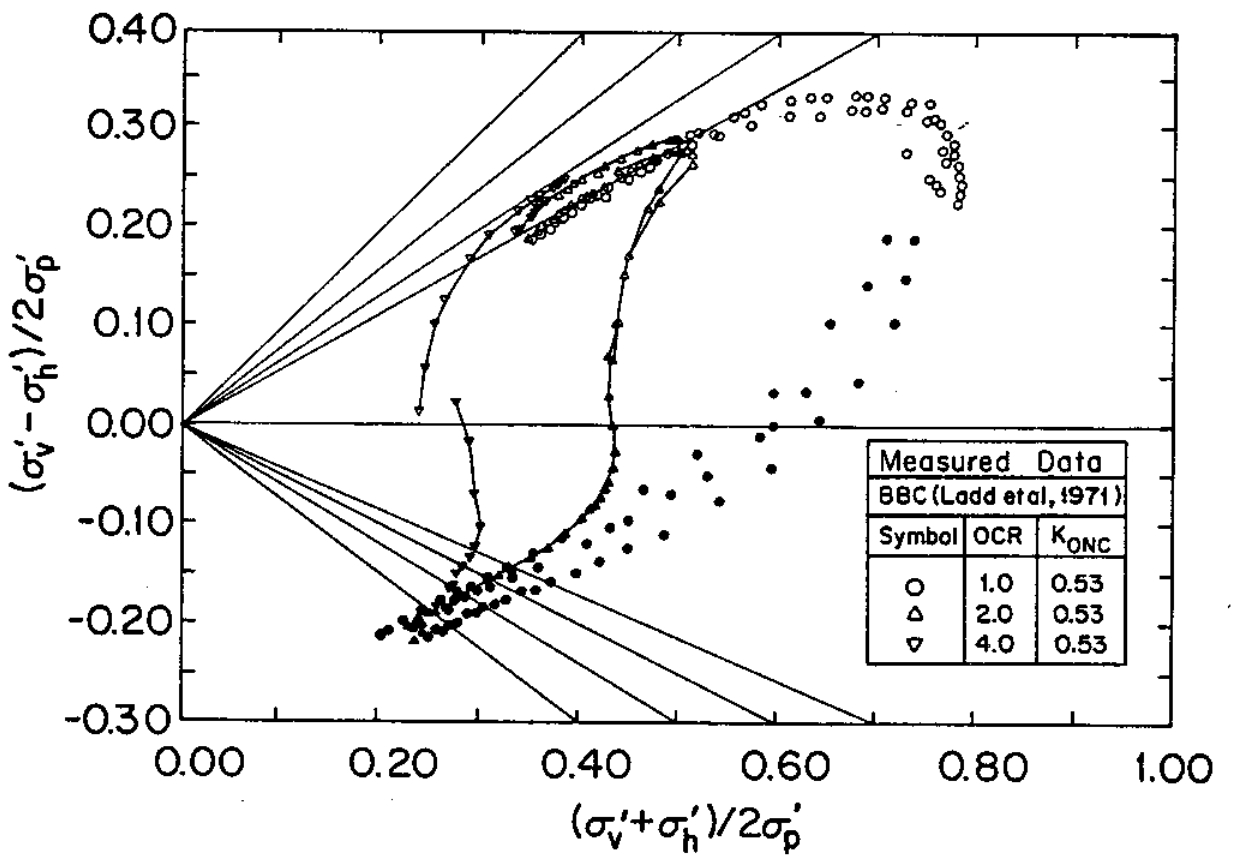

a) Effective Stress Paths

9. Comparison of Model Predictions and Measured Data for K_0-Consolidated, Undrained Plane Strain Compression and Extension Tests on Boston Blue Clay

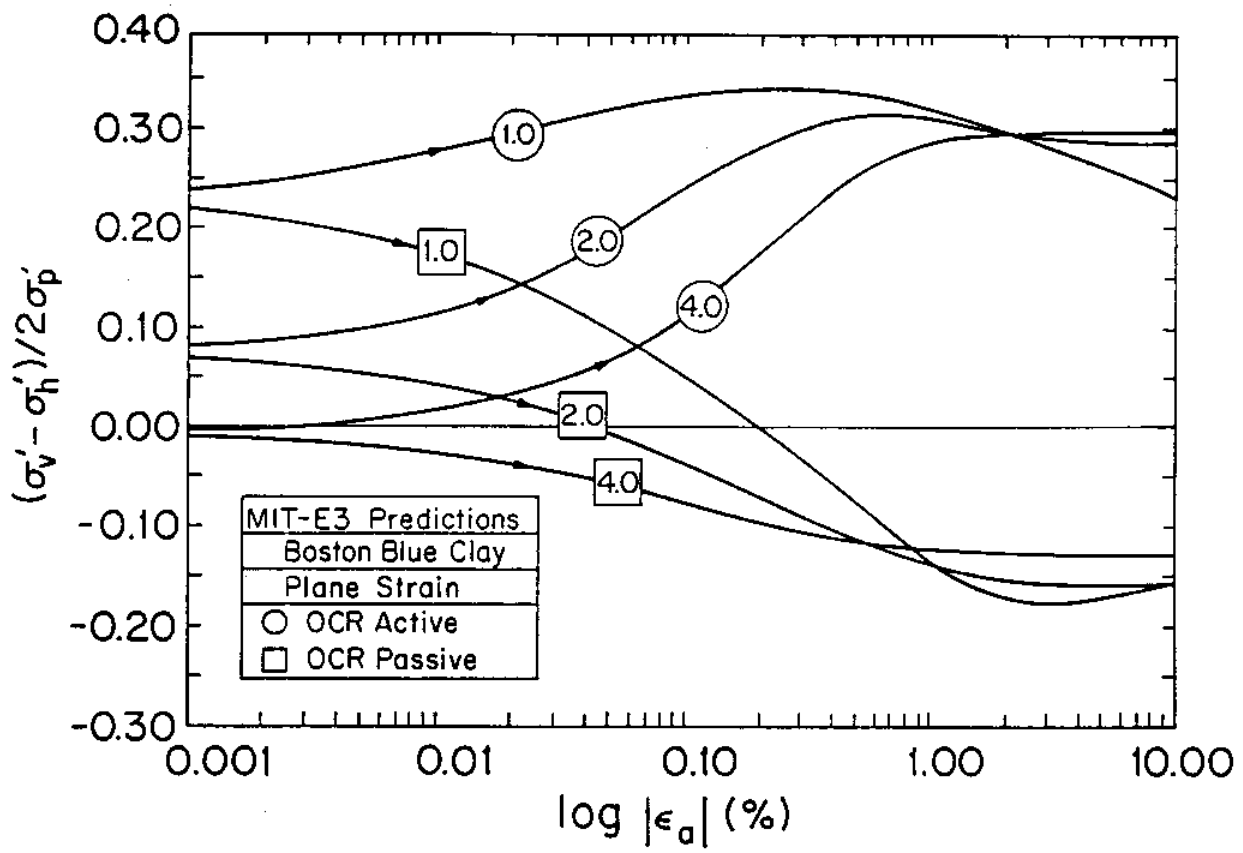

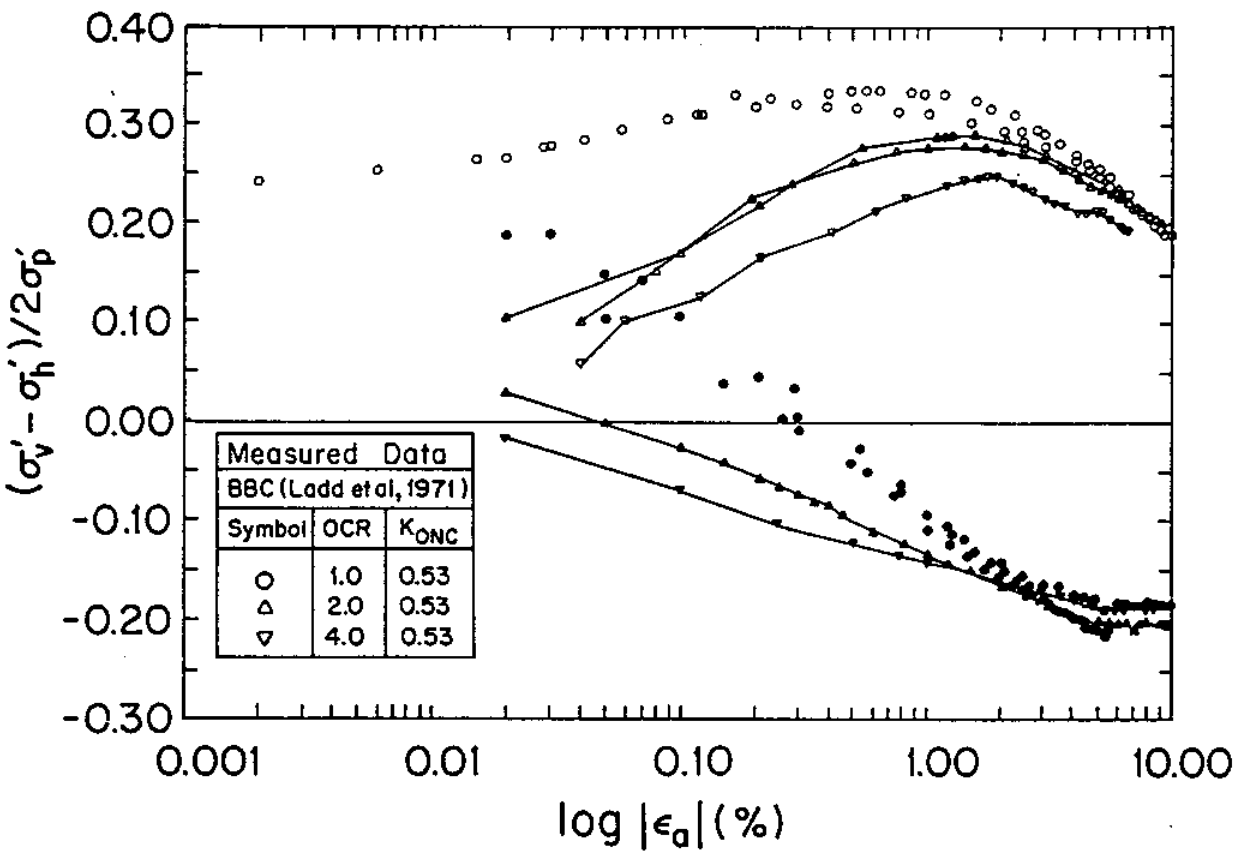

b) Stress-Strain Response

9. Comparison of Model Predictions and Measured Data for K_0-Consolidated, Undrained Plane Strain Compression and Extension Tests on Boston Blue Clay

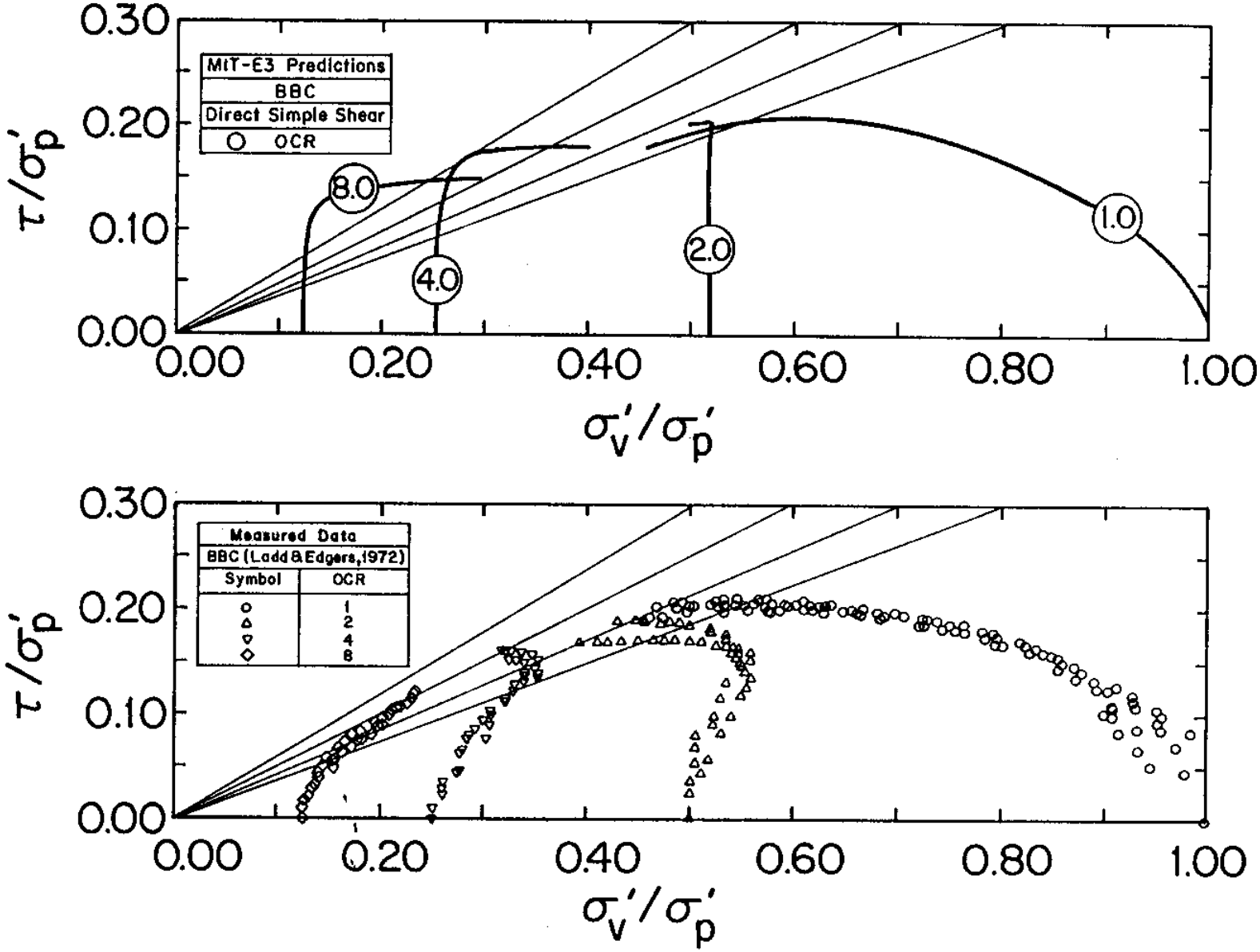

a) Effective Stress Paths

10. Comparison of Model Predictions and Measured Data for K_0-Consolidated, Undrained Direct Simple Shear Tests on Boston Blue Clay

b) Stress-Strain Response

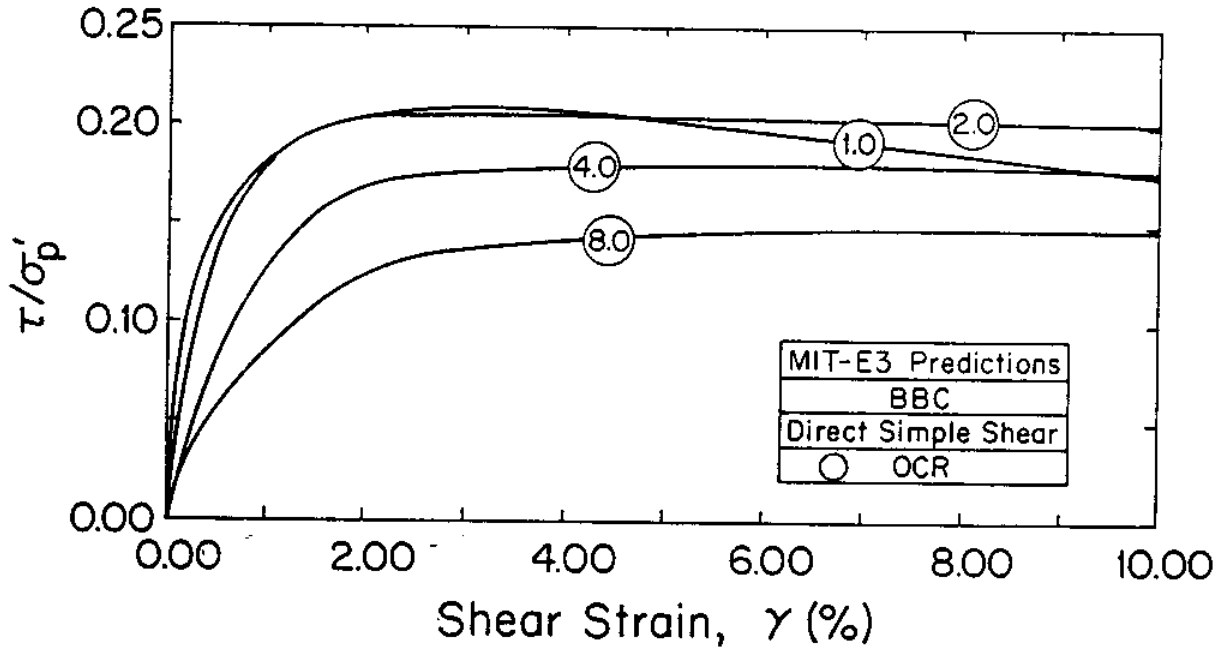

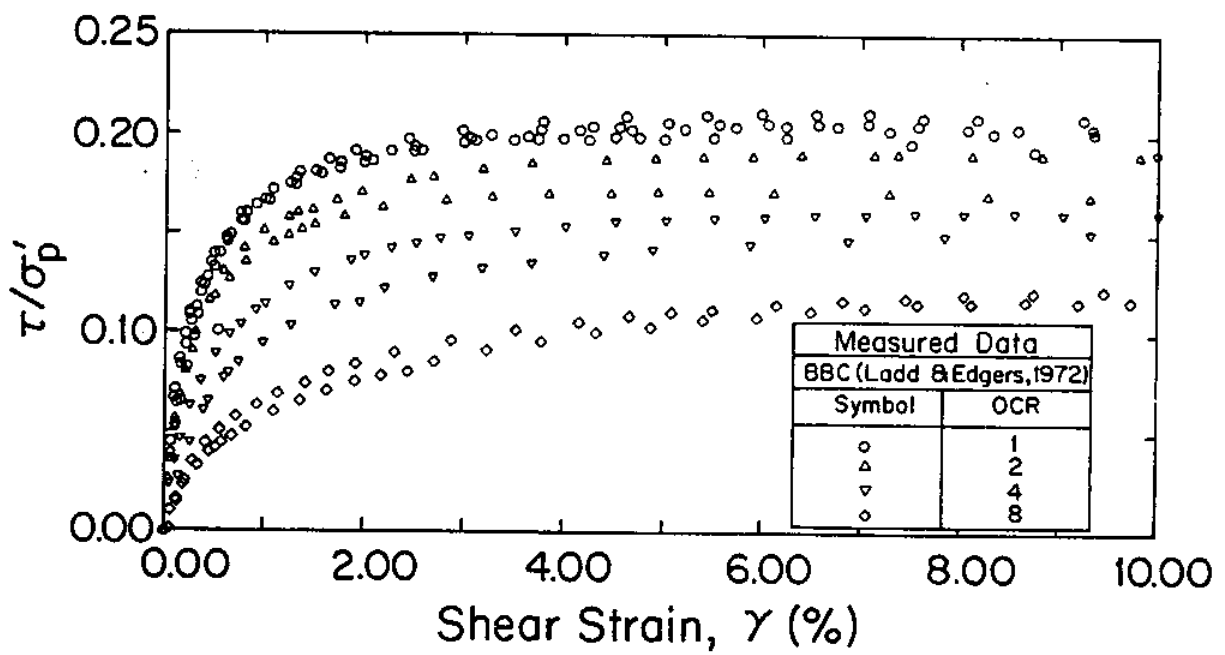

10. Comparison of Model Predictions and Measured Data for K_0-Consolidated, Undrained Direct Simple Shear Tests on Boston Blue Clay

c) Shear stress versus log Strain

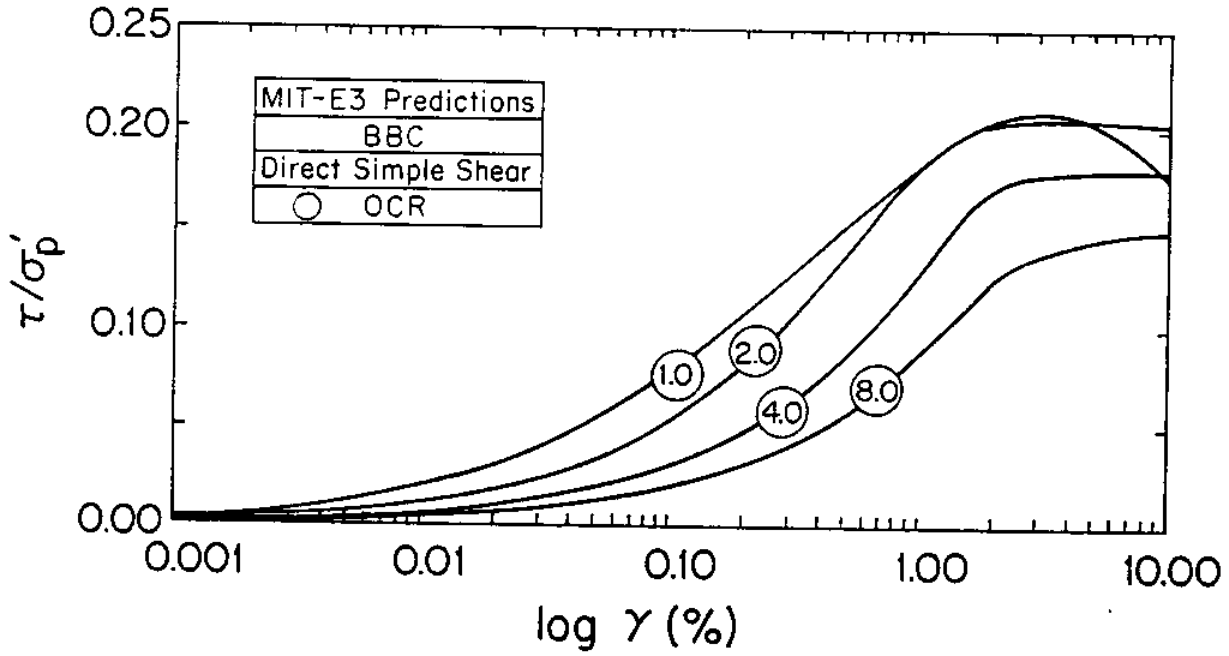

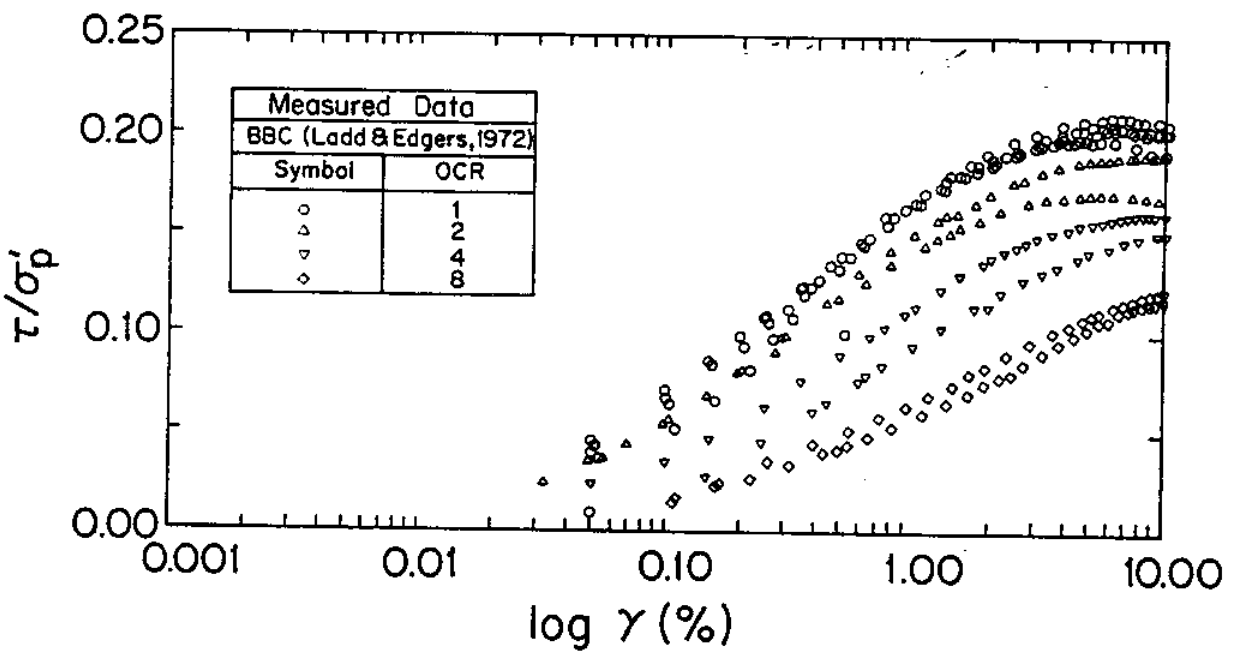

10. Comparison of Model Predictions and Measured Data for K_0-Consolidated, Undrained Direct Simple Shear Tests on Boston Blue Clay

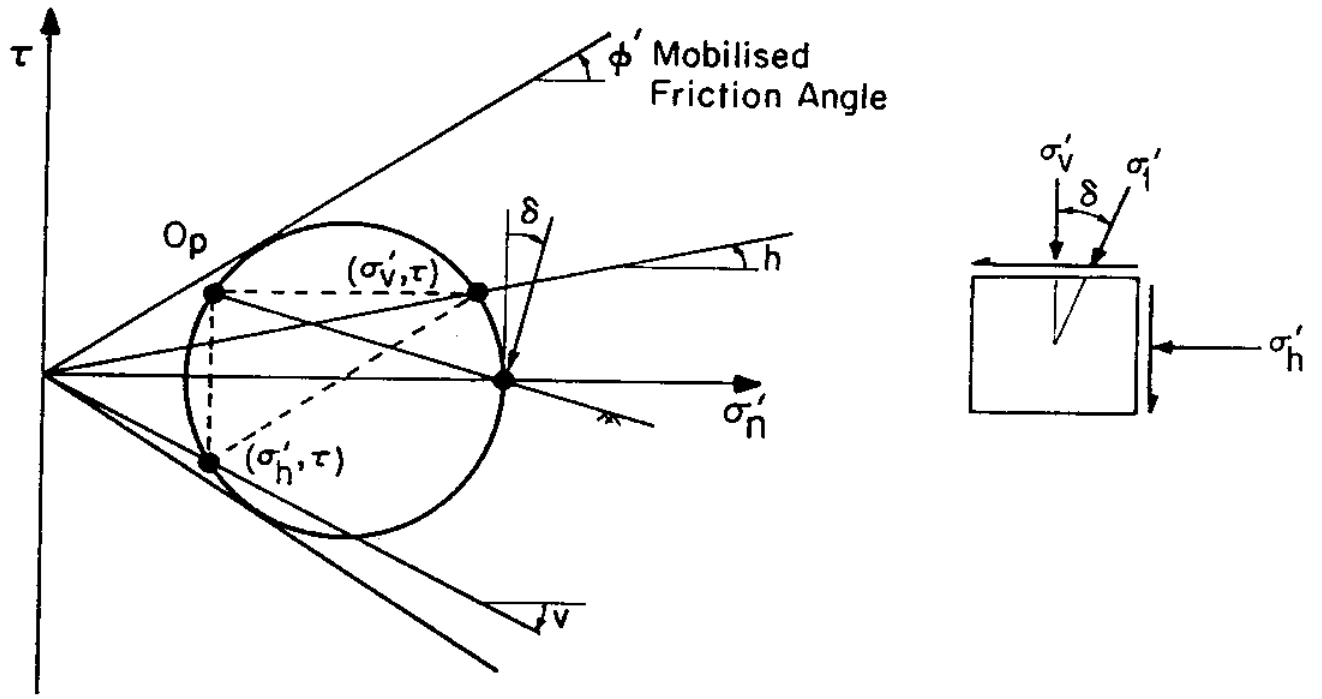

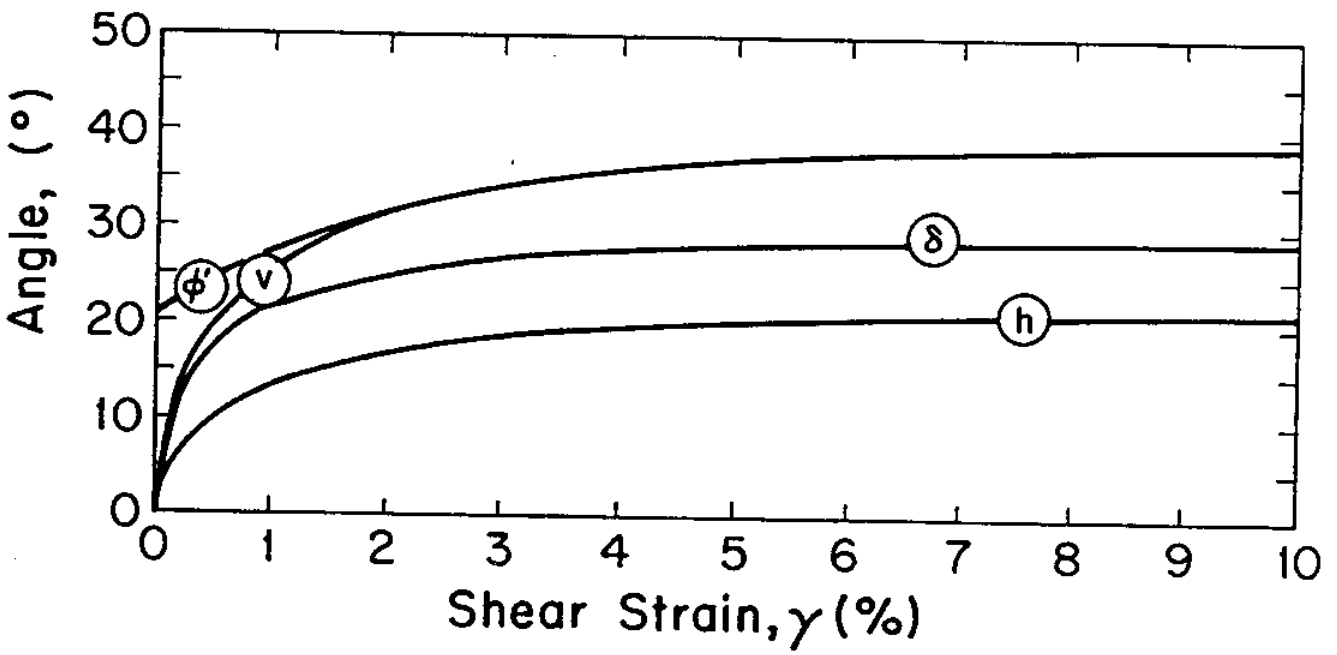

11. MIT-E3 Predictions of Principal Stress Rotation in for Undrained Direct Simple Shear of K_0-Normally Consolidated BBC

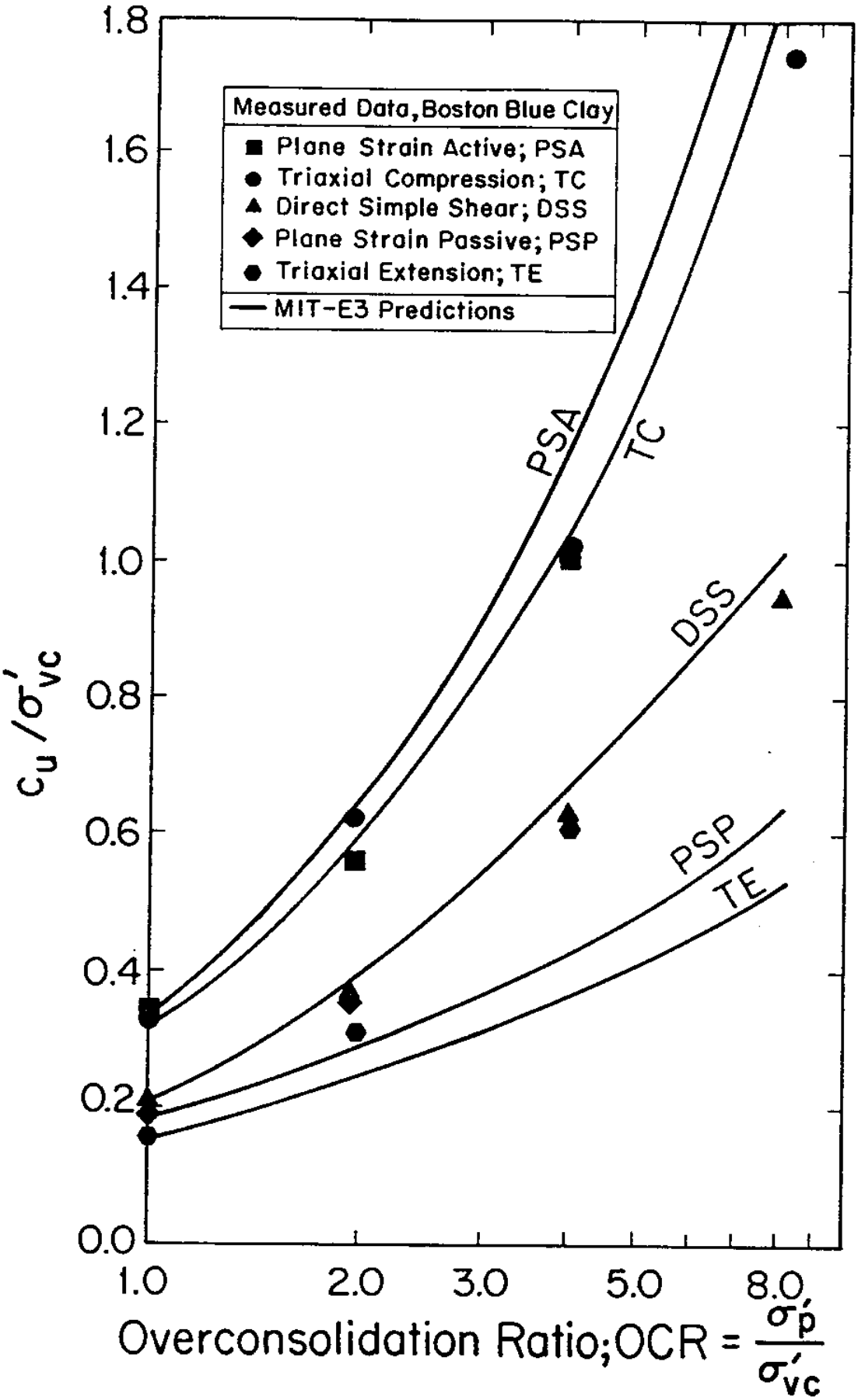

12. Evaluation of MIT-E3 Predictions of Undrained Shear Strength for Various Modes of Shearing

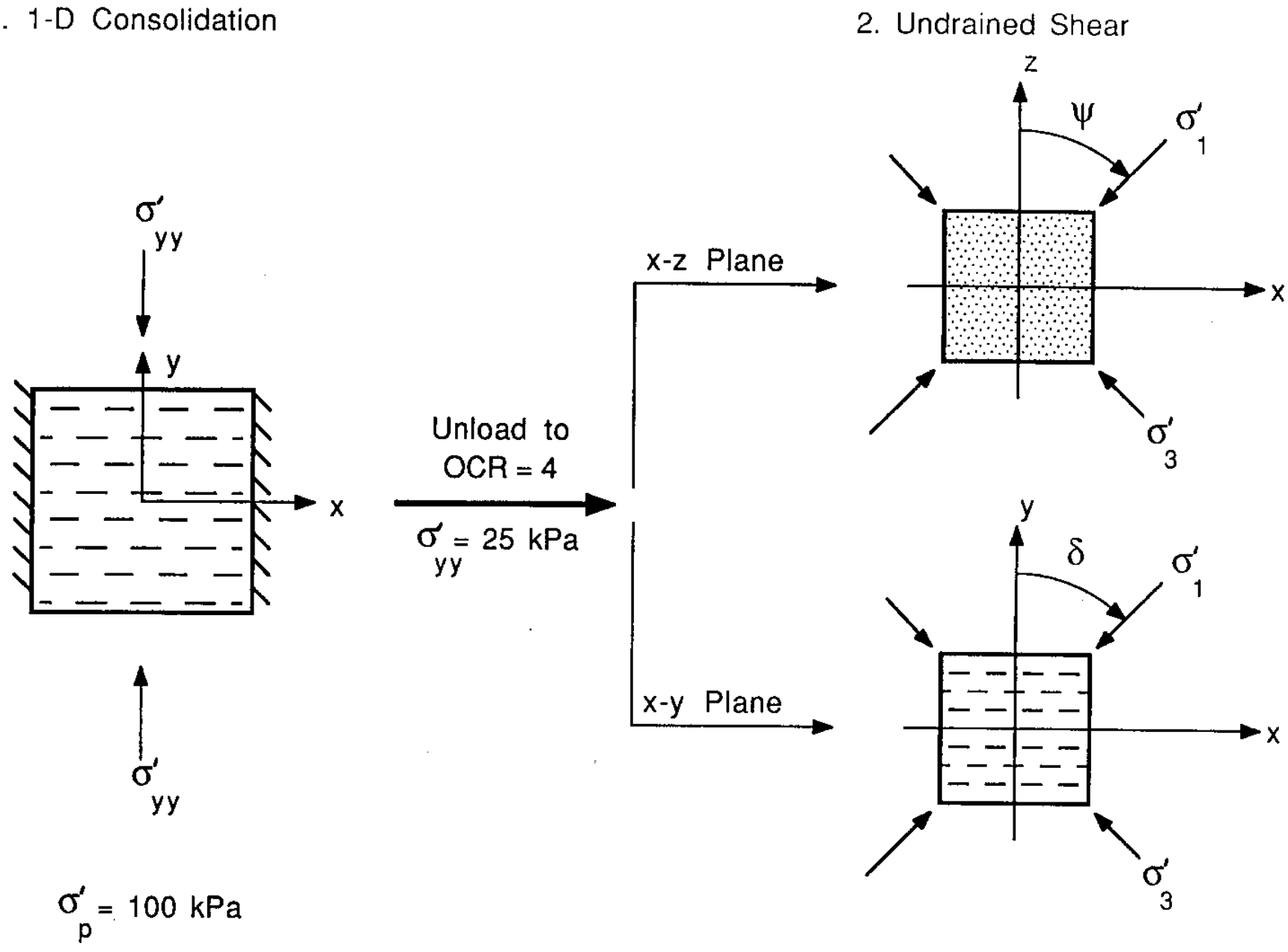

Fig. 13. Experimental Procedure used to Study Anisotropy due to 1-Dimensional Stress History using the Directional Shear Cell (Germaine, 1982; O'Neill, 1985)

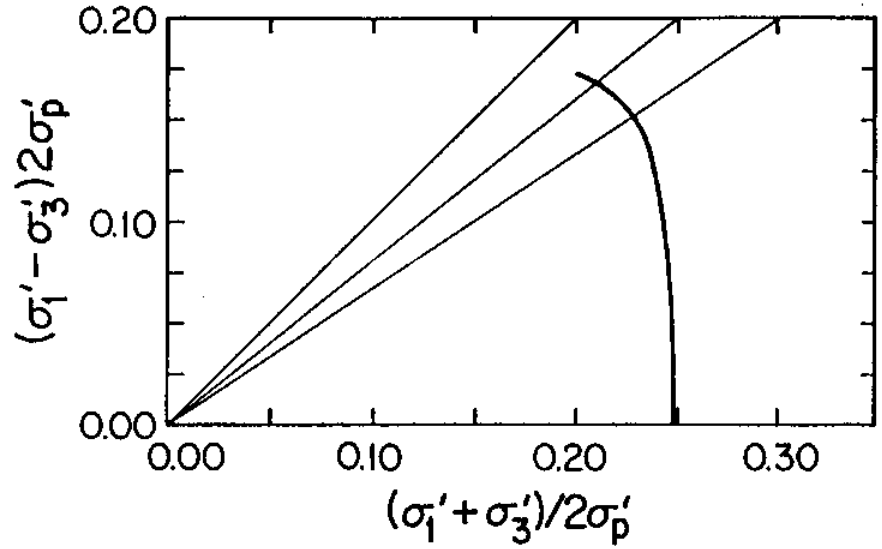

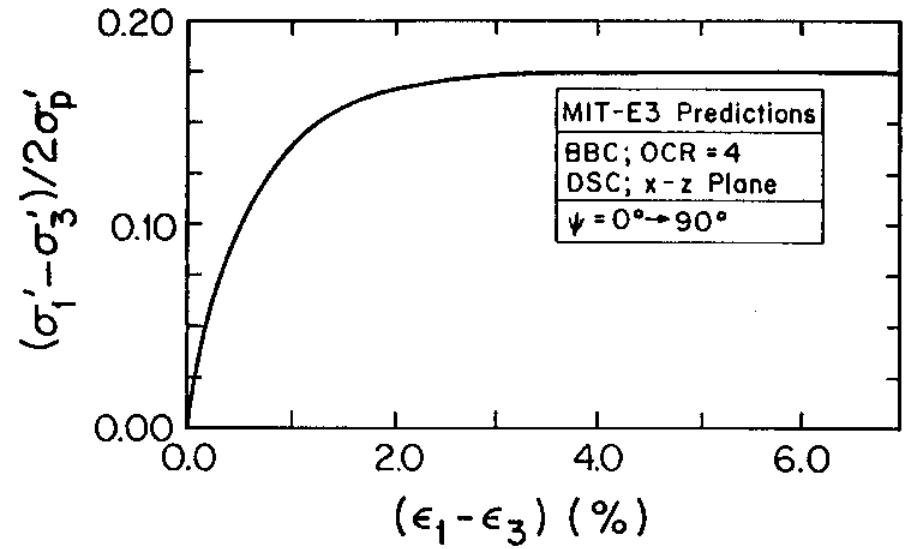

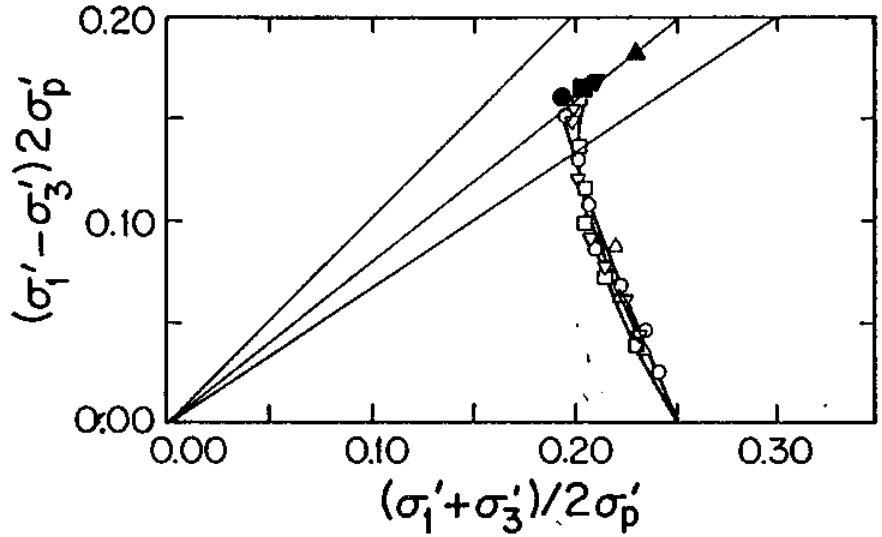

a) Effective Stress Paths

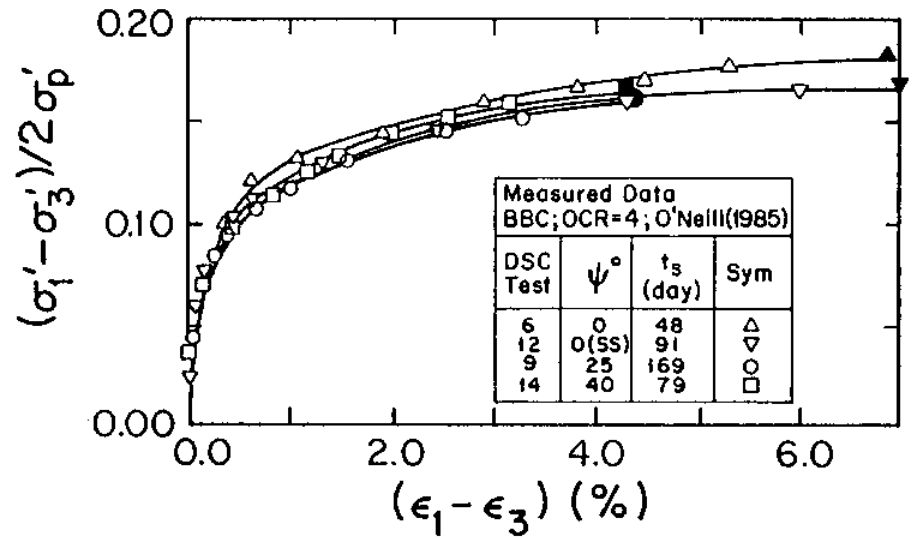

b) Stress-Strain Response

14. Comparison of Model Predictions and Measured Data for BBC at OCR≈4 in Undrained DSC Tests in the Isotropic (x-z) Plane

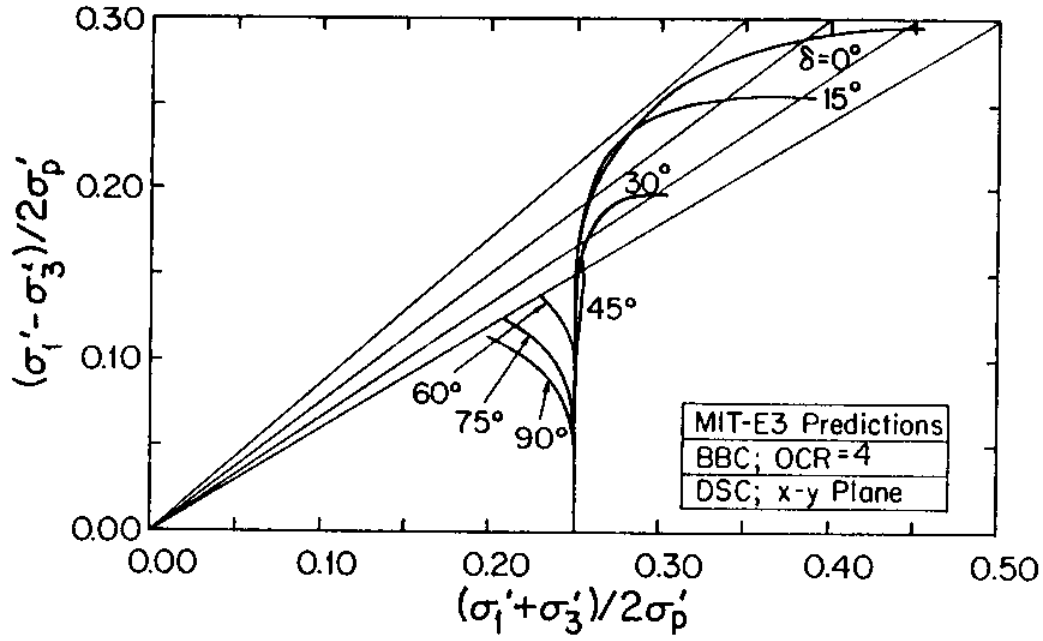

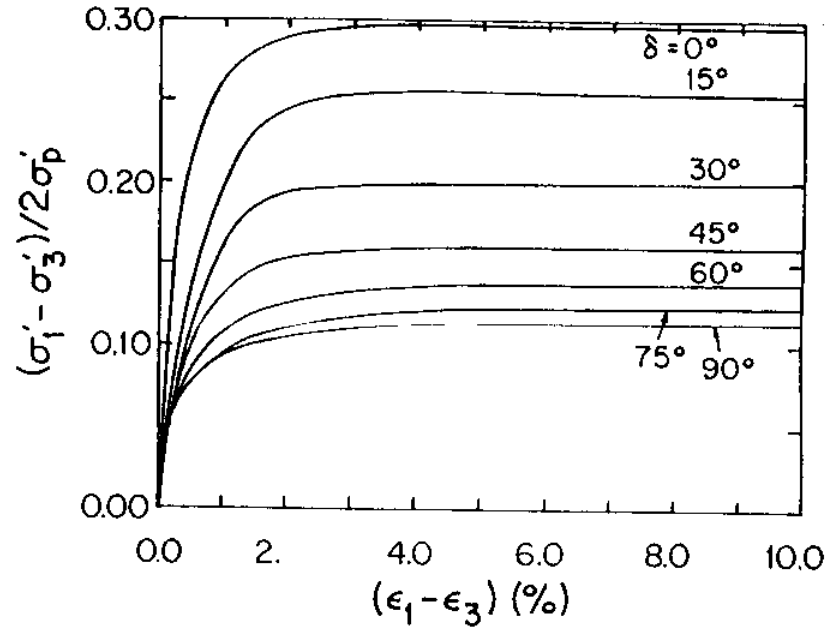

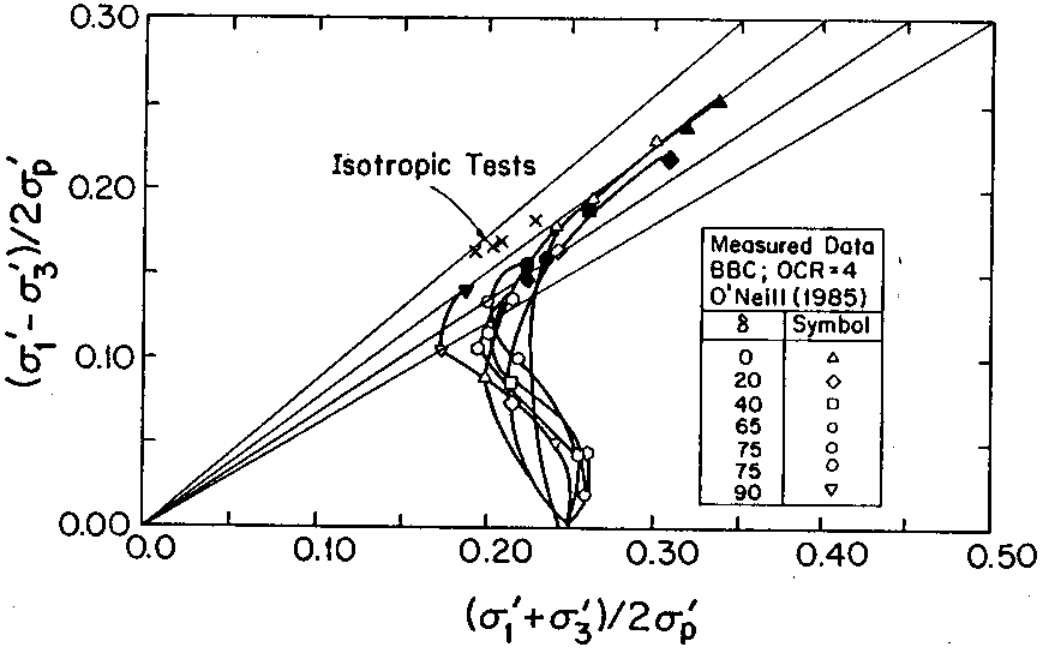

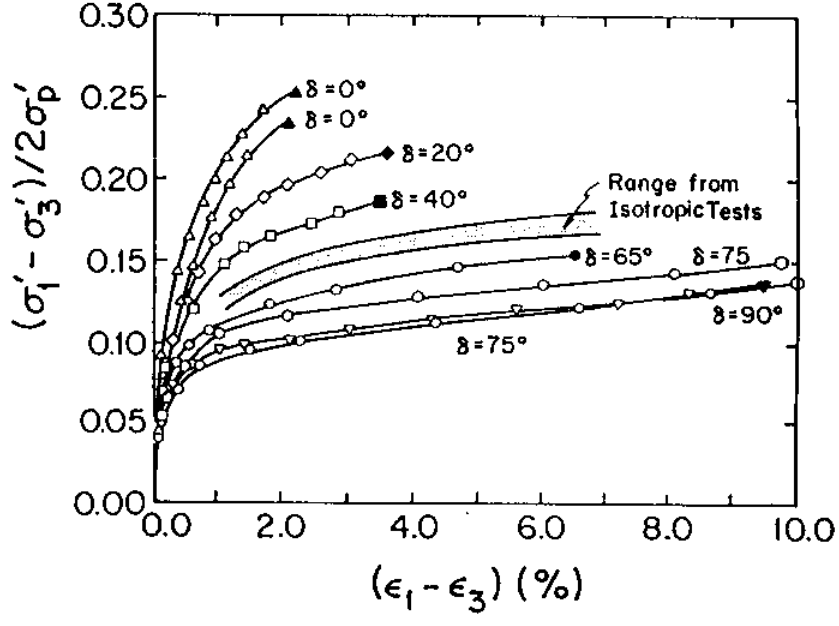

15. Comparison of Model Predictions and Measured Data for BBC at OCR≈4 in Undrained DSC Tests in the x-y Plane for Different Applied δ-Angles

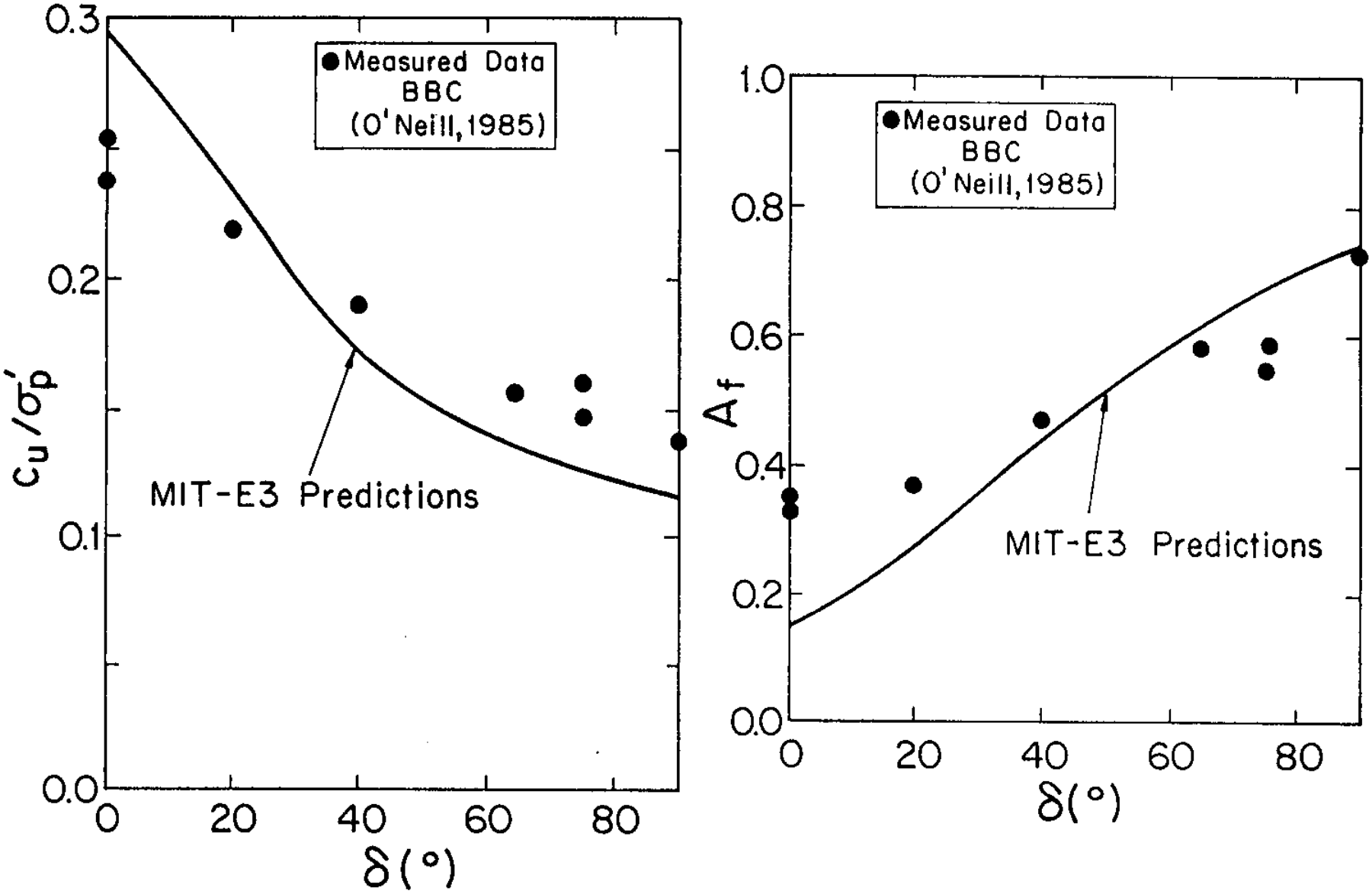

16. Evaluation of MIT-E3 Predictions of Peak Shear Strength Conditions in DSC Tests at OCR≈4

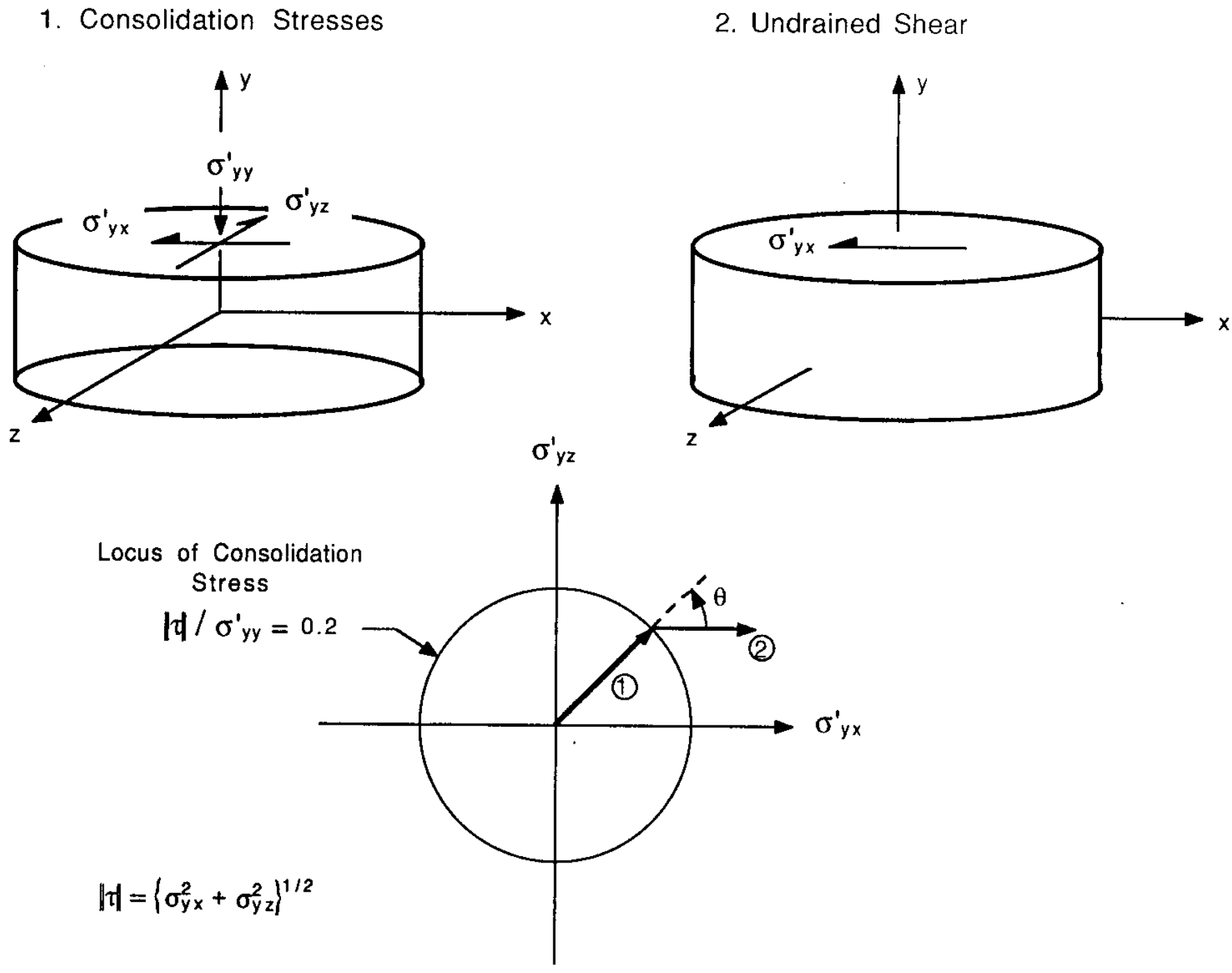

Fig. 17. Principle of the Multi-Directional Direct Simple Shear Apparatus (after DeGroot, 1989)

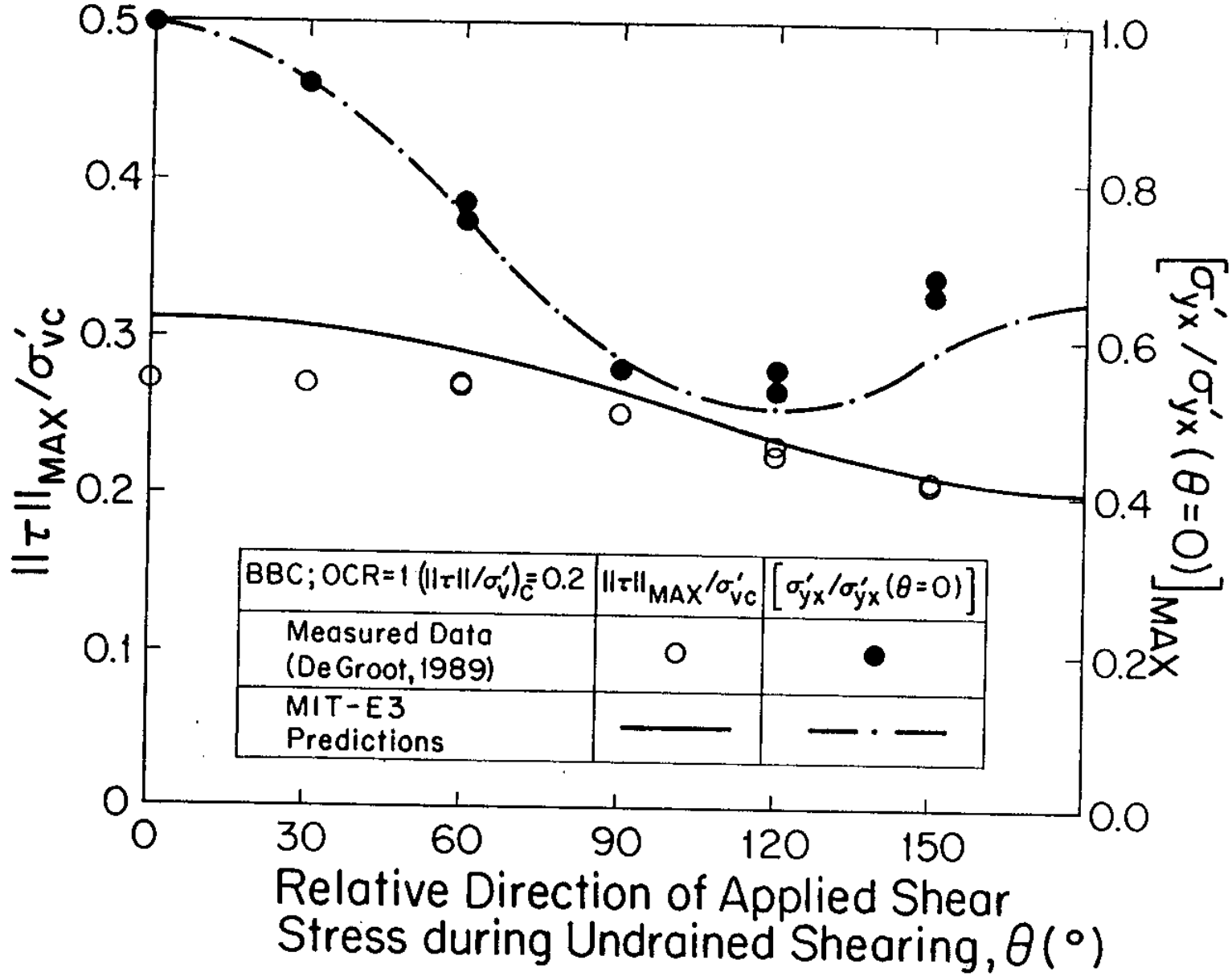

18. Comparison of MIT-E3 Predictions and Measured Undrained Shear Strength for MDSS Tests on K_0-Normally Consolidated Boston Blue Clay

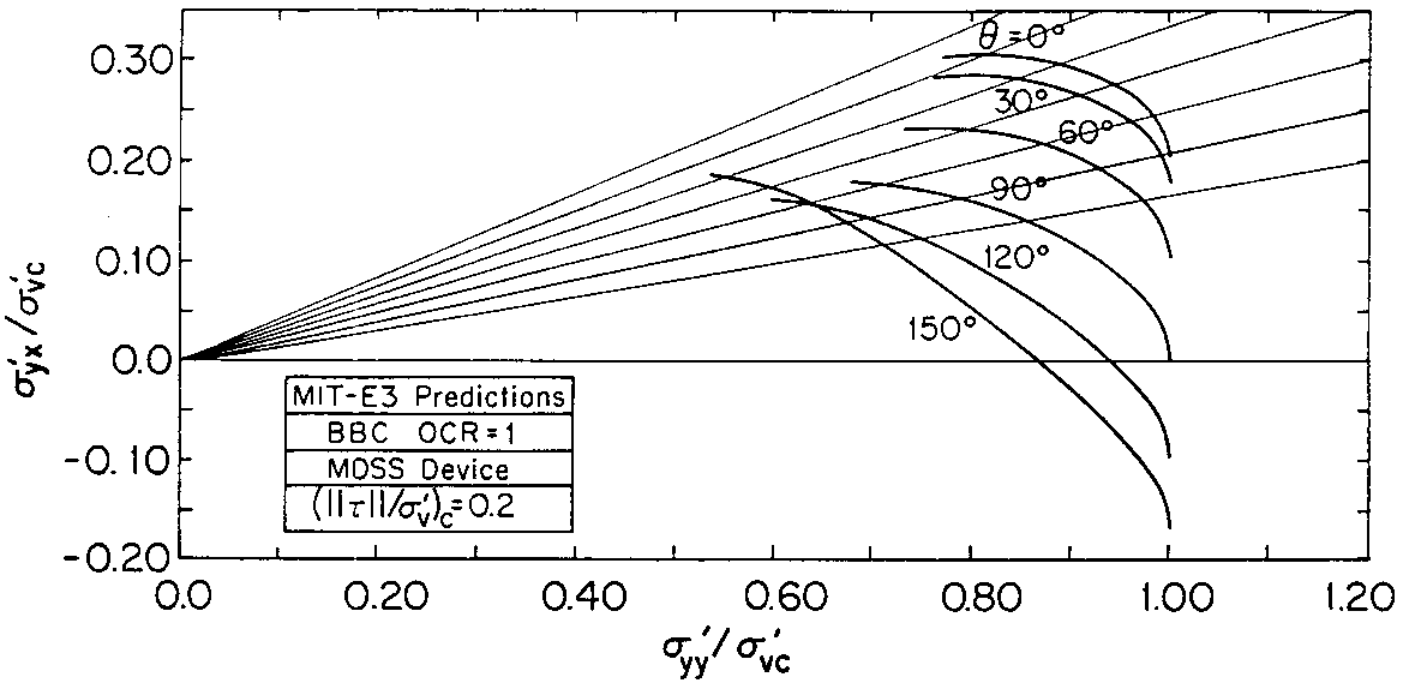

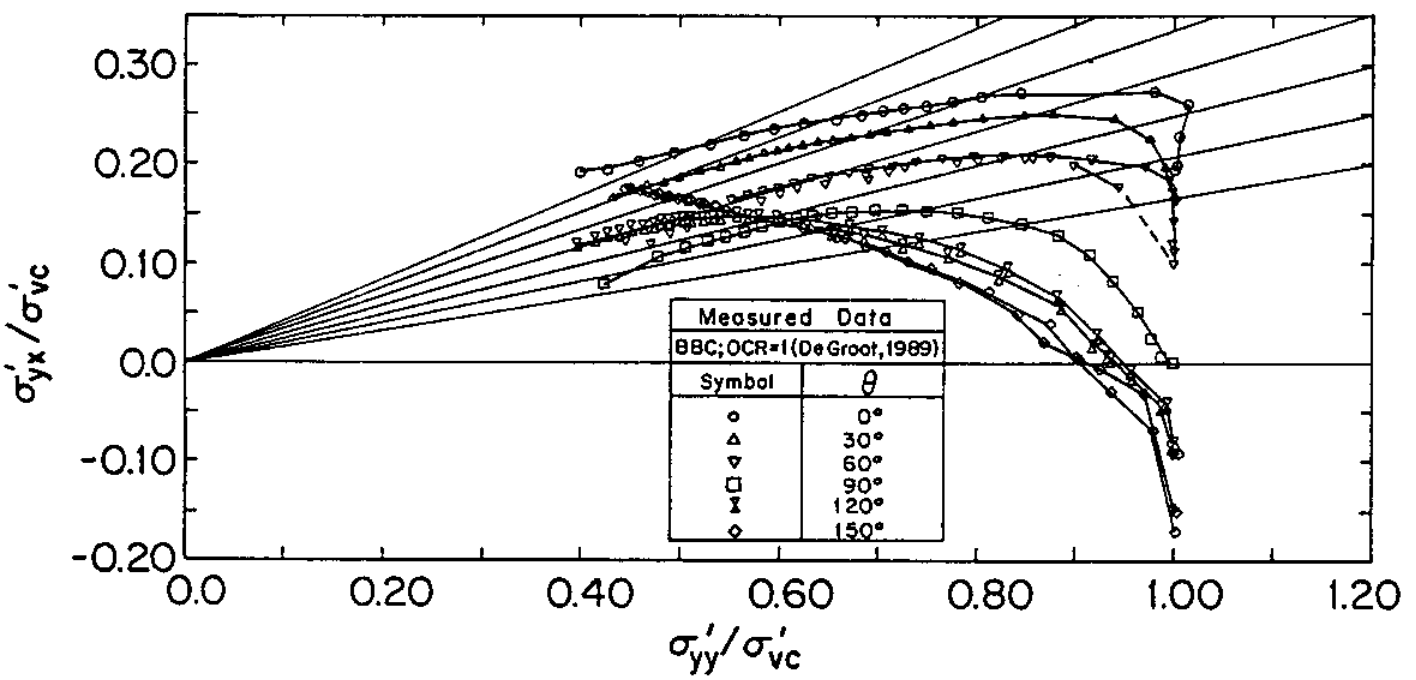

a) Effective Stress Paths

19. Comparison of Model Predictions and Measured Data for MDSS Tests on K_0-Normally Consolidated Boston Blue Clay

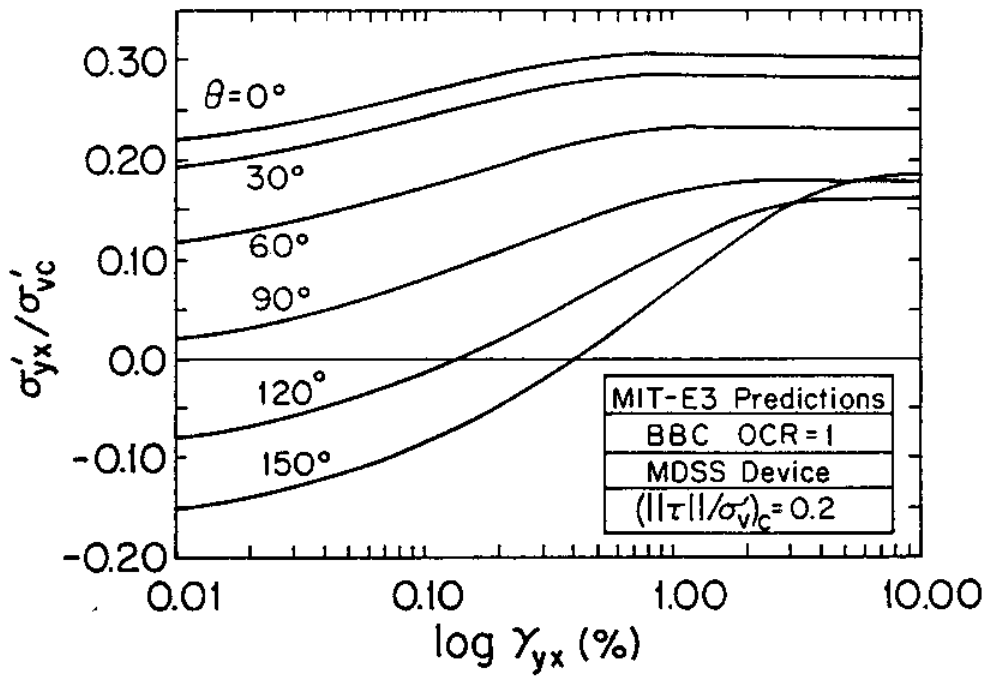

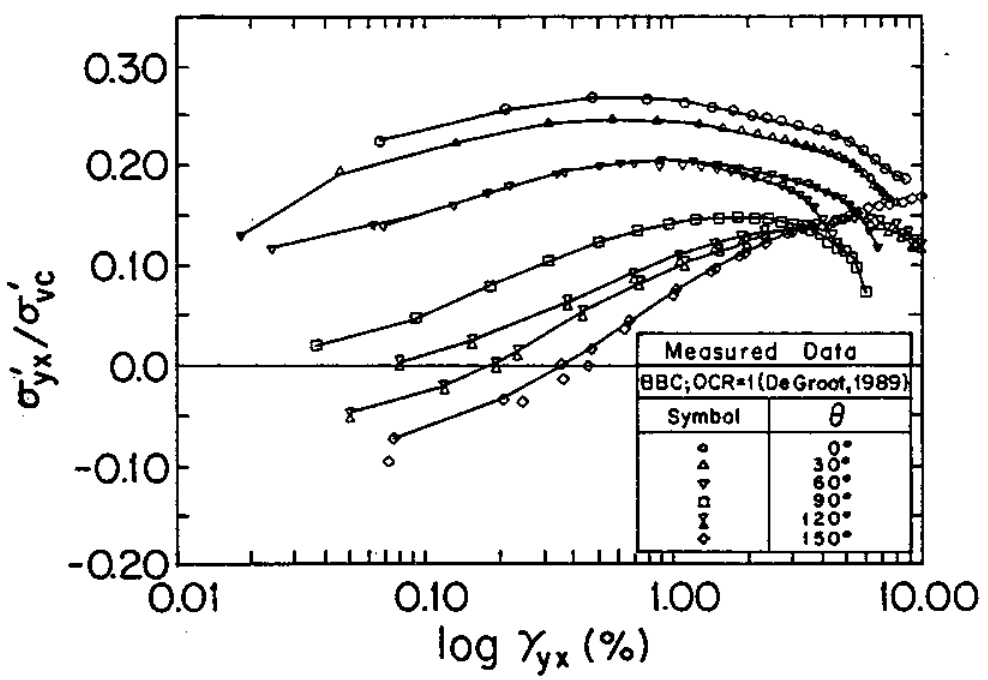

b) Stress-Strain Response in the x-y Plane

19. Comparison of Model Predictions and Measured Data for MDSS Tests on K_0-Normally Consolidated Boston Blue Clay